

**Characterization of BKPyV Interaction with Disialylated Gangliosides
and PKC Regulated Viral Entry**

By

Stacy-ann Adeniqûea Allen-Ramdial

B.A., Boston College, 2007

Thesis

Submitted in partial fulfillment of the requirements for the degree of Doctor of
Philosophy in the Division of Biology and Medicine at Brown University

PROVIDENCE, RHODE ISLAND

MAY 2013

© Copyright 2013 by Stacy-ann Adeniquêa Allen-Ramdial

This dissertation by Stacy-ann A. Allen-Ramdial is accepted in its present form
by the Division of Biology and Medicine as satisfying the
dissertation requirement for the degree of Doctor of Philosophy.

Date _____
Walter J. Atwood, Ph.D., Advisor

Recommended to the Graduate Council

Date _____
Jonathan Reichner, Ph.D., Reader

Date _____
Rebecca Page, Ph.D., Reader

Date _____
Peter R. Shank, Ph.D., Reader

Date _____
Daniel DiMaio, M.D., Ph.D., Outside
Reader

Approved by the Graduate Council

Date _____
Peter Weber, Ph.D.,
Dean of the Graduate School

This dissertation is dedicated to my beloved grandma Sybil Samuels- a woman whose wisdom, courage, strength, honesty, perseverance, and selflessness has afforded her family many opportunities in life. By instilling principles and values in her children and her grandchildren, she taught us all the value of faith, hard work and dedication. Without her I wouldn't have my loving mom, and brother, supportive aunts and uncles, and amazing cousins.

CURRICULUM VITAE

Stacy-ann Adeniquêa Allen-Ramdial

Brown University
Box G-E
Providence RI 02912
Phone: 401-863-3420
Fax: 401-863-9653
Email: Stacy-ann_allen@brown.edu

EDUCATION

- 2007- present** Ph. D candidate, Brown University, Providence, RI
Division of Biology and Medicine, Graduate Program in Pathobiology
- 2007-2010** Masters of Arts, Brown University, Providence, RI
Division of Biology and Medicine, Graduate Program in Pathobiology
- 2003- 2007** Bachelor of Science in Biology, Boston College, Chestnut Hill, MA

RESEARCH EXPERIENCE

December 2007 – present

Structure-Function Analysis of BKV Binding to Disialylated Gangliosides

Thesis research in the Laboratory of Dr. Walter J. Atwood; Dept. of Molecular Biology, Cell Biology and Biochemistry, Brown University, Providence, RI

October 2007 – December 2007

Natural Killer T cell (NKT) Functional Deficiency Alleviates Tissue Damage

Rotation, Laboratory of Dr. Alfred Ayala Division of Surgical Research, Rhode Island Hospital, Providence, RI

January 2006 – January 2007

Lab Focus: Malaria Research

Volunteer work in the laboratory of Dr. Mohammed Shahabuddin; Department of Biology, Boston College, Chestnut Hill, MA

HONORS AND AWARDS

- Frederic Poole Gorham Endowed Fellowship, 2010-2011
- Travel Award, 28th Annual Meeting of the American Society of Virology, 2009
- Boston College Undergraduate Research Fellowship, 2006
- Saint John's Women In Science Award, 2003

PUBLICATIONS

1. Structure-function analysis of human BK polyomavirus-receptor complexes identifies an amino acid switch for binding different ganglioside receptors (In Preparation)
2. Protein Kinase C regulates BKPyV infection (In Preparation)

PRESENTATIONS AND ABSTRACTS

1. **Allen, S.A.**; Neu, U.; Stehle, T.; Atwood, W.J. Unraveling the secrets of BK polyomavirus binding to gangliosides and the consequent effects on viral uptake. Patho-Biology Retreat. Brown University, Providence, Rhode Island. August 28, **2012** (Retreat Talk and Poster Presentation)
2. **Allen, S.A.**; Neu, U.; Blaum, B.; Peters, T.; Stehle, T.; Atwood, W.J. A single point mutation defines BK polyomavirus receptor specificity. American Society of Virology 30th Annual Meeting. University of Minnesota, Minneapolis Minnesota. July 16-20, **2011** (Conference talk)
3. **Allen, S.A.**; Neu, U.; Stehle, T.; Atwood, W.J. Structure-function analysis of BK polyomavirus binding to disialylated gangliosides. New England Science Symposium. Harvard Medical School, Boston, Massachusetts. April 1, **2011** (Poster Presentation)
4. **Allen, S.A.**; Neu, U.; Stehle, T.; Atwood, W.J. Structure-function analysis of BK polyomavirus binding to disialylated gangliosides. Pathobiology Seminar Series. Brown University, Providence, Rhode Island. February 10, **2011** (Departmental Seminar Talk)
5. **Allen, S.A.**; Neu, U.; Stehle, T.; Atwood, W.J. Structure-function analysis of BK polyomavirus binding to disialylated gangliosides. American Society of Virology 29th Annual Meeting, Montana State University, Bozeman, Montana. July 17-21, **2010** (Conference talk)
6. **Allen, S.A.**; Atwood, W.J. The role of gangliosides in human polyomavirus Infection. New England Science Symposium. Harvard Medical School, Boston, Massachusetts. February 28, **2010** (Poster Presentation)
7. **Allen, S.A.**; Atwood, W.J. The role of gangliosides GD1b and GT1b in human polyomavirus entry and infection. American Society for Virology 28th Annual Meeting, University of British Columbia Vancouver, BC, Canada. July 11-15, **2009** (Conference Talk)

PROFESSIONAL DEVELOPMENT

- Teaching Certificate III, Sheridan Center for Teaching and Learning; Brown University (2011).
- Research Collaboration; University of Tübingen (Germany) (2010)
- New England Science Symposium; Harvard University (2010).
- The Biomedical Science Careers Program; Brown University (2010).
- Teaching Certificate I, Sheridan Center for Teaching and Learning Brown University (2008).

TEACHING EXPERIENCE

- “Exploring Infectious Disease: The exotic misconception” – Instructor Summer and Continuing Studies; Brown University (2009 and 2011)
- “Demystifying the Ph.D Experience”-Senior Scholar for Initiative to Maximize Student Development; Brown University (2010)
- Immunology - Teaching Assistant
Department of Biology; Brown University (2008)
- “Medical Microbiology: Germs in the News” -Teaching Assistant Summer and Continuing Studies; Brown University (2008)

PROFESSIONAL AFFILIATIONS

- American Society of Virology

SERVICE

- Beneficent Congregational Church (2010-2013)
- Boston College Alumni Association - Day of Service (2008-2012)
- Samuel M. Nabrit Graduate Students Association (2007-2011)
- ALANA Mentoring Program (2007- 2010)
- Graduate Student Mentor (2008 – 2009)

ACKNOWLEDGEMENTS

First and foremost I would like to say thanks to God for the strength that kept me going and for the faith to believe that I can pursue anything. Additionally, I have been supported by many individuals to whom I would like to express my deepest gratitude.

I would like to express sincere gratitude to my advisor Dr. Walter Atwood for providing me an opportunity to complete my thesis work in his laboratory. I am extremely grateful for his support, encouragement, candor and for allowing me to grow as a scientist and an individual. Thank you for allowing me to represent your lab at local and international conferences and through our international collaboration. Thank you also for all the “surprise” cakes and for taking the time to celebrate something as simple as growing one year older.

Thank you to the members of my committee Dr. Jonathan Reichner, Dr. Rebecca Page, Dr. Peter Shank and the past member of my committee Dr. Shuping Tong for their support, mentoring and constructive criticism. I would like to extend special thanks to Dr. Daniel DiMaio for serving as my outside reader and for taking the time to traveling here today. Special thanks also to Dr. Thilo Stehle and Dr. Ursula Neu for their invaluable contribution to our collaborative partnership and for their overwhelming support in making this project a success. To the Pathobiology Graduate Program, the IMSD program, the administrative staff, the staff in the Ship street core and fellow students, thank you for creating such a memorable environment and graduate school experience.

I take this opportunity to thank the current members of the Atwood lab: Dr. Melissa Maginnis, Dr. Gretchen Gee, Dr. Christian Nelson, Dr. Aaron Derdowski, Dr. Sheila Haley, Bethany O’Hara, Benedetta Assetta, Steve Zins, our visiting student Luisa

Stroh and the former lab members: Dr. Aisling Dugan, Dr. Joslynn Jordan, Dr. Megan Stanifer, and Dr. Kate Manley for their encouragement, guidance, support, constructive criticism and advice. A special thank you to Melissa, Benny and Beth, I can't say thank you enough for your tremendous support, mentorship, kindness and help.

I am immensely blessed to have a cohort of overwhelmingly supportive family and friends. I'd like to express my overwhelming gratitude to my mom Ceceline Samuels for all her sacrifices, encouragement and her love. I am proud to be representing her today. Thank you to my relatives for keeping me grounded and for being unwavering in their support of all my dreams. Special thanks to my Grandma Sybil and Aunt Pam who were instrumental in laying the foundation that has been so fundamental to my current and future success, and my Aunt Verene for making sure I never lose faith during the tough times in college and during grad school. Thank you also to my extended family for your well wishes, encouragement and love. You've believed in this journey and your encouragement has meant a lot. My experience wouldn't be the same without my church family and friends. Thank you to Pastor Todd, Pastor Nicole and the Beneficent church family for being so gracious and welcoming. Thank you to my friends especially Tania, Bonnie and Leon for, sharing new experiences and for all the fun memories. Thanks to Tania for helping me to always feel like I'm back in Jamaica and for being a sister.

Last and definitely not least, a very special thank you to my husband Sunerine R. Ramdial for loving me unconditionally, for celebrating all my accomplishments as if they were his own, for encouraging me to be better, and for supporting all my endeavors with great enthusiasm. Thank you for spending those long hours with me in lab and for being my personal computer engineer. I am truly blessed to have you in my life.

PREFACE

The work presented in this Ph.D thesis was conducted in the laboratory of Dr. Walter J. Atwood, Dr. Thilo Stehle, Dr. Thomas Peters, and Dr. Ten Feizi. I have designed/executed experiments and prepared figures presented herein with the following exceptions:

1. The crystallography and all related structural data and models in Chapter 2 were completed by Dr. Ursula Neu in the laboratory of Dr. Thilo Stehle at the University of Tübingen.
2. The NMR data in Chapter 2 were completed by Dr. Bärbel S. Blaum in the laboratories of Dr. Thomas Peters at the University of Lübeck and of Dr. Thilo Stehle at the University of Tübingen.
3. The Glycan array screen in Chapter 2 was completed by Dr. Yan Liu and Dr. Angelina de Sa Palma in the laboratory of Dr. Ten Feizi at Imperial College London.
4. Additionally the intellectual contributions of Dr. Melissa Maginnis, and Bethany O'Hara were critical for the work presented in Chapter 3. Benedetta Assetta and Aaron Derdowski assisted with the confocal microscopy work presented in Chapter 3.

TABLE OF CONTENTS

Title Page-----	i
Copyright Page-----	ii
Signature Page-----	iii
Dedication Page -----	iv
Curriculum Vitae-----	v
Acknowledgements-----	viii
Preface-----	x
Table of Contents-----	xi
List of Figures-----	xiv
List of Abbreviations-----	xvi

Chapter 1: Introduction

Title Page -----	1
Polyomavirus Classification -----	2
Polyomavirus BK and Pathogenesis -----	5
Polyomavirus Associated Nephropathy -----	6
Hemorrhagic Cystitis -----	9
BKPyV Genome Organization -----	11
BKPyV Capsid Organization -----	16
BKPyV Lifecycle -----	19

Attachment	20
Signaling and Entry	25
Trafficking to the ER	28
Nuclear Entry and Egress	31
Specific Aims	33
Literature Cited	35

Chapter 2: Structure-function analysis of BKPyV binding to disialylated gangliosides

Title page	53
Abstract	54
Introduction	55
Materials and Methods	57
Results	64
Discussion	77
Literature Cited	81
Figures	86

Chapter 3: Regulation of BKPyV infection by PKC

Title page	99
Abstract	100

Introduction	-----101
Materials and Methods	-----104
Results	-----109
Discussion	-----113
Literature Cited	-----117
Figures	-----123

Chapter 4: Discussion and Future Directions

Title page	-----127
BKPyV engagement of b-series ganglioside	-----128
PKC regulation of BKPyV entry	-----137
Summary	-----143
Literature Cited	-----145

LIST OF FIGURES

Chapter 1

Figure 1: Phylogenetic relationship among polyomaviruses	2
Figure 2: The polyomavirus genome	11
Figure 3: The crystal structure of KIPyV and WUPyV	17
Figure 4: Schematic of BKPyV lifecycle	19
Figure 5: Structure and diversity of sialic acid	22
Figure 6: Biosynthetic pathway for glycosphingolipids	24
Figure 7: Organization of lipid rafts and caveolae domains	25
Figure 8: Proposed model of BKPyV early entry	29

Chapter 2

Figure 1: B-series gangliosides are receptors for BKPyV	86
Figure 2: BKPyV primarily engages the disialic acid motif of b-series gangliosides	88
Figure3: Structure of a BKPyV VP1-GD3 oligosaccharide complex	89
Figure 4: Proposed model of BKPyV VP1-GD1b oligosaccharide complex	91
Figure 5: BKPyV engagement of sialic acid is important for spread and infectivity	92

Figure 6: Comparison of carbohydrate binding sites of BKPyV, SV40 and JCPyV ----	93
Figure 7: The K68S mutation retargets BKPyV to the SV40 receptor GM1 -----	94
Figure 8: K68S specifically interacts with NeuNAc-GM1 -----	96
Figure 9: K68S BKPyV uses N-acetyl GM1 as a receptor -----	97
 Chapter 3:	
Figure 1: Transient inhibition of PKC increases BKPyV infection -----	123
Figure 2: GT1B and GFX synergize to further enhance BKPyV infection -----	124
Figure 3: Inhibition of PKC causes membrane localization -----	125
Figure 4: Inhibition of PKC causes BKPyV accumulation in an antibody sensitive location -----	126

ABBREVIATIONS

AA	Amino acid
BKPyV	BK virus
Bp	Base pairs
BSA	Bovine serum albumin
Cav-1	Caveolin-1
CMV	Cytomegalovirus
CTX	Cholera toxin
DAG	Diacylglycerol
DBD	DNA binding domain
DHODH	Dihydroorotic acid dehydrogenase
DMSO	Dimethyl Sulfoxide
DNA	Deoxyribonucleic Acid
dsDNA	Double-stranded DNA
EGFR	Epidermal growth factor receptor
EM	Electron microscopy
ER	Endoplasmic reticulum
ERAD	ER-associated degradation
GalNAc	N-Acetylgalatosamine
GFX	Bisindolylmaleimide I
H2A	Histone 2A
H2B	Histone 2B
H3	Histone 3
H4	Histone 4
HBV	Hepatitis B virus
HC	Hemorrhagic cystitis
HCV	Hepatitis C virus
HIV	Human immunodeficiency virus
HLA	Human leukocyte antigen
HPyV6	Human polyomavirus 6
HPyV7	Human polyomavirus 7
HPyV9	Human polyomavirus 9
JCPyV	John Cunningham Virus
KIPyV	Karolinska Institute polyomavirus
LT-Ag	Large Tumor Antigen
MCC	Merkel Cell Carcinoma
MCPyV	Merkel cell polyomavirus
MHC(I)	Major Histocompatibility Complex class I protein

MPyV	Mouse polyomavirus
mRNA	Messenger RNA
NCCR	Non-Coding Control Region
Neu5Ac	N-Acetyl- neuraminic acid
NeuNAc	N-Acetyl- neuraminic acid
NeuNGc	N-glycolyl-neuraminic acid
NFAT	Nuclear factor of activating T-cells
NFκB	Nuclear factor kappa light chain enhancer of activated B cells
NLS	Nuclear localization signal
NMR	Nuclear Magnetic Resonance
PBS	Phosphate Buffer Saline
PCR	polymerase chain reaction
PKA	Protein Kinase A
PKC	Protein Kinase C
PML	Progressive Multifocal Leukoencephalopathy
PP2A	Protein phosphatase 2A
pRb	Retinoblastoma protein
PS	Phosphatidylserine
PVN	Polyomavirus Induced Nephropathy
RNA	Ribonucleic Acid
RSV	Respiratory Syncytial Virus
Ser/Thr	Serine/Threonine
STD	Saturation Transfer Difference
SV40	Simian vacuolating Virus 40
t-Ag	Small t-Antigen
TLC	Thin Layer Chromatography
TSPyV	Trichodysplasia spinulosum polyomavirus
VLPs	Virus like particles
VP1	Viral Protein 1
VP2	Viral Protein 2
VP3	Viral Protein 3
VSV	Vesicular stomatitis virus
WUPyV	Washington University polyomavirus

CHAPTER 1

INTRODUCTION

POLYOMAVIRUS CLASSIFICATION

Polyomaviruses are members of the Polyomaviridae family. In addition to the family, Polyomaviridae and Papillomaviridae were once members of the Papovaviridae family. However this taxonomical classification is no longer used and Polyomaviridae and Papillomaviridae were split into two categorically unique families because of their distinct modes of replication, genome organization and evolutionary history (1,146). In addition to these changes, further distinctions have recently been made regarding classification of the Polyomaviridae family, which once consisted of only the Polyomavirus genus. The taxonomical changes produced three polyomavirus genera and reflect biological differences and nucleotide sequence divergence among the species (Figure 1) (64). Wukipolyomavirus and Orthopolyomavirus represent the mammalian genera and Avipolyomavirus represents the avian genus (64).

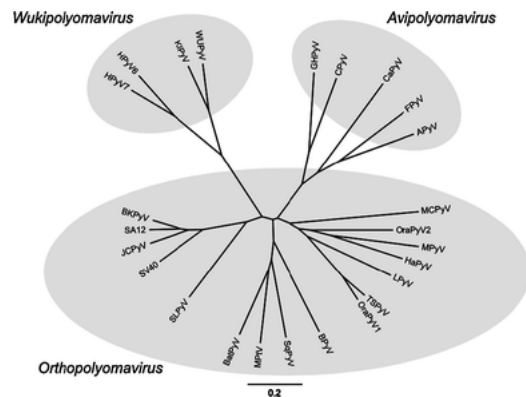


Figure 1: Phylogenetic relationship among polyomaviruses. The polyomaviruses are divided into three genera based on whole genome sequences. The avian polyomaviruses are listed under the genera Avipolyomavirus and the mammalian polyomaviruses are divided into two genera, Wukipolyomavirus and Orthopolyomavirus. Printed image from; Springer, John, Buck, Allander, Atwood, Garcea, Imperiale, Major, Ramqvist, Cole, *Taxonomical developments in the family Polyomaviridae, 1627-1634*, Copyright 2011 with kind permission from Springer Science and Business Media.

Polyomaviruses are small, approximately 40-45nm in diameter; they are icosahedral in shape and lack a viral envelope (24,64). Polyomaviruses have circular double-stranded deoxyribonucleic acid (dsDNA) genomes that are roughly 5000 base pairs (bp) in length and replicate in the nucleus using host cell DNA polymerase (1,34,64). Primary infection is usually asymptomatic and is believed to occur by respiratory and/or fecal-oral transmission during childhood. Infection persists as a latent infection in the host (24). Polyomaviruses infect a wide range of species and at present there are over twenty identified polyomaviruses. The prototypical polyomaviruses are Simian vacuolating virus 40 (SV40) and Mouse Polyomavirus (MPyV), which have been extensively studied (34). To date nine human polyomaviruses have been identified: BKPyV and JCPyV were identified in 1971 and named with the initials of the first patient from which they were isolated; Karolinska Institute polyomavirus (KIPyV) and Washington University polyomavirus (WUPyV) in 2007, Merkel cell polyomavirus (MCPyV) in 2008, Human polyomavirus 6 (HPyV6), Human polyomavirus 7 (HPyV7) and Trichodysplasia spinulosum polyomavirus (TSPyV) in 2010, and Human polyomavirus 9 (HPyV9) in 2011 (4,24,39,42,43,64,107,130,131,155).

Human polyomaviruses have been isolated and can cause clinically relevant infections in the kidney, urinary tract, respiratory tract, neuroendocrine cells in the dermis, and the brain. BKPyV was isolated from the urine of a kidney transplant patient and JCPyV from patient derived brain tissue as the etiological agent of the neurodegenerative disease Polyomavirus Multifocal Leukoencephalopathy (PML) (42,103,107). KIPyV and WUPyV were isolated from respiratory aspirates of patients with respiratory tract infections (4,43). MCPyV was isolated directly from tumors of

patients with Merkel Cell carcinoma (MCC) and is associated with most Merkel cell carcinomas (39). The discovery of MCPyV as the cause of a human cancer is noteworthy as it emphasizes the etiological role of a polyomavirus in a human cancer. HPyV6, HPyV7 and TSPyV were isolated from the skin of healthy patients, however TSPyV is associated with the rare skin disease Trichodysplasia spinulosa in immunocompromised patients (130,155). HPyV9 was isolated from urine and blood of immunocompromised kidney transplant recipients (131).

BKPyV and JCPyV have been extensively characterized and are considered the prototype human polyomaviruses. Phylogenetic analysis of whole genome sequences reveal that BKPyV is closely related to JCPyV (Figure 1); they share approximately 75% overall sequence homology (24,34). Even though BKPyV and JCPyV are so closely related, they display strikingly different biological characteristics such as receptor usage, mode of entry and pathogenesis. Phylogenetic analysis shows that KIPyV, WUPyV HPyV6 and HPyV7 are distantly related to other polyomaviruses but are closely related to each other (Figure 1). A comparison of KIPyV and WUPyV sequence identity to JCPyV and BKPyV shows only 28% sequence similarities (24,64). The disparate sequence identities of KIPyV, WUPyV, HPyV6, HPyV7 are so distinct from other mammalian polyomaviruses that they have been classified under a separate genera, Wukipolyomavirus, while all other mammalian polyomaviruses are classified under the genus Orthopolyomavirus (Figure 1) (64).

POLYOMAVIRUS BK AND PATHOGENESIS

Polyomavirus BKPyV is a significant human pathogen. It is widely distributed worldwide with seroprevalence reported to vary between 40 and 95% in the human population (24). Epidemiological studies of human polyomavirus seroprevalence in adults (> 21yrs) and children (< 21yrs) produced similar statistical results, indicating that primary polyomavirus exposure occurs at an early age (24,70,73). To further support this, serological evidence exists demonstrating the potential for vertical transmission of BKPyV during pregnancy or soon after delivery, and studies of BKPyV seroprevalence in children show that seroprevalence peaks between the ages of 5 and 9 years (9,72,145).

The initial site of infection for BKPyV is not known, however it has been hypothesized that initial infection may occur orally in the tonsils via the respiratory route as studies have revealed low levels of BKPyV DNA in the tonsillar tissue of immunocompetent patients and patients with acute upper respiratory disease (17,45). The presence of BKPyV in urine further suggests the possibility of oral transmission from contaminated food and water (56). From the initial site of infection BKPyV disseminates to the blood. Viremia can present itself with flu-like symptoms that may likely be the result of the immune response, which ultimately clears the infection from the blood (56). Following clearance from the blood, BKPyV is thought to establish a state of non-replicative infection, latency, or a low level persistent asymptomatic infection in the epithelial cells of the genitourinary tract, specifically the epithelial lining of the collective ducts and Bowman's capsule (56,103,137). BKPyV can be reactivated periodically but most often reactivation is due to immunosuppression leading to an increase in viral replication (56).

Approximately 50% of healthy (non-transplanted) kidneys contain non-replicating BKPyV (153). Reactivation occurs in approximately 0.3-5% of healthy individuals, and is characterized by increased viruria and viremia, and morphological changes such as the presence of viral inclusion bearing cells in the uroepithelial (28,54,56,153). Reactivation of BKPyV, however is primarily seen in individuals who are immune compromised. Reactivation is reported in 20-40% of human immunodeficiency virus (HIV) infected patients, 22-100% of bone marrow transplant recipients, 10-60% of kidney transplant recipients, up to 50% of solid organ (non-kidney) transplants, and in individuals with inherited immune dysfunction though this remains controversial (54,56,92,119,122,124,153). The prevalence BKPyV shedding can also increase for pregnant women, individuals with advanced age, and individuals with diabetes mellitus as a result of down regulation of the immune response (54,122,153). Because of the significant correlation between immunosuppression and reactivation, immunosuppression is widely considered the key modulator of BKPyV reactivation (54,56).

Polyomavirus Associated Nephropathy

Disease associated with viral reactivation is relatively rare, however a small number of viruric individuals experience complications due to BKPyV reactivation. Complications include the development of Polyomavirus Associated Nephropathy (PVN) in kidney transplant recipients and Hemorrhagic Cystitis (HC) in bone marrow transplant patients (8,42,53,169). BKPyV is responsible for the majority of PVN cases with 1-10% prevalence of PVN in kidney transplant recipients (53,56,104). PVN is characterized by signs of nuclear inclusions in tubular epithelial cells, sloughing of epithelial cells,

enlarged irregular nuclei and chromatin smudging (53,104). Diagnosis of PVN includes observation of BKPyV in urine samples and plasma, quantification of viral inclusion bearing cells (“decoy cells”) in the uroepithelial, PCR detection of BKPyV DNA and quantification of viral particles by electron microscopy (EM) (53,104).

PVN is a serious complication of renal transplantation. Kidney transplant patients who develop PVN have a 10-70% graft failure rate (104,162). The primary risk factor for developing PVN is immunosuppression associated with allograft transplantation (53,153). However, the risk for developing PVN following organ transplant other than kidney transplant is so low that it is believed that immunosuppression, as a risk factor, may be confounded by other factors (153). Additional risk factors associated with PVN include: older age (>50years), male gender, BKPyV sero-negativity prior to transplant (10-40% prevalence), diabetes, caucasian ethnicity, impaired BKPyV specific T-cell response, co-infections, drug toxicity, human leukocyte antigen (HLA) compatibility, mutation of BKPyV and tissue injury (54,53,55,118,133,151,153).

Since the late 1990s there has been a systematic increase in the incidence of PVN, which could indicate new risk factors and/or increased awareness (53). A common argument for the “re-emergence” of PVN is the use of more potent immunosuppressants such as Tacrolimus and Mycophenolate mofetil (53). While neither drug necessarily causes PVN, approximately 5% of patients treated with high doses of Tacrolimus, for example show signs of BKPyV nephropathy (54,53,104). Due to the lack of specific BKPyV antiviral therapy, treatment of PVN is difficult. The current strategies for treatment of PVN include decreasing immunosuppression by using less potent immunosuppressants such as Cyclosporine A, and coupling immunosuppressive therapy

with the use of broad spectrum antiviral drugs such as Cidofovir, and Leflunomide (54,53,104,153).

As with any treatment regimen there is the risk of unwanted side effects. The goal of treatment regimens that reduce immunosuppression is to allow for improved immune clearance of BKPyV, but reducing immunosuppression can have the unintended consequence of graft rejection (153). Treatment with immunosuppressants such as Cyclosporine A also has unwanted side effects. Cyclosporine A binds and inhibits calcineurin activity thus blocking the activation of the transcription factor Nuclear Factor of Activating T-cells (NFAT), which is necessary for regulation of BKPyV infection and viral transcription (57,65). Because calcineurin and NFAT are important for cellular processes in both the target cell type and other cell types in the body, inhibiting their activity can have toxic effects (95,139). Antiviral therapies likewise have unwanted side effects. Cidofovir is transported to tubular epithelial cells and targets viral DNA polymerase to inhibit viral replication of viruses like cytomegalovirus (CMV), which encode their own DNA polymerase (22,54). BKPyV does not encode its own viral DNA polymerase and relies on host DNA polymerase for its replication. It is believed that Cidofovir works by reversing the effects of LT-Ag on p53 and pRB resulting in apoptosis of infected cells (22). The effectiveness of Cidofovir in inhibiting BKPyV replication is thus related to the drug's effect on the host cell replication. This cell specific, versus virus specific effect, can result in highly nephrotoxic side effects (6,53). Leflunomide likewise has shown promise as treatment for BKPyV because of its antiviral and immunosuppressive properties. Leflunomide metabolizes to the active metabolite A77 1726, which inhibits dihydroorotic acid dehydrogenase (DHODH), the enzyme that

catalyzes the synthesis of pyrimidine (66). Previous research has shown that Leflunomide disrupts CMV infection *in vivo* possibly by blocking virion assembly (163,164). Leflunomide has been shown to reduce BKPyV infection during *in vitro* and *in vivo* studies, though the mechanism of inhibition is not known (66,167). Additionally, Leflunomide was also shown to inhibit the transcription factors Activator Protein 1 (AP-1) and Nuclear Factor Kappa light chain enhancer of activated B cells (NFκB), which are important transcription factors that contribute to transcriptional regulation of BKPyV (65,84). While Leflunomide shows promise because of its antiviral properties, like Cyclosporine A its target of cellular factors can result in inadvertent cytotoxic effects. The combination of improved diagnostic criteria and continued refinement of treatment options and standards allows for much optimism that the incidence of PVN will decrease in the near future.

Hemorrhagic Cystitis

Hemorrhagic cystitis (HC) is a complication of bone marrow transplants in which the patient develops inflammation of the bladder. It has an incidence of 5-60% of transplants in adults and children (8,16,54). HC is caused by the side effects of toxins, chemotherapy, radiation and viral infections such as adenovirus and BKPyV infections (16,54,110). Early onset HC is ascribed to the toxic effects of drugs used during bone marrow transplants such as cyclophosphamide, while late onset HC is usually associated with BKPyV infection in 50% of adult transplant cases (2,16,54,169). BKPyV associated HC pathogenesis is hypothesized to result from over reaction of the immune system in response to the increase in BKPyV antigen during the process of immune recovery. This results in an excessive inflammatory response which damages the urothelium (54). There

is no effective therapy for BKPyV associated HC in bone marrow transplant patients (110). Treatment is restricted to alleviating pain, bladder irrigation and the use of the antiviral Cidofovir for patients with co-infections with CMV (8,54). The antibiotic Ciprofloxacin, a DNA gyrase inhibitor has been evaluated as a treatment option for HC. Ciprofloxacin is an antibiotic belonging to the family of broad spectrum family of antibiotics called quinolones. Quinolones have been shown to inhibit the helicase activity of Large T Antigen for SV40 and are believed to function in the same manner for BKPyV Large T-Antigen (3,134). Treatment with Ciprofloxacin was demonstrated to have no overall benefit as the rate of HC was not significantly reduced and the effectiveness of Ciprofloxacin was most apparent when BKPyV viral levels are low, which is not useful as the development of HC is preceded by high BKPyV viral level as detected in urine samples (77,117).

The drug levofloxacin may also be an effective treatment option for HC. Levofloxacin is also a quinolone and was observed to inhibit BKPyV infection when added to cells treated with BKPyV-containing urine samples from patients that had undergone bone marrow transplants (77). More recent studies have looked at the effects of levofloxacin on the prevention of BKPyV viremia in renal transplant recipients and on BKPyV infection in renal proximal tubular cells. The results show that levofloxacin lowers the rate of BKPyV viremia in patients and significantly lowers BKPyV infection in a dose dependent manner in proximal tubular cells yielding ~90% inhibition at a concentration that is not cytotoxic and can be achieved in urine and kidney (41,134).

BKPyV GENOME ORGANIZATION

Polyomaviruses have a conserved genome that is divided into three regions: the non-coding regulatory region (NCRR) also known as the non-coding control region (NCCR), the early coding region and the late coding region (Figure 2) (1,34).

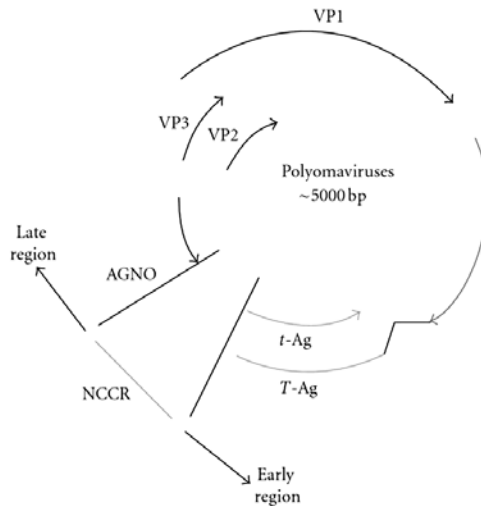


Figure 2: The Polyomavirus Genome. The polyomavirus genome is divided into three regions: The non-coding control region (NCCR) and the early and late coding region. The NCCR contains the origin of replication (ORI) and controls transcription of the early and late genes and regulates replication. The early coding region codes for: Large T-Antigen (LT-Ag) and small t-Antigen (t-Ag) and the late coding region codes for the structural proteins VP1, VP2, VP3 and the regulatory protein agnoprotein in some polyomaviruses. Printed image from; Clinical and Developmental Immunology, Delbue, Comar, Ferrante, *Review on the Relationship between Human Polyomavirus-Associated Tumors and Host Immune System, 1-10*, Copyright 2012 with permission from Serena Delbue et al.

The non-coding regulatory region is 300-500 bp and separates the early and late coding regions (34). The NCCR contains the origin of replication (Ori), a bi-directional promoter, the LT-Ag binding site, the TATA box, and cellular transcription control sequences (1,26,27,34,56). Unlike the early and late coding regions that have conserved sequences, the NCCR is subjected to considerable sequence variability in BKPyV. The NCCR of archetypal BKPyV is divided into 4 transcription factor sequence blocks

labeled P, Q, R and S. Variability in the NCCR can result from duplications and rearrangements of these blocks which can result in improved replication and transcriptional advantages (65,87,88). For example, compared to the archetypal strain of BKPyV, which has one “P” block, the Dunlop strain of BKPyV with three repeats of the “P” block shows enhanced transcription and more efficient replication (48,87,88,165). Sequence variability in the NCCR may play a role in viral reactivation. The BKPyV promoter is dependent on the activity of NFAT, in addition to AP-1 and NFκB, to regulate viral transcription. Recent work has shown that rearrangements in the NCCR or treatment with NFAT modulators such as the immunosuppressant Tacrolimus has the potential to disrupt transcriptional regulation by NFAT and mimic viral reactivation suggesting potential mechanism for drug induced reactivation (65).

The polyomavirus early coding region contains the genetic information for the viral regulatory tumor antigen proteins. The gene products encoded by the early coding region are LT-Ag and t-Ag, which are produced by alternative splicing of a pre-messenger RNA (mRNA) precursor. The splicing variants produce a ~700 amino acid and an ~170 amino acid product respectively (Figure 1) LT-Ag and t-Ag are the first genes to be transcribed. LT-Ag is necessary for viral replication; however, t-Ag is not necessary as a deletion in the coding region for t-Ag does not affect viral propagation in culture. LT-Ag and t-AG were named as such because early studies found that they were dominant tumor antigens in animals with virally induced tumors (64,87,146). (60).

The BKPyV LT-Ag shares >70% amino acid sequence homology with the SV40 LT-Ag (87). Studies with SV40 LT-Ag revealed that LT-Ag possesses transforming properties. SV40 LT-Ag has been shown to bind and inactivate retinoblastoma

susceptible protein (pRb), its relatives and the tumor suppresser protein p53 resulting in activation of the transcription factors of the E2F family, which stimulate cell cycle progression and host cell DNA replication (23,38,111,146,147). Like SV40, BKPyV LT-Ag has been shown to induce transformation of cells by binding to members of the retinoblastoma family of proteins and p53 (49,50,87). Stimulating DNA replication creates an environment suitable for initiation of viral DNA synthesis as the same factors and substrates required for DNA synthesis in the cell, such as DNA polymerase, are likewise essential for viral DNA replication (34,56).

Once the cell has entered S-phase, LT-Ag binds to the Ori and recruits host DNA polymerase, α -primase, and proceeds to unwind the DNA which stimulates bi-directional replication of the viral genome (60,146). Because polyomavirus replication is dependent on host cell replication, it is believed that characteristics of uroepithelial cells as continuously proliferating predispose these cells to BKPyV infection and create a favorable environment for reactivation (53). The functional interaction between LT-Ag and DNA polymerase is species specific and this defines in part the narrow host cell tropism of BKPyV and polyomaviruses in general (34,83). In addition to stimulating DNA synthesis, LT-Ag also has the ability to auto-regulate its own expression such that at peak expression of LT-Ag, early gene transcription is suppressed and late gene transcription is initiated (34,56).

Unlike LT-Ag, the function of t-Ag has not been as extensively defined. BKPyV t-Ag shares 73% overall sequence homology with SV40 t-Ag (87). Small t-Ag has been shown to support viral replication and cell transformation by stimulating cell proliferation and DNA synthesis in SV40 (34,87,146). Work done with SV40 t-Ag has shown it to be

important for optimal SV40 replication, as it supports effective replication by binding and inhibiting the cellular phosphatase protein phosphatase 2A (PP2A), resulting in cell cycle progression and viral replication (59,166). BKPyV t-Ag was also shown to bind PP2A however its function is not well understood (87). BKPyV t-Ag is not necessary for human polyomavirus infection as infection progresses in the absence of the protein. Additionally its role in cell transformation remains questionable though the current evidence indicates that it may play a supporting role for T-Ag function (34,87).

BKPyV late gene transcription is controlled by the late coding region, which codes for the structural proteins, viral protein 1, 2 and 3 (VP1, VP2 and VP3), and the regulatory protein agnoprotein (1,34). The three structural proteins, like LT-Ag and t-Ag, are produced by alternative splicing of a common precursor mRNA. However, VP1 is translated in a different reading frame from VP2 and VP3 (87,146). VP1 is the major structural protein while VP2 and VP3 are minor components of the virion (87,146). The structural proteins are translated in the cytoplasm and then translocate to the nucleus where they are necessary for the packaging of new viral particles and release of the viral progeny (34). The structural proteins all share common domains which include the nuclear localization signal (NLS), the DNA binding domain (DBD) and the protein-protein interacting domain. These domains are necessary for capsid formation, viral genome encapsidation, and maturation of the viral particle (87).

In addition to the structural proteins, the regulatory protein agnoprotein is also encoded in the late coding region for BKPyV and the polyomaviruses JCPyV and SV40 (44). Other than BKPyV and JCPyV, none of the other human polyomaviruses seem to encode this protein (44). The BKPyV and JCPyV agnoprotein share >50% sequence

similarity with SV40 (44). BKPyV agnoprotein is a 66 amino acid phospho-protein that is modulated by protein kinases such as protein kinase C (PKC) and protein kinase A (PKA) (63,87). Post-translational modification of BKPyV agnoprotein by phosphorylation is thought to direct the cellular localization of the expressed protein primarily to the cytosol and perinuclear region (44,63). Additionally phosphorylation of BKPyV agnoprotein may be residue specific such that phosphorylation of a specific residue may lead to increased stability or phosphorylation of another residue may result in targeting for degradation (44,63). BKPyV agnoprotein seems to be dispensable however. In studies where BKPyV agnoprotein was mutated resulting in an alteration in the initiation codon, BKPyV was able to successfully propagate in a number of cell lines (87). Additionally, when growth of a BKPyV mutant lacking agnoprotein was compared to the growth of wild type BKPyV, the mutant successfully grew albeit at a reduced level compared to wild type (44,94). Similarly, deletions in agnoprotein of SV40 reduce viral spread (87).

Studies of JCPyV agnoprotein provide additional insight into the potential function of agnoprotein in the BKPyV viral life cycle. Agnoprotein has been shown to regulate gene expression in JCPyV by binding to LT-Ag and down regulating early gene expression and DNA replication (44,125). It has also been shown to interact with p53 leading to suppression of the cell cycle presumably in order to allow efficient virion assembly (21). Additionally, JCPyV agnoprotein has been shown to interact with heterochromatin protein 1 α resulting in destabilization of the nuclear envelop, which promotes release of the viral progeny (106). The function of agnoprotein in progeny

release may address why agnoprotein deficient SV40 and BKPyV mutants show reduced viral spread.

BKPyV CAPSID ORGANIZATION

VP1, as the major polyomavirus structural protein, accounts for approximately 70% of the virion mass (1,64,146). The capsid is composed of 360 copies of VP1 which forms 72 pentamers (146). A capsid is formed when the neighboring VP1 C-terminals of a pentamer interact with a neighboring pentamer, such that each pentamer shares five C-terminal protrusions while simultaneously accepting five C-terminal protrusions (79,127,126,128,141). Additionally, the N-terminus of the accepting VP1 monomer interacts with the invading C-terminus arms to further aid in capsid formation (79,128,141). These interactions of the C-terminus and the N-terminus are stabilized by calcium ions and disulfide bonds (78,79,128,141). The crystal structure of a number of polyomaviruses, including the prototypical polyomavirus SV40 and MPyV, and the human polyomaviruses JCPyV, MCPyV, WUPyV and KIPyV have been determined providing a wealth of information on polyomavirus VP1 structure and its interaction with whole and partial receptor components (Figure 3) (79,98-101,141,143). Additionally, a previous study produced a model of BKPyV based on its homology to SV40 but no crystal structure of BKPyV has been published (32). These studies which provide a basis for further characterization of BKPyV with its receptors has lead to a more extensive characterization of BKPyV as described in chapter 2.

VP1 is a polypeptide formed by two opposing beta sheets with anti-parallel strands that fold into a jelly-roll β -barrel structure (Figure 3) (32,128,141). This conformation gives rise to multiple exposed loops that link the beta sheets and point

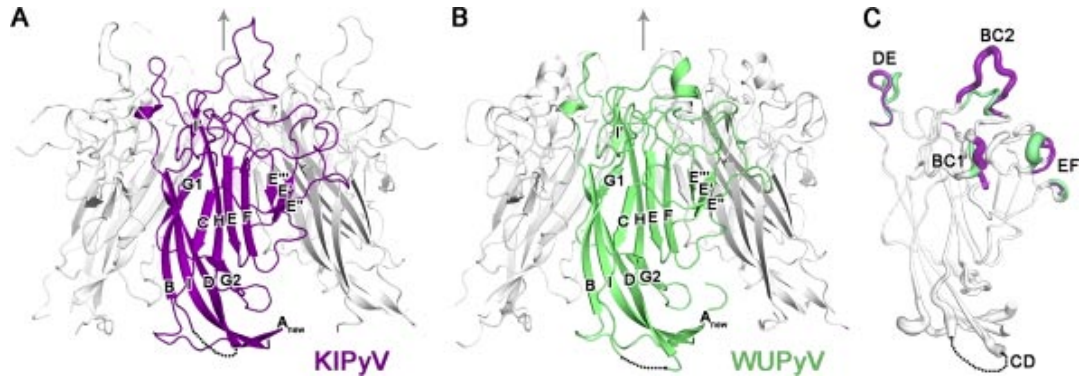


Figure 3: The Crystal structure of KIPyV and WUPyV. (A) Structures of KIPyV and (B) WUPyV VP1 pentameric capsomeres are shown as ribbon traces with a single monomer highlighted in color. KIPyV and WUPyV adopt the anti-parallel β -sandwich conformation typical of polyomavirus VP1 capsid protein. The gray arrow indicates the exterior of the pentamer and the fivefold axis of symmetry. (C) Superposition of KIPyV and WUPyV VP1 monomers highlighting, in their respective colors, differences in their outer loops. Printed image from; Journal of Virology, Neu, Wang, Macejak, Garcea, Stehle, *Structures of the major capsid proteins of the human Karolinska Institutet and Washington University polyomaviruses*, 7384-7392, Copyright 2001 with permission from American Society of Microbiology.

toward the exterior of the capsid (Figure 3) (141). The β -strands are conventionally labeled CHEF and BIDG (Figure 3), and the loops connecting the strands are conventionally labeled BC, HI, DE and FG (128,142). Polyomavirus structural data indicate that the VP1 surface is formed primarily by the BC, DE and HI loops (98-101,142,143). The loops of VP1 define the receptor binding site and are the most variable regions in VP1 (32,99,100). This is emphasized in (Figure 3C) where individual monomers of KIPyV and WUPyV are superimposed to show the differences in their outer loops. Early studies with SV40 and MPyV show that much of the sequence divergence in VP1 are located in the outer loops of VP1 indicating that differences in VP1 sequence homology translate to differences in surface loop structure and interaction with receptors (101,141,144). Additional studies characterizing and comparing the

structure of the various polyomaviruses support the finding that differences in the sequences of the outer loops of VP1 result in differences in receptor interactions and requirements (82,98-100).

VP1 loops also function as the major antigenic determinants for polyomaviruses. Their importance in this capacity is highlighted by the fact that four distinct antigenic BKPyV subtypes have been identified based on VP1 sequence variations between amino acid 61 and 83 (1,32,56,62). The VP1 binding region of all BKPyV subtypes interact with receptor(s) that contain an α 2-3 linked sialic acid (32,56). It is still not fully determined whether the serological differences between subtypes are due to variations in receptor usage (47,152).

VP2 and VP3 are the minor capsid proteins. They are not exposed and do not play a role in virus-receptor interactions (128). A single copy of VP2 or VP3 interacts with five copies of VP1, through hydrophobic interactions to form a viral pentamer (34). When VP1 and VP2 or VP3 are co-expressed without the viral genome they can assemble into virus like particles (VLPs) that resemble a complete virion. VLP and VP1 pentamer assembly can, however, occur independent of VP2 or VP3 (34,126,128,146). In addition to their role in capsid formation, VP2 and VP3 are believed to be necessary for proper encapsidation of the newly synthesized viral genome as both VP2 and VP3 share a DNA binding domain in addition to a VP1 interacting domain (34,64).

BKPyV LIFECYCLE

The polyomavirus lifecycle is divided into two stages, the early and the late stage. The early stage is defined by virus binding to host cell receptor, endocytosis, trafficking to the nucleus, uncoating of the DNA and expression of the early genes (Figure 4). The late stage consists of viral DNA replication, expression of the late genes, virus assembly and release (34).

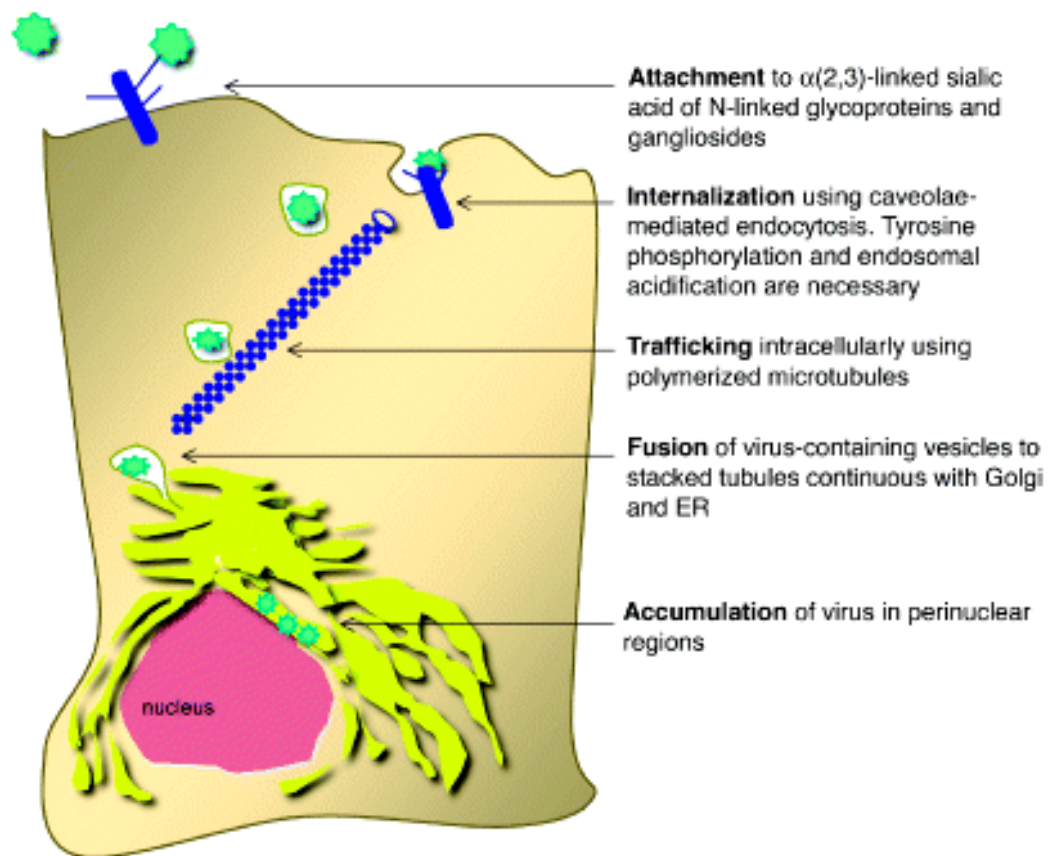


Figure 4: Schematic of BKPyV lifecycle. Printed image from; Transplant Infectious Disease, Dugan, Eash, Atwood, *Update on BK virus entry and intracellular trafficking*, 62-67, Copyright 2006 with permission from John Wiley and Sons.

Attachment

The initial step in the establishment of polyomavirus infection is interaction of the virus with receptors present on the cell surface. Receptor interaction is an important means for the process of engagement and internalization. Receptors enrich viruses on target cells, provide accessibility to co-receptors, and support efficient viral release (46). As a critical step in the viral lifecycle this interaction can define tissue tropism and contribute to disease pathogenesis if the interaction leads to productive infection. The ongoing characterization of polyomaviruses and their receptor usage has shown that the expression and function of viral receptors contribute to the restricted host range and tissue tropism. Characterization of virus attachment mechanism and the subsequent signaling effect is thus an important step in understanding BKPyV infection and disease.

BKPyV, as previously mentioned, interacts with host cells via the capsid protein VP1. A proteinaceous receptor for BKPyV has yet to be identified. It is possible that BKPyV engages a proteinaceous receptor as the polyomaviruses JCPyV, SV40 and MPyV have been demonstrated to utilize a proteinaceous receptor for entry. JCPyV used the serotonergic receptor 5HT_{2A}R, SV40 uses the Major Histocompatibility Complex class I protein (MHC I) and MPyV uses the Integrin $\alpha 4\beta 1$ (7,10,12,36). Though a proteinaceous receptor has not been identified, early studies have shown that BKPyV requires an $\alpha(2-3)$ linked sialic acid on a N-linked glycoprotein (30,31). Subsequent work identified two $\alpha(2-8)$ linked sialic acid containing glycosphingolipids, gangliosides GD1b and GT1b as receptors for BKPyV (31,81). How BKPyV engages its ganglioside receptors and the effects of this engagement are still not fully defined.

In studies characterizing BKPyV receptor(s), sialic acid was presented as a common receptor component (31,81). It is not surprising that sialylated receptors play a role in BKPyV infection as sialic acids have been shown to influence attachment and entry of both DNA viruses, including other polyomaviruses, and RNA viruses (149). Sialic acids decorate the surfaces of vertebrate cells, mediate cellular interactions with the environment, and regulate the affinity of receptors through their negative charge and hydrophilicity (158,161). They are highly expressed in the glomerular basement membrane which, likely plays a role in defining tissue tropism for BKPyV (158). Sialic acid, also known as neuraminic acid, is a nine carbon acidic sugar typically found on terminating branches of N-glycans, O-glycans and glycosphingolipids (Figure 5 and 6) (158,161). The diversity of sialic acid is determined by substitutions of the hydroxyl groups on carbon position R4, R5, R7, R8 and R9 (Figure 5A) (161). Substitution at carbon position 5 with an N-Acetyl group gives rise to N-Acetyl-neuraminic acid (Neu5Ac), which is the most common linkage in the sialic acid family and the predominant sialic acid type in humans (Figure 5B) (156,157,161). While the predominant sialic acid in humans is Neu5Ac, simians express mostly N-glycolyl-neuraminic acid (NeuNGc), which humans no longer naturally express (11,91,156,159). In NeuNGc, the N-Acetyl group at R5 is replaced by an N-glycolyl group (Figure 5). The differences in the species specific expression of these two types of sialic acids and additional sialic acid modifications has implications for pathogen specific interactions, variations in resistance and susceptibility to infection (11,52,71,159,158).

Additional sialic acid diversity arises from the various glycosidic linkages formed between the second carbon of sialic acid and other sialic acids or carbohydrates. The

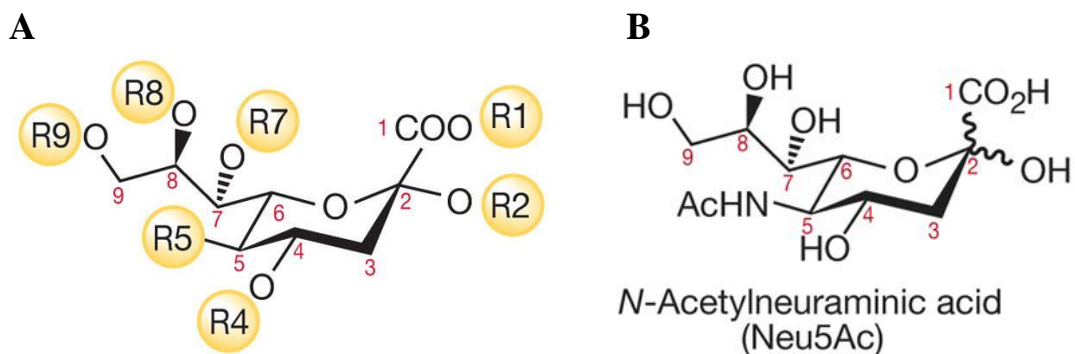


Figure 5: Structure and Diversity of Sialic Acid. (A) The 9-carbon backbone common to all sialic acids is shown in chair conformation with the carbon positions at R1, R2, R4, R5, R7, R8 and R9, which can be modified to create diversity, highlighted. (B) Substitution of hydrogen on carbon position 5 (R5) with an N-acetyl group gives rise to N-Acetyl-neuraminic acid. Modified printed image from; Essentials of Glycobiology, Varki, Schauer, *Sialic Acids, Ch 14*, Copyright 2009 with permission The Consortium of Glycobiology Editors, La Jolla, California.

most common alpha linkages are alpha 2 linkages to carbon position 3 and 6 of galactose (gal) and an alpha 2 linkage to carbon 6 of N-Acetylgalactosamine (GalNAc) (Figure 5) (161). To further add to this, polysialylation of higher order glycosphingolipids commonly occurs via an alpha 2 linkage to carbon position 8 of another sialic acid (161). Linkages and modifications made to sugars and sialic acids show tissue and cell specific expression and are determined by native sialic acid and carbohydrate specific sialyltransferases and glycosyltransferases (161). These unique features help to define species and tissue tropism for many pathogens. For example, influenza pathogenesis is defined in part by sialic acid linkages, and in recent years there has been growing concern that mutations in avian influenza, which naturally uses $\alpha(2-3)$ linked sialic acid in bird intestinal epithelium, could switch allowing it to use the $\alpha(2-6)$ -linked sialic, which is

highly expressed in the airway epithelium of humans. This could result in a human pandemic (13,158).

Sialic acid modification of glycosphingolipids produces a unique subfamily of glycosphingolipids known as gangliosides (Figure 6) (96,160). Gangliosides are found localized to lipid rafts which are enriched with sphingolipids and cholesterol, are dynamin dependent and clathrin independent (Figure 7) (116). Because of the presence of varying numbers of sialic acid molecules, gangliosides poses a relatively strong electronegative charge (Figure 6) (96). Gangliosides are synthesized in the Golgi and the ER after which a majority is transported to the cell membrane. They are oriented in the plasma membrane such that the ceramide is inserted into the lipid bilayer and the oligosaccharide backbone faces the extracellular space (96,160). Gangliosides have been characterized as receptors or co-receptors that mediate the attachment and entry of microbes including viruses and bacteria (86,108,154). They also mediate cell-cell interactions, modulate signal transduction pathways and can define the internalization pathway into the cell (96,140,149). Gangliosides are widely expressed in mammalian tissue with the highest amount found in the brain and the second largest amount found in the kidney (58). Gangliosides are found in cell types that are susceptible to BKPyV infection such as kidney and tonsillar cells (45,58,81,136). Characterization of the native gangliosides in adult kidney shows an abundance of many polysialylated gangliosides including gangliosides GD1b and GT1b (Figure 6). These gangliosides are differentially expressed in sites of BKPyV infection such as the cortical tubular, medullary and glomerular tissue (58).

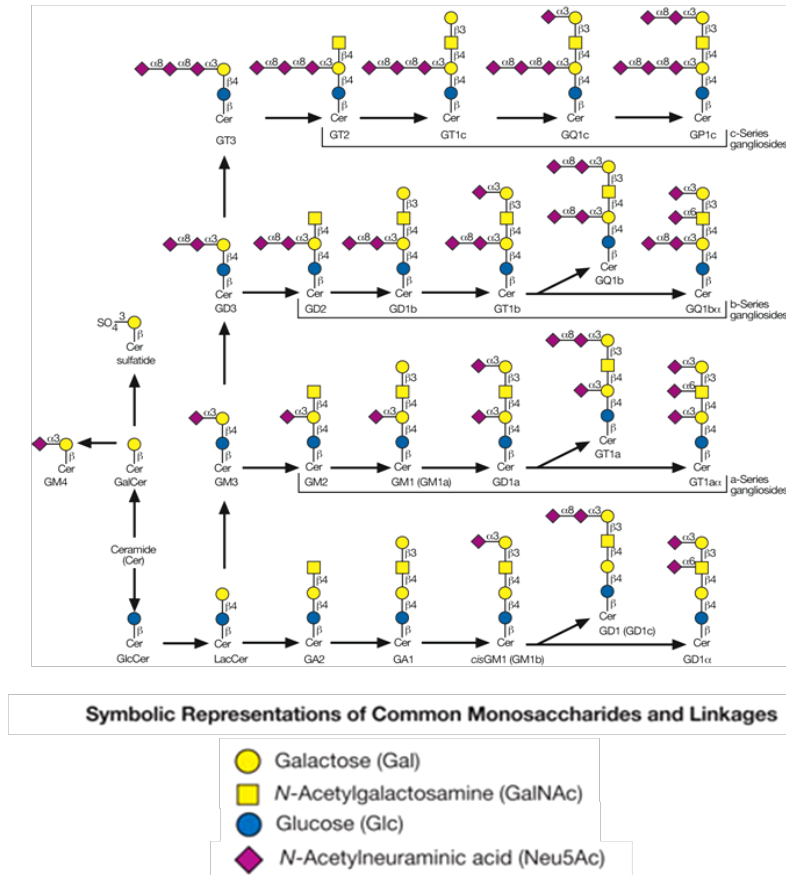


Figure 6: Biosynthetic pathway for glycosphingolipids. Modified printed image from; Essentials of Glycobiology, Varki, Schauer, *Glycosphingolipids, Ch 10*, Copyright 2009 with permission from The Consortium of Glycobiology Editors, La Jolla, California.

A number of polyomaviruses other than BKPyV use gangliosides as receptors. These includes MPyV, which uses terminal $\alpha(2-3)$ -linked sialic acid on GD1a and GT1b; SV40 which uses GM1, and MCPyV which uses GT1b (37,149,154). By thin layer chromatography (TLC) JCPyV VLPs were shown in a previous study to bind to gangliosides GM3, GD2, GD3, GD1b, GT1b, GQ1b and GD1a; Additionally, ganglioside GT1b was also shown to inhibit JCPyV infection (74). A recent study to characterize the mechanism of JCPyV attachment to cells however found that JCPyV binds specifically to

a linear sialylated pentasaccharide (LSTc) found on glycoproteins and glycolipids but did not show binding to GT1b (99). In this study JCPyV binding to an oligosaccharide receptor was evaluated by examining purified JCPyV pentamer binding to glycan arrays containing carbohydrates found on N- and O-linked glycoproteins and glycolipids such as GT1b (99). It is possible that the discrepancy seen between these two studies could result from differences in the interaction of virus and pentamers with receptor components and the sensitivity of the assay used to evaluate binding.

Signaling and Entry

Following engagement of cellular receptors, BKPyV must efficiently enter cells and traffic to the nucleus for successful infection. Effective virus-receptor interactions induce the activation of intracellular signaling pathways that promote entry and trafficking. BKPyV has been shown to enter cells via caveolae-mediated endocytosis (Figure 6) (35,89). Entry into cells is relatively slow with a majority of the virus entering within four hours post binding (35,89). Caveolae are 50-100nm flask shaped invaginations of the plasma membrane (Figure 7) (115,121,123). They are thought to be specialized forms of lipid rafts characterized by the presence of the caveolae scaffolding protein caveolin-1 (Cav-1) (Figure 7) (121,123). Caveolae domains serve as platforms for the aggregation of proteins, a majority of which are signal transducing molecules (112,123). The compartmentalization of signaling molecules in caveolae domains is thought to create a micro-environment where signals are concentrated and modified by local kinases and phosphatases in a controlled manner producing an efficient downstream intra-cellular signal (140). Signaling molecules can associate with lipid rafts via three modes: they can be constitutively present, induced to translocate from the membrane to

lipid rafts or induced to translocate from the cytosol to lipid rafts by an agonist (67). Signaling molecules associated with lipid rafts or caveolae domains include: receptor tyrosine kinases such as the Epidermal Growth Factor Receptor (EGFR), non-receptor tyrosine kinases such as the SRC family kinases and non receptor serine/threonine kinases such as PKC (35,123). In addition to associating with caveolae domains, a number of signaling molecules have been shown to directly interact with Cav-1 (67,123).

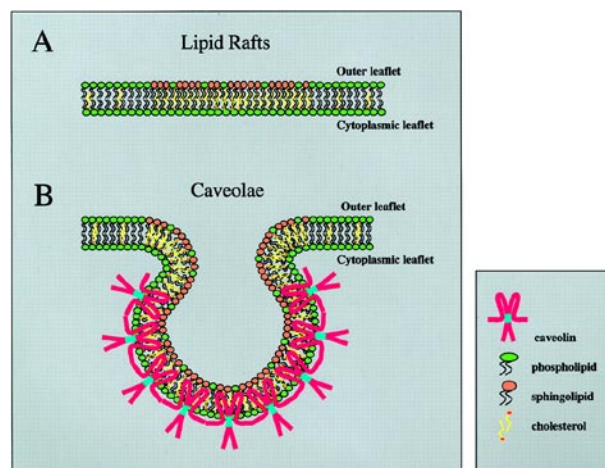


Figure 7: Organization of lipid rafts and caveolae domains. (A) Lipid rafts are enriched with cholesterol (yellow) and exoplasmic oriented sphingolipids (orange). (B) Caveolae domains form upon integration of Caveolin-1 protein (red), which interacts with cholesterol and sphingolipids causing small flask shaped invaginations. Image from; Pharmacological Reviews, Razani, Woodman, Lisanti, *Caveolae: From Cell Biology to Animal Physiology*, 431-467, Copyright 2002 with permission from The American Society for Pharmacology and Experimental Therapeutics.

Cav-1 has been shown to modulate the activity of various signaling molecules in caveolae domains by directly interacting with cholesterol and sphingolipids, and sphingolipid derivatives creating a scaffolding for the signaling functions (Figure 7) (40,93,123). A number of glycosphingolipids have been characterized for mediating signal transduction through lipid rafts and caveolae (67-69,75). These glycosphingolipids,

whether ligand mediated or as a result of exogenous ganglioside addition, can directly mediate signal transduction, or cause the association of protein kinases within lipid rafts. This can lead to auto-phosphorylation or trans-phosphorylation of kinases and their substrates facilitating internalization and trafficking (67). Common signal transduction events mediated by glycosphingolipids include: calcium flux, activation of Src family kinases and activation of MAP kinases (67).

Glycosphingolipids such as gangliosides are considered determinants of caveolae-mediated endocytosis (114,115,120,121,123,148). SV40 and Cholera Toxin (CTX) use the ganglioside GM1 to enter cells via caveolae-mediated endocytosis (5,14,154). The endocytosis of SV40 and CTX has been extensively studied and serve as models for gangliosides mediated signaling in BKPyV uptake. CTX and antibody mediated cross-linking studies demonstrate that binding to GM1 causes clustering of these glycosphingolipids in lipid domains resulting in unique signaling events that cannot be mimicked by a non-specific receptor (67,168). In addition to clustering, engagement of gangliosides receptors at the plasma membrane, or clustering of gangliosides independent of a ligand is shown to selectively stimulate caveolae-mediated endocytosis (135). This occurs because glycosphingolipids directly influence membrane invagination of the plasma membrane and regulates recycling of caveolae vesicles back to the plasma membrane (11,108,114,149). This process has been shown to be PKC and SRC dependent (135).

Due to the similarities between their receptor requirements and modes of entry it is hypothesized that BKPyV engagement of its ganglioside receptors induces signals similar to SV40 engagement of GM1. A comparative study of the kinome for SV40 and

Vesicular stomatitis virus (VSV), which enters cells by clathrin-mediated endocytosis, revealed that the signaling profile for caveolae and clathrin mediated uptake is highly segregated and specialized (112). Of the 590 human kinases screened, 80 kinases were shown to specifically regulate caveolae mediated entry of SV40 (112). Additional work has also shown that SV40 activates primary response genes by inducing the activities of tyrosine kinases (18). BKPyV also requires tyrosine kinases as treatment with the tyrosine kinase inhibitor Genistein was demonstrated to significantly reduce infection (18,35). SV40 induces an ERK/MAP kinase independent signaling pathway which may be dependent on PKC (18). Likewise, BKPyV does not directly induce the MAP kinase pathway upon binding (132). Additionally, a number of studies have demonstrated that the BKPyV gangliosides receptors GD1b and GT1b, and other members of the b-series family of gangliosides (Figure 6), modulate PKC activity suggesting that BKPyV signaling pathway may also include PKC (67-69,75).

Trafficking to the ER

Though little is known about the signaling events leading to BKPyV ganglioside-mediated caveolae uptake, more progress has been made in understanding the trafficking of BKPyV from the plasma membrane to the nucleus. Once BKPyV is internalized into caveolae vesicles, it is shown to localize soon after entry to a low pH compartment, likely an endosomal/lysosomal compartment, where the capsid is thought to undergo initial conformational changes to support release of the viral genome into the nucleus (Figure 8) (33,35,61). From this low pH compartment BKPyV was thought to traffic to caveosomes (Figure 8) (29,61,89). Caveosomes were identified with SV40 as immobile, cav-1 positive, pH neutral endosomes that lack markers of clathrin coated pits and early

endosomes (113). A recent study, completed by the researchers that initially proposed the caveosome, questions the existence of these structures (51,109). The study found that what was once thought to be unique structures may actually be late endosomes decorated with un-degraded Cav-1(51).

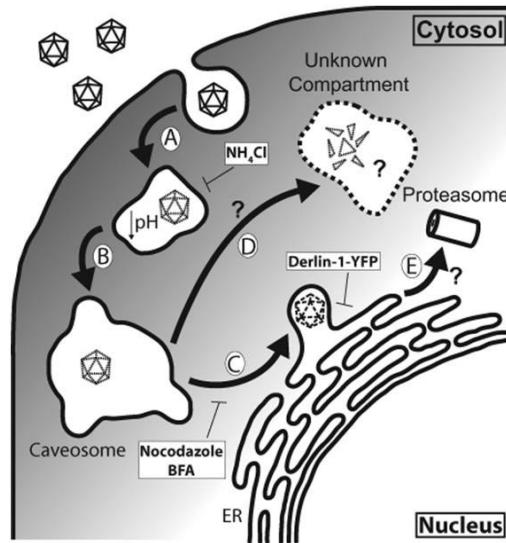


Figure 8: Proposed model of BKPyV early entry. BKPyV enters cells via caveolae-mediated endocytosis into a low pH compartment. BKPyV is then trafficked via microtubules to the ER where it interacts with Derlin-1, which mediates escape to the cytosol prior to movement to the nucleus. Printed image from; Journal of Virology, Jiang, Abend, Tsai, Imperiale, *Early Events during BKV Virus Entry and Disassembly*, 1350-1358. Copyright 2009 with permission from American Society of Microbiology.

Caveolae mediated endocytosis has been shown to retrograde traffic cargo via the Golgi to the Endoplasmic Reticulum (ER) or bypass the Golgi and go directly to the ER (76). Studies have shown that upon entry, BKPyV co-localizes with CTX which traffics to the Golgi (35,102). Additionally, examination of PVN tissue in a recent study notes aggregates of BKPyV in close proximity with the Golgi complex also suggesting that BKPyV may traffic to the Golgi (29). However, studies in cell culture examining BKPyV

co-localization with the Golgi indicate that BKPyV bypasses or transiently interacts with the Golgi (90). It is still not conclusively known whether BKPyV traffics to the Golgi.

BKPyV traffics via microtubules to the ER where the capsid is further destabilized (33,35,61,81,89). Trafficking of BKPyV to the ER takes approximately 8-12 hours post absorption (33,61). BKPyV trafficking mimics the pathway necessary for ganglioside turnover as ganglioside uptake and trafficking to the ER requires a low pH compartment to facilitate recycling from the plasma membrane to the ER (35,61,81,150). Gangliosides traffic to the ER. However it is not known whether BKPyV remains associated with its ganglioside receptors as it traffics to the ER. It is likely that BKPyV does remain associated with its ganglioside receptors as a recent study looking at MPyV trafficking to the ER reports that lipid binding sites for MPyV are present in the ER and that MPyV undergoes ganglioside specific sorting from the low pH endolysosome to the ER (120,154).

Once in the ER, the BKPyV capsid is rearranged (61). In a recent study to determine when and where capsid rearrangement occurs, it was observed that 8-12 hours post infection there is a reduction in the disulfide bonds that crosslink the pentamers of VP1 indicating capsid rearrangement (61). This reduction in disulfide bonds occurs during the time frame of trafficking to the ER and is believed to be facilitated by oxidoreductases present in the ER (61,89). In the ER additional host factors interact with BKPyV and are thought to assist in mediating ER escape. Like SV40, BKPyV associates with Derlin-1 in the ER (61,105,128,129). Derlin-1 is a member of the ER-associated degradation (ERAD) pathway. It is known to target misfolded proteins from the ER to the cytosol and was previously shown to assist in SV40 escape from the ER (61,80,128).

Derlin-1 may also directly participate in transporting BKPyV from the ER to the cytosol (61,128). In addition to Derlin-1, VP2 or VP3 may also aid in the movement of BKPyV to the cytosol as both proteins have been shown to associate with and destabilize the ER membrane for SV40 and MPyV (19,20,25,128).

Nuclear entry and egress

The process of binding, endocytosis and trafficking leads to the ultimate outcome of genome release into the nucleus for replication. However, nuclear targeting of BKPyV, capsid assembly, and steps that mediate egress are poorly understood. There are questions as to whether BKPyV fully uncoats in the nucleus or in the perinuclear space and if the BKPyV genome is deposited into the nucleus alone or with the viral capsid. Since BKPyV and SV40 share such similarities in sequence homology, entry requirements, and trafficking, it is thought that targeting of the BKPyV genome may occur similar to SV40. It is hypothesized that once SV40 escapes the ER to the cytosol, the low calcium environment supports trafficking of the viral genome to the nucleus as the low calcium environment may compromise pentamer stability (61,129). Additionally, the targeting of the SV40 genome into the nucleus is shown to require VP3, which may direct entry through the nuclear pore complex (15,97).

Once inside the nucleus BKPyV early gene transcription is initiated resulting in the expression of the early genes LT-Ag and small T-Ag and initiation of DNA synthesis (34,56,146). Following DNA synthesis late gene expression is initiated resulting in the production of the structural proteins VP1, VP2 and VP3 and the regulatory protein agnoprotein (1,34) Translation of the early and late gene transcripts occurs in the cytoplasm after which the protein products translocate to the nucleus (34,138).

Translocation of the structural proteins results in capsid formation and packaging of the viral DNA with histones H2A, H2B, H3 and H4, which form a mini-chromosome structure (34,85). Following assembly of the complete virus particle, the progeny is released by lytic burst (34).

SPECIFIC AIMS

BKPyV is a human polyomavirus that infects a large percentage of the population without normally causing disease. However, due to improved immunosuppressive therapy and an increase in the number of kidney transplants, BKPyV, which establishes a latent infection in the kidney, can be reactivated to cause polyomavirus induced nephropathy resulting in loss of the transplanted kidney. Understanding how BKPyV interacts with its receptors is an important aspect of understanding how BKPyV reactivation leads to disease progression.

The identification and characterization of viral receptors is an area of central importance as virus-receptor interactions can define cell, tissue and host tropism and determine the signaling functions that promote successful infection. BKPyV binds to the gangliosides GD1b and GT1b which are sialylated glycosphingolipids. Previous studies have characterized the sialic acid linkages that are necessary for BKPyV infection, and defined to some extent the amino acid residues on VP1 that are critical for engagement of sialic acid. A number of polyomaviruses also use ganglioside receptors for infection. Included in this group is the prototypical polyomavirus SV40 which uses ganglioside GM1 as a receptor. BKPyV and SV40 share significant sequence homology in their VP1 region. The characterization of the SV40 VP1 binding region with ganglioside GM1 provides a means for comparison and further characterization of the BKPyV binding to not just sialic acid but the additional carbohydrate components of its ganglioside receptors.

The main objective of this dissertation is to characterize BKPyV binding to ganglioside receptors and investigate the function of ganglioside mediated BKPyV

induced signaling events. The first aim of this dissertation is to determine the binding epitope for BKPyV and define the structural basis of binding specificity. In Chapter two we hypothesized that the disialic acid motif is the binding epitope for BKPyV and that the second, internal, sialic acid of the disialic acid motif defines receptor specificity. Additionally we believe that the additional carbohydrate moiety on GD1b and GT1b may influence the interaction with BKPyV. The second aim of this dissertation is to investigate the role of ganglioside induced signaling in BKPyV uptake. In Chapter 3 we hypothesized that PKC regulates ganglioside mediated BKPyV caveolae entry.

LITERATURE CITED

1. **Ahsan, N., K. Shah.** 2002. Polyomaviruses: An Overview. *Graft* **5**: 10.
2. **Ali, N., M.U. Shaikh, S. Hasan.** 2011. BK Virus Associated Late Onset Haemorrhagic Cystitis After Allogeneic Peripheral Blood Stem Cell Transplant. *Indian journal of hematology & blood transfusion : an official journal of Indian Society of Hematology and Blood Transfusion* **27**: 177-9.
3. **Ali, S.H., A. Chandraker, J.A. DeCaprio.** 2007. Inhibition of Simian virus 40 large T antigen helicase activity by fluoroquinolones. *Antiviral therapy* **12**: 1-6.
4. **Allander, T., K. Andreasson, S. Gupta, A. Bjerkner, G. Bogdanovic, M.A. Persson, T. Dalianis, T. Ramqvist, B. Andersson.** 2007. Identification of a third human polyomavirus. *J Virol* **81**: 4130-6.
5. **Anderson, H.A., Y. Chen, L.C. Norkin.** 1996. Bound simian virus 40 translocates to caveolin-enriched membrane domains, and its entry is inhibited by drugs that selectively disrupt caveolae. *Molecular biology of the cell* **7**: 1825-34.
6. **Andrei, G., R. Snoeck, M. Vandeputte, E. De Clercq.** 1997. Activities of various compounds against murine and primate polyomaviruses. *Antimicrobial agents and chemotherapy* **41**: 587-93.
7. **Atwood, W.J., L.C. Norkin.** 1989. Class I major histocompatibility proteins as cell surface receptors for simian virus 40. *J Virol* **63**: 4474-7.
8. **Bedi, A., C.B. Miller, J.L. Hanson, S. Goodman, R.F. Ambinder, P. Charache, R.R. Arthur, R.J. Jones.** 1995. Association of BK virus with failure of prophylaxis against hemorrhagic cystitis following bone marrow transplantation. *J Clin Oncol* **13**: 1103-9.
9. **Boldorini, R., S. Allegrini, U. Miglio, A. Paganotti, N. Cocca, M. Zaffaroni, F. Riboni, G. Monga, R. Viscidi.** 2011. Serological evidence of vertical transmission of JC and BK polyomaviruses in humans. *J Gen Virol* **92**: 1044-50.

10. **Breau, W.C., W.J. Atwood, L.C. Norkin.** 1992. Class I major histocompatibility proteins are an essential component of the simian virus 40 receptor. *J Virol* **66**: 2037-45.
11. **Campanero-Rhodes, M.A., A. Smith, W. Chai, S. Sonnino, L. Mauri, R.A. Childs, Y. Zhang, H. Ewers, A. Helenius, A. Imberty, T. Feizi.** 2007. N-glycolyl GM1 ganglioside as a receptor for simian virus 40. *J Virol* **81**: 12846-58.
12. **Caruso, M., L. Belloni, O. Sthandier, P. Amati, M.I. Garcia.** 2003. Alpha4beta1 integrin acts as a cell receptor for murine polyomavirus at the postattachment level. *J Virol* **77**: 3913-21.
13. **Childs, R.A., A.S. Palma, S. Wharton, T. Matrosovich, Y. Liu, W. Chai, M.A. Campanero-Rhodes, Y. Zhang, M. Eickmann, M. Kiso, A. Hay, M. Matrosovich, T. Feizi.** 2009. Receptor-binding specificity of pandemic influenza A (H1N1) 2009 virus determined by carbohydrate microarray. *Nat Biotechnol* **27**: 797-9.
14. **Chinnapen, D.J.F., H. Chinnapen, D. Saslowsky, W.I. Lencer.** 2007. Rafting with cholera toxin: endocytosis and trafficking from plasma membrane to ER. *Fems Microbiol Lett* **266**: 129-37.
15. **Clever, J., M. Yamada, H. Kasamatsu.** 1991. Import of simian virus 40 virions through nuclear pore complexes. *Proceedings of the National Academy of Sciences of the United States of America* **88**: 7333-7.
16. **Comar, M., P. D'Agaro, M. Andolina, N. Maximova, F. Martini, M. Tognon, C. Campello.** 2004. Hemorrhagic cystitis in children undergoing bone marrow transplantation: a putative role for simian virus 40. *Transplantation* **78**: 544-8.
17. **Comar, M., N. Zanotta, M. Bovenzi, C. Campello.** 2010. JCV/BKV and SV40 viral load in lymphoid tissues of young immunocompetent children from an area of north-east Italy. *J Med Virol* **82**: 1236-40.
18. **Dangoria, N.S., W.C. Breau, H.A. Anderson, D.M. Cishek, L.C. Norkin.** 1996. Extracellular simian virus 40 induces an ERK/MAP kinase-independent signalling pathway that activates primary response genes and promotes virus entry. *J Gen Virol* **77 (Pt 9)**: 2173-82.

19. **Daniels, R., N.M. Rusan, P. Wadsworth, D.N. Hebert.** 2006. SV40 VP2 and VP3 insertion into ER membranes is controlled by the capsid protein VP1: implications for DNA translocation out of the ER. *Molecular cell* **24**: 955-66.
20. **Daniels, R., N.M. Rusan, A.K. Wilbuer, L.C. Norkin, P. Wadsworth, D.N. Hebert.** 2006. Simian virus 40 late proteins possess lytic properties that render them capable of permeabilizing cellular membranes. *J Virol* **80**: 6575-87.
21. **Darbinyan, A., N. Darbinian, M. Safak, S. Radhakrishnan, A. Giordano, K. Khalili.** 2002. Evidence for dysregulation of cell cycle by human polyomavirus, JCV, late auxiliary protein. *Oncogene* **21**: 5574-81.
22. **De Clercq, E.** 2003. Clinical potential of the acyclic nucleoside phosphonates cidofovir, adefovir, and tenofovir in treatment of DNA virus and retrovirus infections. *Clinical microbiology reviews* **16**: 569-96.
23. **DeCaprio, J.A., J.W. Ludlow, J. Figge, J.Y. Shew, C.M. Huang, W.H. Lee, E. Marsilio, E. Paucha, D.M. Livingston.** 1988. SV40 large tumor antigen forms a specific complex with the product of the retinoblastoma susceptibility gene. *Cell* **54**: 275-83.
24. **Delbue, S., M. Comar, P. Ferrante.** 2012. Review on the relationship between human polyomaviruses-associated tumors and host immune system. *Clin Dev Immunol* **2012**: 542092.
25. **Delos, S.E., L. Montross, R.B. Moreland, R.L. Garcea.** 1993. Expression of the polyomavirus VP2 and VP3 proteins in insect cells: coexpression with the major capsid protein VP1 alters VP2/VP3 subcellular localization. *Virology* **194**: 393-8.
26. **Deyerle, K.L., J.A. Cassill, S. Subramani.** 1987. Analysis of the early regulatory region of the human papovavirus BK. *Virology* **158**: 181-93.
27. **Deyerle, K.L., S. Subramani.** 1988. Linker scan analysis of the early regulatory region of human papovavirus BK. *J Virol* **62**: 3378-87.
28. **Drachenberg, C.B., H.H. Hirsch, E. Ramos, J.C. Papadimitriou.** 2005. Polyomavirus disease in renal transplantation: review of pathological findings and diagnostic methods. *Hum Pathol* **36**: 1245-55.

29. **Drachenberg, C.B., J.C. Papadimitriou, R. Wali, C.L. Cubitt, E. Ramos.** 2003. BK polyoma virus allograft nephropathy: ultrastructural features from viral cell entry to lysis. *Am J Transplant* **3**: 1383-92.
30. **Dugan, A.S., S. Eash, W.J. Atwood.** 2005. An N-linked glycoprotein with alpha(2,3)-linked sialic acid is a receptor for BK virus. *J Virol* **79**: 14442-5.
31. **Dugan, A.S., S. Eash, W.J. Atwood.** 2006. Update on BK virus entry and intracellular trafficking. *Transpl Infect Dis* **8**: 62-7.
32. **Dugan, A.S., M.L. Gasparovic, N. Tsomaia, D.F. Mierke, B.A. O'Hara, K. Manley, W.J. Atwood.** 2007. Identification of amino acid residues in BK virus VP1 that are critical for viability and growth. *J Virol* **81**: 11798-808.
33. **Eash, S., W.J. Atwood.** 2005. Involvement of cytoskeletal components in BK virus infectious entry. *J Virol* **79**: 11734-41.
34. **Eash, S., K. Manley, M. Gasparovic, W. Querbes, W.J. Atwood.** 2006. The human polyomaviruses. *Cellular and molecular life sciences : CMLS* **63**: 865-76.
35. **Eash, S., W. Querbes, W.J. Atwood.** 2004. Infection of vero cells by BK virus is dependent on caveolae. *J Virol* **78**: 11583-90.
36. **Elphick, G.F., W. Querbes, J.A. Jordan, G.V. Gee, S. Eash, K. Manley, A. Dugan, M. Stanifer, A. Bhatnagar, W.K. Kroeze, B.L. Roth, W.J. Atwood.** 2004. The human polyomavirus, JCV, uses serotonin receptors to infect cells. *Science* **306**: 1380-3.
37. **Erickson, K.D., R.L. Garcea, B. Tsai.** 2009. Ganglioside GT1b is a putative host cell receptor for the Merkel cell polyomavirus. *J Virol* **83**: 10275-9.
38. **Ewen, M.E., J.W. Ludlow, E. Marsilio, J.A. DeCaprio, R.C. Millikan, S.H. Cheng, E. Paucha, D.M. Livingston.** 1989. An N-terminal transformation-governing sequence of SV40 large T antigen contributes to the binding of both p110Rb and a second cellular protein, p120. *Cell* **58**: 257-67.
39. **Feng, H., M. Shuda, Y. Chang, P.S. Moore.** 2008. Clonal integration of a polyomavirus in human Merkel cell carcinoma. *Science* **319**: 1096-100.

40. **Fra, A.M., M. Masserini, P. Palestini, S. Sonnino, K. Simons.** 1995. A photo-reactive derivative of ganglioside GM1 specifically cross-links VIP21-caveolin on the cell surface. *Febs Lett* **375**: 11-4.
41. **Gabardi, S., S.S. Waikar, S. Martin, K. Roberts, J. Chen, L. Borgi, H. Sheashaa, C. Dyer, S.K. Malek, S.G. Tullius, N. Vadivel, M. Grafals, R. Abdi, N. Najafian, E. Milford, A. Chandraker.** 2010. Evaluation of fluoroquinolones for the prevention of BK viremia after renal transplantation. *Clinical journal of the American Society of Nephrology : CJASN* **5**: 1298-304.
42. **Gardner, S.D., A.M. Field, D.V. Coleman, B. Hulme.** 1971. New human papovavirus (B.K.) isolated from urine after renal transplantation. *Lancet* **1**: 1253-7.
43. **Gaynor, A.M., M.D. Nissen, D.M. Whiley, I.M. Mackay, S.B. Lambert, G. Wu, D.C. Brennan, G.A. Storch, T.P. Sloots, D. Wang.** 2007. Identification of a novel polyomavirus from patients with acute respiratory tract infections. *PLoS Pathog* **3**: e64.
44. **Gerits, N., U. Moens.** 2012. Agnoprotein of mammalian polyomaviruses. *Virology* **432**: 316-26.
45. **Goudsmit, J., P. Wertheim-van Dillen, A. van Strien, J. van der Noordaa.** 1982. The role of BK virus in acute respiratory tract disease and the presence of BKV DNA in tonsils. *J Med Virol* **10**: 91-9.
46. **Greber, U.F.** 2002. Signalling in viral entry. *Cellular and molecular life sciences : CMLS* **59**: 608-26.
47. **Hale, A.D., D. Bartkeviciute, A. Dargeviciute, L. Jin, W. Knowles, J. Staniulis, D.W. Brown, K. Sasnauskas.** 2002. Expression and antigenic characterization of the major capsid proteins of human polyomaviruses BK and JC in *Saccharomyces cerevisiae*. *Journal of virological methods* **104**: 93-8.
48. **Hara, K., Y. Oya, H. Kinoshita, F. Taguchi, Y. Yogo.** 1986. Sequence reiteration required for the efficient growth of BK virus. *J Gen Virol* **67 (Pt 11)**: 2555-9.

49. **Harris, K.F., J.B. Christensen, M.J. Imperiale.** 1996. BK virus large T antigen: interactions with the retinoblastoma family of tumor suppressor proteins and effects on cellular growth control. *J Virol* **70**: 2378-86.
50. **Harris, K.F., J.B. Christensen, E.H. Radany, M.J. Imperiale.** 1998. Novel mechanisms of E2F induction by BK virus large-T antigen: requirement of both the pRb-binding and the J domains. *Molecular and cellular biology* **18**: 1746-56.
51. **Hayer, A., M. Stoeber, D. Ritz, S. Engel, H.H. Meyer, A. Helenius.** 2010. Caveolin-1 is ubiquitinated and targeted to intraluminal vesicles in endolysosomes for degradation. *The Journal of cell biology* **191**: 615-29.
52. **Herrmann, M., C.W. von der Lieth, P. Stehling, W. Reutter, M. Pawlita.** 1997. Consequences of a subtle sialic acid modification on the murine polyomavirus receptor. *J Virol* **71**: 5922-31.
53. **Hirsch, H.H.** 2002. Polyomavirus BK nephropathy: a (re-)emerging complication in renal transplantation. *Am J Transplant* **2**: 25-30.
54. **Hirsch, H.H.** 2005. BK virus: opportunity makes a pathogen. *Clin Infect Dis* **41**: 354-60.
55. **Hirsch, H.H., C.B. Drachenberg, J. Steiger, E. Ramos.** 2006. Polyomavirus-associated nephropathy in renal transplantation: critical issues of screening and management. *Advances in experimental medicine and biology* **577**: 160-73.
56. **Hirsch, H.H., J. Steiger.** 2003. Polyomavirus BK. *Lancet Infect Dis* **3**: 611-23.
57. **Ho, S., N. Clipstone, L. Timmermann, J. Northrop, I. Graef, D. Fiorentino, J. Nourse, G.R. Crabtree.** 1996. The mechanism of action of cyclosporin A and FK506. *Clinical immunology and immunopathology* **80**: S40-5.
58. **Holthofer, H., J. Reivinen, A. Miettinen.** 1994. Nephron segment and cell-type specific expression of gangliosides in the developing and adult kidney. *Kidney international* **45**: 123-30.

59. **Howe, A.K., S. Gaillard, J.S. Bennett, K. Rundell.** 1998. Cell cycle progression in monkey cells expressing simian virus 40 small t antigen from adenovirus vectors. *J Virol* **72**: 9637-44.
60. **Imperiale, M.J.** 2001, The human polyomaviruses: an overview, In: Khalili, K., Stoner, G.L. (Eds.) *Human Polyomaviruses: Molecular and Clinical Perspectives*. Wiley-Liss, New York, pp. 53-71.
61. **Jiang, M., J.R. Abend, B. Tsai, M.J. Imperiale.** 2009. Early events during BK virus entry and disassembly. *J Virol* **83**: 1350-8.
62. **Jin, L., P.E. Gibson, J.C. Booth, J.P. Clewley.** 1993. Genomic typing of BK virus in clinical specimens by direct sequencing of polymerase chain reaction products. *J Med Virol* **41**: 11-7.
63. **Johannessen, M., M.R. Myhre, M. Dragset, C. Tummler, U. Moens.** 2008. Phosphorylation of human polyomavirus BK agnoprotein at Ser-11 is mediated by PKC and has an important regulative function. *Virology* **379**: 97-109.
64. **Johne, R., C.B. Buck, T. Allander, W.J. Atwood, R.L. Garcea, M.J. Imperiale, E.O. Major, T. Ramqvist, L.C. Norkin.** 2011. Taxonomical developments in the family Polyomaviridae. *Arch Virol* **156**: 1627-34.
65. **Jordan, J.A., K. Manley, A.S. Dugan, B.A. O'Hara, W.J. Atwood.** 2010. Transcriptional regulation of BK virus by nuclear factor of activated T cells. *J Virol* **84**: 1722-30.
66. **Josephson, M.A., D. Gillen, B. Javaid, P. Kadambi, S. Meehan, P. Foster, R. Harland, R.J. Thistlethwaite, M. Garfinkel, W. Atwood, J. Jordan, M. Sadhu, M.J. Millis, J. Williams.** 2006. Treatment of renal allograft polyoma BK virus infection with leflunomide. *Transplantation* **81**: 704-10.
67. **Kasahara, K., Y. Sanai.** 2000. Functional roles of glycosphingolipids in signal transduction via lipid rafts. *Glycoconj J* **17**: 153-62.
68. **Katoh, N.** 1995. Inhibition by gangliosides GM3, GD3 and GT1b of substrate phosphorylation by protein kinase C in bovine mammary gland and its reversal by phosphatidylserine. *Life sciences* **56**: 157-62.

69. **Katoh, N.** 1995. Inhibition by phospholipids, lysophospholipids and gangliosides of melittin-induced phosphorylation in bovine mammary gland. *Toxicology* **104**: 73-81.
70. **Kean, J.M., S. Rao, M. Wang, R.L. Garcea.** 2009. Seroepidemiology of human polyomaviruses. *PLoS Pathog* **5**: e1000363.
71. **Keppler, O.T., P. Stehling, M. Herrmann, H. Kayser, D. Grunow, W. Reutter, M. Pawlita.** 1995. Biosynthetic modulation of sialic acid-dependent virus-receptor interactions of two primate polyoma viruses. *J Biol Chem* **270**: 1308-14.
72. **Knowles, W.A.** 2006. Discovery and epidemiology of the human polyomaviruses BK virus (BKV) and JC virus (JCV). *Advances in experimental medicine and biology* **577**: 19-45.
73. **Knowles, W.A., P. Pipkin, N. Andrews, A. Vyse, P. Minor, D.W. Brown, E. Miller.** 2003. Population-based study of antibody to the human polyomaviruses BKV and JCV and the simian polyomavirus SV40. *J Med Virol* **71**: 115-23.
74. **Komagome, R., H. Sawa, T. Suzuki, Y. Suzuki, S. Tanaka, W.J. Atwood, K. Nagashima.** 2002. Oligosaccharides as receptors for JC virus. *J Virol* **76**: 12992-3000.
75. **Kreutter, D., J.Y. Kim, J.R. Goldenring, H. Rasmussen, C. Ukomadu, R.J. DeLorenzo, R.K. Yu.** 1987. Regulation of protein kinase C activity by gangliosides. *J Biol Chem* **262**: 1633-7.
76. **Le, P.U., I.R. Nabi.** 2003. Distinct caveolae-mediated endocytic pathways target the Golgi apparatus and the endoplasmic reticulum. *J Cell Sci* **116**: 1059-71.
77. **Leung, A.Y., M.T. Chan, K.Y. Yuen, V.C. Cheng, K.H. Chan, C.L. Wong, R. Liang, A.K. Lie, Y.L. Kwong.** 2005. Ciprofloxacin decreased polyoma BK virus load in patients who underwent allogeneic hematopoietic stem cell transplantation. *Clin Infect Dis* **40**: 528-37.
78. **Li, P.P., A. Naknishi, M.A. Tran, K. Ishizu, M. Kawano, M. Phillips, H. Handa, R.C. Liddington, H. Kasamatsu.** 2003. Importance of Vp1 calcium-

binding residues in assembly, cell entry, and nuclear entry of simian virus 40. *J Virol* **77**: 7527-38.

79. **Liddington, R.C., Y. Yan, J. Moulai, R. Sahli, T.L. Benjamin, S.C. Harrison.** 1991. Structure of simian virus 40 at 3.8-Å resolution. *Nature* **354**: 278-84.
80. **Lilley, B.N., H.L. Ploegh.** 2004. A membrane protein required for dislocation of misfolded proteins from the ER. *Nature* **429**: 834-40.
81. **Low, J.A., B. Magnuson, B. Tsai, M.J. Imperiale.** 2006. Identification of gangliosides GD1b and GT1b as receptors for BK virus. *J Virol* **80**: 1361-6.
82. **Magaldi, T.G., M.H. Buch, H. Murata, K.D. Erickson, U. Neu, R.L. Garcea, K. Peden, T. Stehle, D. DiMaio.** 2012. Mutations in the GM1 binding site of simian virus 40 VP1 alter receptor usage and cell tropism. *J Virol* **86**: 7028-42.
83. **Mahon, C., B. Liang, I. Tikhanovich, J.R. Abend, M.J. Imperiale, H.P. Nasheuer, W.R. Folk.** 2009. Restriction of human polyomavirus BK virus DNA replication in murine cells and extracts. *J Virol* **83**: 5708-17.
84. **Manna, S.K., B.B. Aggarwal.** 1999. Immunosuppressive leflunomide metabolite (A77 1726) blocks TNF-dependent nuclear factor-kappa B activation and gene expression. *Journal of immunology* **162**: 2095-102.
85. **Meneguzzi, G., P.F. Pignatti, G. Barbanti-Brodano, G. Milanesi.** 1978. Minichromosome from BK virus as a template for transcription *in vitro*. *Proceedings of the National Academy of Sciences of the United States of America* **75**: 1126-30.
86. **Merritt, E.A., S. Sarfaty, F. van den Akker, C. L'Hoir, J.A. Martial, W.G. Hol.** 1994. Crystal structure of cholera toxin B-pentamer bound to receptor GM1 pentasaccharide. *Protein Sci* **3**: 166-75.
87. **Moens, U., O.P. Rekvig.** 2001, Molecular biology of BK virus and clinical and basic aspects of BK virus renal infection, In: Khalili, K., Stoner, G.L. (Eds.) *Human Polyomaviruses: Molecular and Clinical Perspectives*. Wiley-Liss, New York, pp. 359-408.

88. **Moens, U., M. Van Ghelue.** 2005. Polymorphism in the genome of non-passaged human polyomavirus BK: implications for cell tropism and the pathological role of the virus. *Virology* **331**: 209-31.
89. **Moriyama, T., J.P. Marquez, T. Wakatsuki, A. Sorokin.** 2007. Caveolar endocytosis is critical for BK virus infection of human renal proximal tubular epithelial cells. *J Virol* **81**: 8552-62.
90. **Moriyama, T., A. Sorokin.** 2008. Intracellular trafficking pathway of BK Virus in human renal proximal tubular epithelial cells. *Virology* **371**: 336-49.
91. **Muchmore, E.A., S. Diaz, A. Varki.** 1998. A structural difference between the cell surfaces of humans and the great apes. *American Journal of Physical Anthropology* **107**: 187-98.
92. **Munoz, P., M. Fogeda, E. Bouza, E. Verde, J. Palomo, R. Banares, B.K.V.S. Group.** 2005. Prevalence of BK virus replication among recipients of solid organ transplants. *Clin Infect Dis* **41**: 1720-5.
93. **Murata, M., J. Peranen, R. Schreiner, F. Wieland, T.V. Kurzchalia, K. Simons.** 1995. VIP21/caveolin is a cholesterol-binding protein. *Proceedings of the National Academy of Sciences of the United States of America* **92**: 10339-43.
94. **Myhre, M.R., G.H. Olsen, R. Gosert, H.H. Hirsch, C.H. Rinaldo.** 2010. Clinical polyomavirus BK variants with agnogene deletion are non-functional but rescued by trans-complementation. *Virology* **398**: 12-20.
95. **Naesens, M., D.R. Kuypers, M. Sarwal.** 2009. Calcineurin inhibitor nephrotoxicity. *Clinical journal of the American Society of Nephrology : CJASN* **4**: 481-508.
96. **Nagai, Y., M. Iwamori.** 1995, Cellular biology of gangliosides, In: Rosenberg, A. (Ed.) *Biology of Sialic Acids*. Plenum Press, New York, pp. 197-242.
97. **Nakanishi, A., J. Clever, M. Yamada, P.P. Li, H. Kasamatsu.** 1996. Association with capsid proteins promotes nuclear targeting of simian virus 40 DNA. *Proceedings of the National Academy of Sciences of the United States of America* **93**: 96-100.

98. **Neu, U., H. Hengel, B.S. Blaum, R.M. Schowalter, D. Macejak, M. Gilbert, W.W. Wakarchuk, A. Imamura, H. Ando, M. Kiso, N. Arnberg, R.L. Garcea, T. Peters, C.B. Buck, T. Stehle.** 2012. Structures of Merkel cell polyomavirus VP1 complexes define a sialic acid binding site required for infection. *PLoS Pathog* **8**: e1002738.
99. **Neu, U., M.S. Maginnis, A.S. Palma, L.J. Stroh, C.D. Nelson, T. Feizi, W.J. Atwood, T. Stehle.** 2010. Structure-function analysis of the human JC polyomavirus establishes the LSTc pentasaccharide as a functional receptor motif. *Cell host & microbe* **8**: 309-19.
100. **Neu, U., J. Wang, D. Macejak, R.L. Garcea, T. Stehle.** 2011. Structures of the major capsid proteins of the human Karolinska Institutet and Washington University polyomaviruses. *Journal of Virology* **85**: 7384-92.
101. **Neu, U., K. Woellner, G. Gauglitz, T. Stehle.** 2008. Structural basis of GM1 ganglioside recognition by simian virus 40. *Proceedings of the National Academy of Sciences of the United States of America* **105**: 5219-24.
102. **Nichols, B.J., A.K. Kenworthy, R.S. Polishchuk, R. Lodge, T.H. Roberts, K. Hirschberg, R.D. Phair, J. Lippincott-Schwartz.** 2001. Rapid cycling of lipid raft markers between the cell surface and Golgi complex. *The Journal of cell biology* **153**: 529-41.
103. **Nickeleit, V., H.H. Hirsch, I.F. Binet, F. Gudat, O. Prince, P. Dalquen, G. Thiel, M.J. Mihatsch.** 1999. Polyomavirus infection of renal allograft recipients: from latent infection to manifest disease. *J Am Soc Nephrol* **10**: 1080-9.
104. **Nickeleit, V., H.K. Singh.** 2002, Polyomavirus Allograft Nephropathy: Clinical-Pathological Correlations, In: Madame Curie Bioscience Database [Internet]. Landes Bioscience (formerly, Eurekah Bioscience Database).
105. **Norkin, L.C., H.A. Anderson, S.A. Wolfrom, A. Oppenheim.** 2002. Caveolar endocytosis of simian virus 40 is followed by brefeldin A-sensitive transport to the endoplasmic reticulum, where the virus disassembles. *J Virol* **76**: 5156-66.
106. **Okada, Y., T. Suzuki, Y. Sunden, Y. Orba, S. Kose, N. Imamoto, H. Takahashi, S. Tanaka, W.W. Hall, K. Nagashima, H. Sawa.** 2005. Dissociation of heterochromatin protein 1 from lamin B receptor induced by

human polyomavirus agnoprotein: role in nuclear egress of viral particles. *EMBO Rep* **6**: 452-7.

107. **Padgett, B.L., D.L. Walker, G.M. ZuRhein, R.J. Eckroade, B.H. Dessel.** 1971. Cultivation of papova-like virus from human brain with progressive multifocal leucoencephalopathy. *Lancet* **1**: 1257-60.
108. **Pang, H., P.U. Le, I.R. Nabi.** 2004. Ganglioside GM1 levels are a determinant of the extent of caveolae/raft-dependent endocytosis of cholera toxin to the Golgi apparatus. *J Cell Sci* **117**: 1421-30.
109. **Parton, R.G., M.T. Howes.** 2010. Revisiting caveolin trafficking: the end of the caveosome. *The Journal of cell biology* **191**: 439-41.
110. **Pavlakakis, M., A. Haririan, D.K. Klassen.** 2006. BK virus infection after non-renal transplantation. *Advances in experimental medicine and biology* **577**: 185-9.
111. **Peden, K.W., A. Srinivasan, J.M. Farber, J.M. Pipas.** 1989. Mutants with changes within or near a hydrophobic region of simian virus 40 large tumor antigen are defective for binding cellular protein p53. *Virology* **168**: 13-21.
112. **Pelkmans, L., E. Fava, H. Grabner, M. Hannus, B. Habermann, E. Krausz, M. Zerial.** 2005. Genome-wide analysis of human kinases in clathrin- and caveolae/raft-mediated endocytosis. *Nature* **436**: 78-86.
113. **Pelkmans, L., J. Kartenbeck, A. Helenius.** 2001. Caveolar endocytosis of simian virus 40 reveals a new two-step vesicular-transport pathway to the ER. *Nature cell biology* **3**: 473-83.
114. **Pelkmans, L., M. Zerial.** 2005. Kinase-regulated quantal assemblies and kiss-and-run recycling of caveolae. *Nature* **436**: 128-33.
115. **Pietiainen, V.M., V. Marjomaki, J. Heino, T. Hyypia.** 2005. Viral entry, lipid rafts and caveosomes. *Annals of medicine* **37**: 394-403.
116. **Pike, L.J.** 2006. Rafts defined: a report on the Keystone Symposium on Lipid Rafts and Cell Function. *J Lipid Res* **47**: 1597-8.

117. **Portolani, M., P. Pietrosevoli, C. Cermelli, A. Mannini-Palenzona, M.P. Grossi, L. Paolini, G. Barbanti-Brodano.** 1988. Suppression of BK virus replication and cytopathic effect by inhibitors of prokaryotic DNA gyrase. *Antiviral research* **9**: 205-18.
118. **Prince, O., S. Savic, M. Dickenmann, J. Steiger, L. Bubendorf, M.J. Mihatsch.** 2009. Risk factors for polyoma virus nephropathy. *Nephrology, dialysis, transplantation : official publication of the European Dialysis and Transplant Association - European Renal Association* **24**: 1024-33.
119. **Puliyanda, D.P., N. Amet, A. Dhawan, L. Hilo, R.K. Radha, S. Bunnapradist, L. Czer, P. Martin, S. Jordan, M. Toyoda.** 2006. Isolated heart and liver transplant recipients are at low risk for polyomavirus BKV nephropathy. *Clinical transplantation* **20**: 289-94.
120. **Qian, M., D. Cai, K.J. Verhey, B. Tsai.** 2009. A lipid receptor sorts polyomavirus from the endolysosome to the endoplasmic reticulum to cause infection. *PLoS Pathog* **5**: e1000465.
121. **Quest, A.F., L. Leyton, M. Parraga.** 2004. Caveolins, caveolae, and lipid rafts in cellular transport, signaling, and disease. *Biochemistry and cell biology = Biochimie et biologie cellulaire* **82**: 129-44.
122. **Randhawa, P., A. Vats, R. Shapiro.** 2006. The pathobiology of polyomavirus infection in man. *Advances in experimental medicine and biology* **577**: 148-59.
123. **Razani, B., S.E. Woodman, M.P. Lisanti.** 2002. Caveolae: from cell biology to animal physiology. *Pharmacological reviews* **54**: 431-67.
124. **Replog, M.D., G.A. Storch, D.B. Clifford.** 2001. Bk virus: a clinical review. *Clin Infect Dis* **33**: 191-202.
125. **Safak, M., R. Barrucco, A. Darbinyan, Y. Okada, K. Nagashima, K. Khalili.** 2001. Interaction of JC virus agno protein with T antigen modulates transcription and replication of the viral genome in glial cells. *J Virol* **75**: 1476-86.
126. **Salunke, D.M., D.L. Caspar, R.L. Garcea.** 1986. Self-assembly of purified polyomavirus capsid protein VP1. *Cell* **46**: 895-904.

127. **Salunke, D.M., D.L. Caspar, R.L. Garcea.** 1989. Polymorphism in the assembly of polyomavirus capsid protein VP1. *Biophys J* **56**: 887-900.
128. **Sapp, M., P.M. Day.** 2009. Structure, attachment and entry of polyoma- and papillomaviruses. *Virology* **384**: 400-9.
129. **Schelhaas, M., J. Malmstrom, L. Pelkmans, J. Haugstetter, L. Ellgaard, K. Grunewald, A. Helenius.** 2007. Simian Virus 40 depends on ER protein folding and quality control factors for entry into host cells. *Cell* **131**: 516-29.
130. **Schowalter, R.M., D.V. Pastrana, K.A. Pumphrey, A.L. Moyer, C.B. Buck.** 2010. Merkel cell polyomavirus and two previously unknown polyomaviruses are chronically shed from human skin. *Cell host & microbe* **7**: 509-15.
131. **Scuda, N., J. Hofmann, S. Calvignac-Spencer, K. Ruprecht, P. Liman, J. Kuhn, H. Hengel, B. Ehlers.** 2011. A novel human polyomavirus closely related to the african green monkey-derived lymphotropic polyomavirus. *J Virol* **85**: 4586-90.
132. **Seamone, M.E., W. Wang, P. Acott, P.L. Beck, L.A. Tibbles, D.A. Muruve.** 2010. MAP kinase activation increases BK polyomavirus replication and facilitates viral propagation *in vitro*. *Journal of virological methods* **170**: 21-9.
133. **Shah, K.V.** 2000. Human polyomavirus BKV and renal disease. *Nephrology, dialysis, transplantation : official publication of the European Dialysis and Transplant Association - European Renal Association* **15**: 754-5.
134. **Sharma, B.N., R. Li, E. Bernhoff, T.J. Gutteberg, C.H. Rinaldo.** 2011. Fluoroquinolones inhibit human polyomavirus BK (BKV) replication in primary human kidney cells. *Antiviral research* **92**: 115-23.
135. **Sharma, D.K., J.C. Brown, A. Choudhury, T.E. Peterson, E. Holicky, D.L. Marks, R. Simari, R.G. Parton, R.E. Pagano.** 2004. Selective stimulation of caveolar endocytosis by glycosphingolipids and cholesterol. *Molecular biology of the cell* **15**: 3114-22.
136. **Shayman, J.A., N.S. Radin.** 1991. Structure and function of renal glycosphingolipids. *Am J Physiol* **260**: F291-302.

137. **Shinohara, T., M. Matsuda, S.H. Cheng, J. Marshall, M. Fujita, K. Nagashima.** 1993. BK virus infection of the human urinary tract. *J Med Virol* **41**: 301-5.
138. **Shishido-Hara, Y., Y. Hara, T. Larson, K. Yasui, K. Nagashima, G.L. Stoner.** 2000. Analysis of capsid formation of human polyomavirus JC (Tokyo-1 strain) by a eukaryotic expression system: splicing of late RNAs, translation and nuclear transport of major capsid protein VP1, and capsid assembly. *J Virol* **74**: 1840-53.
139. **Sieber, M., R. Baumgrass.** 2009. Novel inhibitors of the calcineurin/NFATc hub - alternatives to CsA and FK506? *Cell communication and signaling : CCS* **7**: 25.
140. **Simons, K., D. Toomre.** 2000. Lipid rafts and signal transduction. *Nat Rev Mol Cell Biol* **1**: 31-9.
141. **Stehle, T., S.J. Gamblin, Y. Yan, S.C. Harrison.** 1996. The structure of simian virus 40 refined at 3.1 Å resolution. *Structure* **4**: 165-82.
142. **Stehle, T., S.C. Harrison.** 1996. Crystal structures of murine polyomavirus in complex with straight-chain and branched-chain sialyloligosaccharide receptor fragments. *Structure* **4**: 183-94.
143. **Stehle, T., S.C. Harrison.** 1997. High-resolution structure of a polyomavirus VP1-oligosaccharide complex: implications for assembly and receptor binding. *EMBO J* **16**: 5139-48.
144. **Stehle, T., Y. Yan, T.L. Benjamin, S.C. Harrison.** 1994. Structure of murine polyomavirus complexed with an oligosaccharide receptor fragment. *Nature* **369**: 160-3.
145. **Stolt, A., K. Sasnauskas, P. Koskela, M. Lehtinen, J. Dillner.** 2003. Seroepidemiology of the human polyomaviruses. *J Gen Virol* **84**: 1499-504.
146. **Strauss, J., E. Strauss.** 2008, DNA-Containing Viruses: Family Polyomaviridae, In: *Viruses and Human Disease*. Academic Press, Boston, pp. 302-08.
147. **Stubdal, H., J. Zalvide, K.S. Campbell, C. Schweitzer, T.M. Roberts, J.A. DeCaprio.** 1997. Inactivation of pRB-related proteins p130 and p107 mediated by

- the J domain of simian virus 40 large T antigen. *Molecular and cellular biology* **17**: 4979-90.
148. **Tagawa, A., A. Mezzacasa, A. Hayer, A. Longatti, L. Pelkmans, A. Helenius.** 2005. Assembly and trafficking of caveolar domains in the cell: caveolae as stable, cargo-triggered, vesicular transporters. *The Journal of cell biology* **170**: 769-79.
 149. **Taube, S., M.X. Jiang, C.E. Wobus.** 2010. Glycosphingolipids as Receptors for Non-Enveloped Viruses. *Viruses-Basel* **2**: 1011-49.
 150. **Tettamanti, G.** 2003. Ganglioside/glycosphingolipid turnover: New concepts. *Glycoconjugate J* **20**: 301-17.
 151. **Tremolada, S., S. Delbue, L. Castagnoli, S. Allegrini, U. Miglio, R. Boldorini, F. Elia, J. Gordon, P. Ferrante.** 2010. Mutations in the external loops of BK virus VP1 and urine viral load in renal transplant recipients. *J Cell Physiol* **222**: 195-9.
 152. **Tremolada, S., S. Delbue, S. Larocca, C. Carloni, F. Elia, K. Khalili, J. Gordon, P. Ferrante.** 2010. Polymorphisms of the BK virus subtypes and their influence on viral *in vitro* growth efficiency. *Virus Res* **149**: 190-6.
 153. **Trofe, J., J. Gordon, P. Roy-Chaudhury, I.J. Koralnik, W.J. Atwood, R.R. Alloway, K. Khalili, E.S. Woodle.** 2004. Polyomavirus nephropathy in kidney transplantation. *Prog Transplant* **14**: 130-40; quiz 41-2.
 154. **Tsai, B., J.M. Gilbert, T. Stehle, W. Lencer, T.L. Benjamin, T.A. Rapoport.** 2003. Gangliosides are receptors for murine polyoma virus and SV40. *Embo J* **22**: 4346-55.
 155. **van der Meijden, E., R.W. Janssens, C. Lauber, J.N. Bouwes Bavinck, A.E. Gorbalenya, M.C. Feltkamp.** 2010. Discovery of a new human polyomavirus associated with trichodysplasia spinulosa in an immunocompromized patient. *PLoS Pathog* **6**: e1001024.
 156. **Varki, A.** 2001. Loss of N-glycolylneuraminic acid in humans: Mechanisms, consequences, and implications for hominid evolution. *Am J Phys Anthropol Suppl* **33**: 54-69.

157. **Varki, A.** 2001. N-glycolylneuraminic acid deficiency in humans. *Biochimie* **83**: 615-22.
158. **Varki, A.** 2008. Sialic acids in human health and disease. *Trends Mol Med* **14**: 351-60.
159. **Varki, A.** 2009. Multiple changes in sialic acid biology during human evolution. *Glycoconj J* **26**: 231-45.
160. **Varki, A., R. Schauer.** 2009, Glycolipids, In: Cummings, R.D., Esko, J.D., Freeze, H., Stanley, P., Bertozzi, C., Hart, G.W., Etzler, M.E. (Eds.) *Essentials of Glycobiology*. Cold Harbour Spring Harbor Laboratory Press, Cold Harbour Spring.
161. **Varki, A., R. Schauer.** 2009, Sialic Acids, In: Cummings, R.D., Esko, J.D., Freeze, H., Stanley, P., Bertozzi, C., Hart, G.W., Etzler, M.E. (Eds.) *Essentials of Glycobiology*. Cold Harbour Spring Harbor Laboratory Press, Cold Harbour Spring.
162. **Vats, A., P.S. Randhawa, R. Shapiro.** 2006. Diagnosis and treatment of BK virus-associated transplant nephropathy. *Advances in experimental medicine and biology* **577**: 213-27.
163. **Waldman, W.J., D.A. Knight, L. Blinder, J. Shen, N.S. Lurain, D.M. Miller, D.D. Sedmak, J.W. Williams, A.S. Chong.** 1999. Inhibition of cytomegalovirus *in vitro* and *in vivo* by the experimental immunosuppressive agent leflunomide. *Intervirology* **42**: 412-8.
164. **Waldman, W.J., D.A. Knight, N.S. Lurain, D.M. Miller, D.D. Sedmak, J.W. Williams, A.S. Chong.** 1999. Novel mechanism of inhibition of cytomegalovirus by the experimental immunosuppressive agent leflunomide. *Transplantation* **68**: 814-25.
165. **Watanabe, S., K. Yoshiike.** 1985. Decreasing the number of 68-base-pair tandem repeats in the BK virus transcriptional control region reduces plaque size and enhances transforming capacity. *J Virol* **55**: 823-5.

166. **Whalen, B., J. Laffin, T.D. Friedrich, J.M. Lehman.** 1999. SV40 small T antigen enhances progression to >G2 during lytic infection. *Exp Cell Res* **251**: 121-7.
167. **Williams, J.W., B. Javaid, P.V. Kadambi, D. Gillen, R. Harland, J.R. Thistlewaite, M. Garfinkel, P. Foster, W. Atwood, J.M. Millis, S.M. Meehan, M.A. Josephson.** 2005. Leflunomide for polyomavirus type BK nephropathy. *N Engl J Med* **352**: 1157-8.
168. **Wolf, A.A., M.G. Jobling, S. Wimer-Mackin, M. Ferguson-Maltzman, J.L. Madara, R.K. Holmes, W.I. Lencer.** 1998. Ganglioside structure dictates signal transduction by cholera toxin and association with caveolae-like membrane domains in polarized epithelia. *The Journal of cell biology* **141**: 917-27.
169. **Xie, Y., Y. Han, D.P. Wu, A.N. Sun, J.N. Cen, L. Yao, C.G. Ruan.** 2009. [The BK virus load in urine in association with the development of hemorrhagic cystitis after hematopoietic stem cell transplantation]. *Zhonghua Xue Ye Xue Za Zhi* **30**: 524-7.

CHAPTER 2

STRUCTURE-FUNCTION ANALYSIS OF BKPYV BINDING TO DISIALYLATED GANGLIOSIDES

Abstract

Human polyomavirus BKPyV causes polyomavirus-associated nephropathy and hemorrhagic cystitis in kidney and bone marrow transplant recipients respectively. Using viral infection assays we show that b-series gangliosides GD3, GD2, GD1b and GT1b can serve as receptors for BKPyV. NMR spectroscopy identifies the α 2,8-disialic acid motif common to these gangliosides as the primary binding epitope for BKPyV. The crystal structure of the BKPyV capsid protein VP1 in complex with GD3 reveals contacts with both sialic acid moieties, providing a basis for the observed specificity. A structure-based model of the GD1b interaction suggests additional, affinity-enhancing contacts, which when evaluated, subtly influence BKPyV binding and growth. Comparison with the crystal structure of Simian virus 40 (SV40) VP1 in complex with the a-series ganglioside GM1 reveals an amino acid at position 68 as the major determinant of specificity. Mutation of this amino acid from lysine in BKPyV to serine in SV40 switches the specificity of BKPyV so it recognizes GM1 versus GD3 both in vitro and in cell culture.

Introduction

The human polyomavirus BK Virus (BKPyV) is a non-enveloped, double-stranded DNA (dsDNA) virus that belongs to the family Polyomaviridae. Other members of the family include Simian Virus 40 (SV40) and Murine Polyomavirus (Polyoma), as well as the human JC Virus (JCPyV), Merkel Cell Polyomavirus (MCPyV) and at least eight other recently discovered human polyomaviruses. BKPyV was first isolated from a kidney transplant recipient in 1970 (12). BKPyV seroprevalence is approximately 70% in the adult population. Following primary infection, BKPyV establishes a persistent asymptomatic infection in the genitourinary tract (15,29,35). A key modulator of BKPyV reactivation is immunosuppression of the host that leads to an increase in viral replication (15). Complications of BKPyV reactivation include the development of polyomavirus-induced nephropathy (PVN) in kidney transplant recipients, and hemorrhagic cystitis (HC) in bone marrow transplant recipients (3,14,15,45). Currently, treatment of PVN and hemorrhagic cystitis includes reduction of immunosuppression for PVN and hyperhydration, irrigation of the bladder, or surgery for HC (15,44).

BKPyV particles are icosahedral with a diameter of 45-50 nm (19). A polyomavirus capsid consists of 72 pentamers of the major capsid protein VP1 (20,39). The minor capsid proteins VP2 and VP3 are likely not exposed in the virus and do not contribute to the primary recognition process. Crystal structures of Polyoma, SV40, MCPyV and JCPyV VP1 receptor complexes show that these are bound in shallow grooves on the outer surface of the virus, which are the most variable areas of VP1, contributing to different receptor specificities (26-28,38,39). BKPyV attachment is mediated by cell-surface sialic acid (33). The most common sialic acid type in humans is

α -5-N-acetyl neuraminic acid (NeuNAc) (42). Gangliosides GD1b and GT1b have been identified as receptors for BKPyV (Fig. 1), but a glycoprotein carrying terminal α 2,3-linked sialic acid has also been implicated as a BKPyV receptor (7,21,36). Gangliosides are ceramide-based glycolipids, which are used as receptors for most of the well characterized polyomaviruses, such as GD1a and GT1b for Polyoma, or GM1 for SV40 (41).

In this study, we use viral infection assays to demonstrate that the b-series gangliosides GD3, GD2, GD1b and GT1b can all enhance BKPyV infection. We then define the common α 2,8-disialic acid motif on these gangliosides as the primary binding epitope for BKPyV by NMR spectroscopy. In order to understand how the disialic acid motif is recognized by the virus, we solved the crystal structure of a BKPyV VP1 pentamer in complex with GD3. Analysis of the complex reveals extensive interaction with the terminal sialic acid and specificity-defining contacts with the second sialic acid of the motif. A molecular model of BKPyV with GD1b revealed that the region of the protein where the left arm of GD1b interacts is also involved in binding. Mutagenesis of VP1 residues in the sialic acid binding site abolishes infectivity. However, mutagenesis of residues that interact with the left arm does not seem to significantly affect infectivity. A comparison with the SV40 VP1-GM1 complex attributes the different viral receptor specificities to one point mutation. Introduction of this mutation into BKPyV enables BKPyV to bind GM1 and abolishes binding to GD3. The specificity of the mutant virus is thus similar to that of SV40, but it preferentially recognizes human-specific GM1 instead of its monkey-specific counterpart.

Materials and Methods

Virus Infection and Transfection Cells (ATCC, Manassas, VA) were maintained at 37°C in Cellgro Minimum Essential Medium Eagle (MEM) supplemented with 5% heat inactivated fetal bovine serum (Atlanta Biologicals) and penicillin (10,000U/ml) and streptomycin (10,000µg/ml) (Gibco). HEK cells (ATCC) were maintained at 37°C in Cellgro Dulbecco's Minimum Essential Medium Eagle (DMEM) supplemented with 10% heat inactivated fetal bovine serum and penicillin-streptomycin as above.

To assess the effects of exogenous addition of b-series gangliosides, Vero cells plated 80% confluent per well. Cells were pre-incubated with media, Dimethyl sulfoxide (DMSO) or gangliosides GM1, GD2, GD3, GD1b, and GT1b (Mateya) at 30, 3 or 0.3µM for 17hrs at 37°C. Prior to infection cells were chilled for 20min at 4°C and washed with 2% MEM. Cells were infected with 1.5×10^3 Fluorescent Forming Units (FFU) of BKPyV per 1.5×10^5 cells for 1hr at 37°C. The infectious media was then removed and replaced with fresh growth media. Infection was scored 72hrs post infection by staining for VP1 and analyzed by indirect immunofluorescence.

Construction of the BKPyV pUC-19 protein expression plasmid was previously described (8). The generation of mutants in the BKPyV VP1 encoding region was performed by site directed mutagenesis using the QuickChange XL site-directed mutagenesis kit (Stratagene, La Jolla, CA). Mutant and WT plasmids were digested with 5.0U of BamHI restriction enzyme (10U/µl) (Promega) per 1µg of DNA for 2.5 hours at 37°C to excise the pUC-19 backbone plasmid from the BKPyV genome. The DNA digest was then incubated at 65°C for 15min to heat inactivate the enzyme. Vero cells or HEK cells seeded in at 30% confluent per well, were transfected with (0.5µg) of digested

mutant or WT BKPyV DNA using Fugene 6 according to the manufacturer's instructions (Roche). Transfection was scored over a 22 day time course for VP1 expression or 13-23 days for T-Ag expression in HEK and Vero cells respectively. For experiments with the K68S mutant, fresh GM1 supplemented media (3 μ M) was added to cells on days 4 and 10 for HEK and days 15 and 20 for Vero cells alone. Cells were washed, fixed and stained for T-Ag. Infection of new vero cells were done by adding 200 μ l of the virus containing supernatants collected 22 days post transfection to Vero cells for 2 hours at 37°C. The infectious supernatant was replaced with fresh media and infection scored 72hrs post infection by staining for VP1.

Indirect Immunofluorescence To detect expression of viral antigens cells were fixed with 2% paraformaldehyde in phosphate buffered saline (PBS) for 20 min at 25°C and permeabilized with 1% Triton-X 100 in PBS for 15 min at 37°C. Cells were incubated with the primary mouse monoclonal antibody PAb597 (1:10), which recognizes SV40 VP1 and cross-reacts with both JCPyV and BKPyV VP1, to stain for VP1 (8), or PAb416 (Ab-2) (0.2mg/ml) (Calbiochem), which recognizes SV40 large T-antigen but crossreacts with JCPyV and BKPyV Large T-antigen (9), used at (.008 μ g/ μ l) to stain for BKPyV T-Ag. After incubation with the primary antibody cells were washed with PBS and incubated with Alexa Fluor 488-labeled goat anti-mouse antibody (Invitrogen). Primary and secondary antibodies were diluted in PBS. The nucleus was counterstained with DAPI (1mg/ml) (Sigma).

Flow Cytometry To assess the effects of the exogenous addition of b-series gangliosides on binding Vero cells were plated in 6 well dishes 1.0×10^6 cells per well. Cells were incubated with media, DMSO and gangliosides GM1, GD3, GD2, GD1b, and GT1b for 17-18hrs. Cells were washed, pelleted by centrifugation and suspended in 100 μ l of purified Alex Fluor 488-labeled wild type BKPyV VP1 pentamer (100 μ g/mL) in PBS on ice for 2 hours with 30 min agitations or PBS alone. Cells were washed, pelleted and fixed in 1% paraformaldehyde and analyzed for pentamer binding using a BD FACSCanto II (Benton, Dickinson, and Company) flow cytometer. The data were analyzed using Flow Jo software (Tree Star Inc.).

To evaluate binding of mutant residues that determine terminal sialic acid binding Vero cells were pelleted by centrifugation and suspended in 100 μ l of purified his-tagged wild type or mutant BKPyV VP1 pentamers (100 μ g/mL) in PBS on ice for 2 hours with 30 min agitations or PBS alone. Cells were washed pelleted and suspended in 100 μ l of Penta-His-AlexaFlour 488 conjugated antibody (10 μ g/mL) (Qiagen) in PBS on ice for 1hr with 15 min agitations. Cells were washed, pelleted and fixed in 1% paraformaldehyde and analyzed as above

To evaluate binding of K68S to NeuNAc-GM1 Vero or HEK cells were incubated with media or 3 μ M GM1 dissolved in DMSO for 17-18hrs. Cells were washed, pelleted by centrifugation and suspended in 100 μ l (10 μ g/mL) (Sigma) of CTX or PBS for 30 min on ice with 10 min agitation. Cells were washed pelleted and incubated with 100 μ l of purified wild type or K68S BKPyV VP1 pentamers (100 μ g/mL) in PBS on ice for 2 hours with 30 min agitations or PBS alone. Cells were washed pelleted and suspended in 100 μ l of Penta-His-AlexaFlour 488 conjugated antibody (10 μ g/mL) (Qiagen) in PBS on

ice for 1hr with 15 min agitations. Cells were washed, pelleted and fixed in 1% paraformaldehyde and analyzed as above

Recombinant protein expression and purification DNA coding for amino acids 30-300 of BKPyV VP1 was amplified by PCR and cloned into the pET15b expression vector (Novagen) in frame with an N-terminal hexahistidine tag (His-tag) and a thrombin cleavage site. The pentameric protein was overexpressed in E.coli BL21 (DE3) and purified by nickel affinity chromatography and gel filtration on Superdex-200, and used for STD NMR. For crystallization, the tag was cleaved with thrombin before gel filtration, leaving the non-native amino acids Gly-Ser-His-Met at the N-terminus. After gel filtration, the protein was in 20 mM HEPES pH 7.5, 150 mM NaCl.

STD NMR measurements All NMR spectra were recorded using 3 mm tubes on a Bruker DRX 500 MHz spectrometer fitted with a 5 mm cryogenic probe at 283 K and processed with TOPSPIN 2.0 (Bruker). For each of the three proteins used for STD NMR (SV40 VP1, WTs BKPyV VP1 and K68S BKPyV VP1) two NMR samples were prepared, one containing 1 mM GM1 oligosaccharide (Alexis) and one containing 1 mM GD3 oligosaccharide (Sigma). Protein concentrations were between 19 μ M and 22 μ M as judged by the absorbance at 280 nm. An additional sample contained 20 μ M WT BKPyV VP1 and 1 mM GD1b oligosaccharide (Elicityl, F). Additional samples were prepared that contained no protein but 1 mM GM1, GD3 or GD1b oligosaccharide. The pure oligosaccharide samples were used to verify that no direct excitation of ligand resonances occurred during STD NMR measurements in the absence of protein, and they served as

samples for the spectral assignment. 0.1 mM trimethylsilyl propionate was then added to the GD3 sample to allow ^1H referencing. The buffer used for all NMR measurements contained 20 mM deuterio-Tris pH 7.5, 150 mM NaCl, and 20 mM deuterio-DTT. Samples were prepared in D_2O and no additional water suppression was used in order not to affect the anomeric proton signals. The off- and on-resonance frequencies were set to 80 ppm and 7 ppm, respectively. The total relaxation delay was 4 s. A cascade of 40 Gaussian-shaped pulses with 50 ms duration each, corresponding to a strength of 65 Hz, and a saturation time of 2 s was used for selective excitation. A 10 ms continuous-wave spin lock filter with a strength of 3.7 kHz was employed in order to suppress residual protein signals. 32 k points were collected and zero filling to 64 k data points was employed. Spectra were multiplied with an exponential line broadening factor of 1 Hz prior to Fourier transformation.

For assignment of the oligosaccharide proton resonances, series of 1D ^1H -TOCSY and COSY spectra as well as ^1H , ^{13}C -HSQC spectra were acquired. Literature values on related oligosaccharides served as additional assignment controls (4,13,17,23). Assignment of the acetate methyl groups was taken from (23) for GD3 and (17) for GM1.

Crystallization and structure determination For crystallization, BKPyV VP1 was supplemented with 20 mM DTT and concentrated to 6.6 – 7.0 mg/ml. The protein was crystallized at 20 °C by sitting drop vapor diffusion against a reservoir of 16-18 % PEG 3,350, 0.1 M HEPES pH 7.5 and 0.25 M LiCl (drop size 300 nl protein + 300 nl reservoir). Crystals were harvested into a reservoir solution containing only 14-16 % PEG 3,350 and cryoprotected by soaking in harvesting solution supplemented with 30 %

(v/v) glycerol for 10 s. They were then flash-frozen in liquid nitrogen. For oligosaccharide complex formation, crystals were soaked in harvesting solution containing 20 mM GD3 oligosaccharide for 15 min before cryoprotection and freezing.

Diffraction data were collected at beamlines X06DA and X06SA at SLS (Villigen, CH). They were processed with xds (18), and the structure was solved by molecular replacement with Phaser (1) using the β -sandwich core of the SV40 VP1 pentamer (3BWQ) as the search model. After rigid body and simulated annealing coordinate refinement in Phenix (2), missing parts of the model such as the surface loops were built in Coot (10). Refinement proceeded by alternating rounds of restrained coordinate and isotropic B-factor refinement in Phenix or Refmac5 (25) and model building in Coot. The fivefold non-crystallographic symmetry among the five VP1 monomers was used as a symmetry restraint throughout refinement. Oligosaccharide residues were located in weighted 2Fo-Fc and Fo-Fc electron density maps and refined with restraints from the CCP4 monomers library; only the α 2,8-glycosidic linkage had to be user-defined. The final models have good stereochemistry and Rfree = 18.4 % (5). Figures showing the x-ray structures were prepared with PyMol (Schrödinger Inc.).

Molecular Modeling There are two main conformations for the α 2,3-linkage between NeuNAc in the right arm of gangliosides and the branching Gal that are observed in crystal structures of protein-ganglioside complexes: trans (t) and gauche (g). These two conformations are exemplified by the SV40 VP1-GM1 complex (pdb id 3bwr) and the Ad37 fiber knob-GD1a complex (pdb id 3noi), respectively. The conformations of the left arm of the gangliosides are similar in the two complexes. For modeling the BKPyV

VP1-GD1b interaction, oligosaccharide coordinates were extracted from the complex structures and NeuNAc 5L was deleted from the GD1a oligosaccharide structure of the Ad37 fiber knob complex to yield GM1 oligosaccharide. Then, both GM1 structures were placed into the BKPyV-GD3 complex by superposing the terminal NeuNAc 3R from GM1 onto the internal NeuNAc 3R in the GD3 complex. The “g” conformation of the a2,3-linkage resulted in the left arm of the oligosaccharide pointing away from the protein, while the “t” conformation resulted in potential contacts with the protein, but no steric clashes. Therefore, the model featuring the “t” conformation was chosen.

Glycan Array Screening The ganglioside dose-response microarray used for screening of BKPyV K68S VP1 was composed of 21 sequence-defined lipid-linked oligosaccharide probes. Three of the probes were asialo versions of gangliosides. The probes were robotically printed in duplicate on nitrocellulose-coated glass slides at the four different probe concentrations of 0.3, 0.8, 1.7 and 5 fmol/spot using a non-contact instrument (30). His-tagged WT or BKPyV K68S VP1 pentamer were diluted in 5 mM HEPES pH 7.4, 150 mM NaCl, 0.3% (v/v) Blocker Casein (Pierce), 0.3% (w/v) bovine serum albumin (Sigma), 2.5 mM DTT and 5 mM CaCl₂, to give a final VP1 concentration of 150 µg/ml. The protein was overlaid onto the arrays at 20 °C for 2 h, followed by incubation with mouse monoclonal anti-poly-histidine and biotinylated antimouse IgG antibodies (both from Sigma). Binding was detected with Alexa Fluor-647-labelled streptavidin (Molecular Probes) and imaged (30). Data analysis was done as described (40).

Results

All b-series gangliosides promote infection of BKPyV. BKPyV utilizes the b-series gangliosides GD1b and GT1b as receptors (21). The carbohydrate moieties of gangliosides typically consist of two branches, termed “arms”, and have regular oligosaccharide sequences and linkages. One arm, the “right” arm by convention, consists entirely of sialic acids and is used to classify gangliosides (Fig. 1A). Those of the b-series, e.g. GD1b and GT1b, carry both NeuNAc 3R and NeuNAc 4R, while those of the a-series, e.g. GM1, carry only NeuNAcs 3R (Fig. 1A). We hypothesized that the linear disialic acid motif on the conserved right arm of b-series gangliosides might be the main binding epitope for BKPyV entry. We therefore tested the effects of all common b-series gangliosides on BKPyV infection by supplementing Vero cells with each ganglioside. Gangliosides GD3, GD2, GD1b and GT1b in DMSO at 0.3, 3.0, and 30 μ M were added to permissive Vero cells for 17-18 h to allow for incorporation into the plasma membrane. Cells were washed to remove residual gangliosides and challenged with BKPyV. Infection was scored 72 h later for VP1 expression. Consistent with previous reports (21), gangliosides GD1b and GT1b enhanced infectivity of Vero cells. However, the b-series gangliosides GD2 and GD3, which had not been tested previously, also enhanced infection of the cells (Fig. 1B). To further add to this, incorporation into the plasma membrane also enhanced attachment to Vero cells for the GD2, GD1b and GT1b at the highest concentration tested as observed by flow cytometry (Fig 1C). Supplementation of cells with the a-series ganglioside GM1, which is the known receptor for SV40 and only carries one NeuNAc on its right arm (41), or DMSO as a control had no effect on infection or binding (Fig. 1B and Fig 1C). The data are further supported by

a glycan array screen (Fig 8B). The ability of different b-series gangliosides to enhance BKPyV infection increased with the length of their left arm, with GD1b and GT1b supporting infection best. GD3 does not have a left arm, while GD2 only carries one GalNAc, GD1b carries GalNAc and Gal, and GT1b has an additional NeuNAc on their left arm (Fig. 1A). However, even short b-series gangliosides were able to serve as receptors for BKPyV, indicating that the α 2,8-disialic acid motif of b-series gangliosides is the minimal requirement for interaction.

BKPyV carbohydrate epitope mapping on b-series gangliosides. To characterize BKPyV receptor interactions in greater detail, we expressed and purified a soluble form of BKPyV VP1 that lacks residues 1-29 at the N-terminus and residues 301-362 at the C-terminus. The expressed protein forms folded pentamers, but is unable to form capsids since it lacks residues required for assembly. We analyzed binding of these pentamers to GD3 and GD1b oligosaccharides by saturation transfer difference (STD) NMR spectroscopy (22). In these experiments, selective excitation of the protein (on-resonance spectrum) is followed by a period in which saturation spreads quickly through the entire protein and, if ligand is bound, is transferred to the ligand. When the ligand dissociates from the protein during the measurement, the small ligand maintains the magnetic imprint of the protein's binding site, which can then be detected (off-resonance spectrum). Subtraction of on- and off-resonance spectra allows for easy visualization of the effect in the difference spectrum, which shows signals for only those parts of the ligand that had been close to the protein.

The strongest saturation transfer from BKPyV VP1 to GD3 was observed for the methyl group of the terminal NeuNAc (NeuNAc 4R), followed by the methyl group of the neighboring NeuNAc (NeuNAc 3R) (Fig. 2A). No significant transfer was observed to any of the anomeric protons between 4.2 and 5.0 ppm, or to the NeuNAc H3 protons. Interestingly, no transfer was also observed for the entire Glc and Gal residues of GD3 (Fig. 2A), indicating that they do not participate in binding BKPyV VP1. Some resonances of the two NeuNAc rings could be unambiguously assigned in the spectral region between 3 and 4 ppm, where heavy signal overlap occurs, among them H5, H7 and H8 from NeuNAc 3R and H5 from NeuNAc 4R. We repeated the same experiment for GD1b oligosaccharide and observed transfer to essentially the same set of protons from the disialyl moiety plus additional transfer to the GD1b left arm (Gal 3L and GalNAc 4L) and the branching Gal 2 residue (Fig. 2B). Resonances H3 from Gal 2 and H4 from GalNAc 3L overlap and cannot be distinguished, but both rings contribute additional unambiguous resonances such as H4 and H1 from Gal 2 and H1 from GalNAc 3L. From the Gal 4L ring, only the anomeric proton can be assigned unambiguously in the STD difference spectrum. This resonance overlaps with the Gal 2 anomeric proton, giving the two doublets the appearance of a triplet in both the reference and the STD difference spectrum. If only one of the two anomeric protons experienced saturation transfer from the protein, the apparent triplet in the reference spectrum would change into a doublet in the difference spectrum, similar to the 4L-H1 and 2-H1 resonances highlighted in Fig. 7. The STD spectra thus suggest that the disialyl moieties in both GD3 and GD1b interact with BKPyV VP1 in a similar way, but that additional contacts are

provided by the second arm in GD1b, likely resulting in increased affinity for GD1b in comparison to GD3.

Contacts between BKPyV VP1 and GD3. To further determine the molecular details of carbohydrate recognition by BKPyV VP1, we crystallized free pentameric BKPyV VP1 with GD3 and solved its structure at a resolution of 1.75 Å (Fig. 3A). The VP1 pentamer is a donut-shaped ring, with the five monomers arranged around a central pore that aligns with the five-fold symmetry axis. The monomers adopt the β -sandwich fold with jelly-roll topology (Fig 3A). The β -strands B, I, D, G and C, H, E, F (designated alphabetically from the N-terminus of the full-length protein) form two anti-parallel β -sheets that stack together. The surface of the protein is decorated with extensive loops linking the β -strands. For clarity, one of the loops, the BC-loop, is further subdivided into BC1 and BC2, facing in different directions (Fig 3B-C). The oligosaccharide binding sites of BKPyV VP1 lie on top of the pentamer which corresponds to the outer surface of the virion (Fig. 3B-C). In all four occupied binding sites on the BKPyV VP1 pentamer, NeuNAc 4R adopts the same position and conformation and shares identical contacts with the protein regardless of the presence or absence of crystal contacts (Fig 3A). The carbohydrate ligand is contacted by residues from the BC1-, HI- and DE-loops of one monomer, with contributions from the BC2-loop of the clockwise neighboring VP1 monomer (BC2cw) and the DE-loop of the counterclockwise neighbor (DEccw) (Fig 3B). Four of the five binding sites within one pentamer are occupied by ligand molecules, while one is inaccessible due to the crystal packing (Fig. 3A). Only the terminal

NeuNAc- α 2,8-NeuNAc motif is found to interact with BKPyV VP1. This corresponds well with the results of the STD NMR experiments (Fig 2).

The terminal NeuNAc 4R is the main contact of GD3 with BKPyV VP1. BKPyV VP1 makes extensive contacts with the different functional groups of NeuNAc 4R (Fig 3D). The sialic acid carboxylate group is recognized by two hydrogen bonds to the side chains of S274 and T276 (Fig. 3D). Additionally, water-mediated hydrogen bonds are formed to the side chain of S273 and the backbone of S274. The O4 hydroxyl group of NeuNAc 4R interacts via water-mediated hydrogen bonds with the side chain of N272 and the backbone nitrogen of F75cw. The N-acetyl group is bound by a hydrogen bond to N272. Moreover, its methyl group inserts into a tight-fitting, hydrophobic pocket on BKPyV VP1 that is formed by L62, F65, F270 and F75cw. In addition, the amide oxygen of the N-acetyl group is bound by a water-mediated hydrogen bond to R169cw. The water mediating this contact is part of a network of water molecules, with contacts to D59, N61 and D74cw. The glycerol chain of NeuNAc lies in a shallow, rimmed groove and makes van der Waals contacts to both the bottom, formed by Q278, and the rim of the groove formed by the side chains of P58, L62, L67 and K68. Additionally, via its O9 hydroxyl group, it forms a single hydrogen bond to the K68 backbone nitrogen. The conformation of the NeuNAc 4R ring is stabilized by an intramolecular hydrogen bond from the carboxylate group to the O8 hydroxyl group.

The second sialic acid of GD3, NeuNAc 3R, makes fewer contacts with the protein (Fig. 3E). It is likely to be more mobile, which is reflected in its weaker electron density and elevated temperature factors in comparison to NeuNAc 4R. The carboxylate group of NeuNAc 3R forms a bidentate salt bridge with the positively charged side chain

of K68 (Fig. 3E). The methyl group of its N-acetyl chain stacks against a hydrophobic surface created by parts of the side chains of H138ccw, S274 and T276. Without any other contacts to the protein, NeuNAc 3R is suspended between the side chain of K68 and the surface that contacts its N-acetyl group. Again, its conformation is stabilized by an intramolecular hydrogen bond between its carboxylate group and the O9 hydroxyl group of its glycerol chain. The prominent role of the van der Waals interaction of the methyl groups is highlighted by the STD NMR spectrum of the GD3-BKPyV VP1 complex, which features prominent saturation transfer to the methyl groups of both NeuNAcs (Fig. 2A). The relative peak height of the NeuNAc methyl groups with respect to other peaks in the spectrum is even higher than in the off-resonance spectrum which serves as reference.

Modeling of the BKPyV-GD1b interaction reveals additional contacts. Our BKPyV-GD3 complex structure enabled us to model the interaction of BKPyV VP1 with the longer GD1b oligosaccharide (Fig. 4). The two observed conformations of the ganglioside core structure were superposed onto the tightly bound disialic acid motif, using the internal NeuNAc 3R as an anchor. The model brings GalNAc 3L and especially Gal 4L within 5 Å of protein residues, without causing steric clashes (Fig. 4A). Protein residues E81 and K83 might be in a position to form hydrogen bonds, while L67 is close enough to engage in van der Waals interactions (Fig. 4B). The model is in accord with the observed increase in BKPyV infection with increasing length of the left arm of b-series gangliosides (Fig. 1B). GD3 meets the minimal requirements for binding, but does not feature a branch and thus is more flexible than other b-series gangliosides. The

branching GalNAc 3L of GD2 restricts flexibility and also could make van der Waals interactions with the protein. GD1b features the Gal that is recognized according to our model, which again increases the strength of binding. The additional NeuNAc of the left arm of GT1b would be tolerated according to our model, but it would likely not interact strongly with the protein.

Carbohydrate binding is crucial for BKPyV spread and infectivity. To test the importance of BKPyV binding to sialylated carbohydrates as a crucial step to infectivity, we mutated residues in the binding site. We first probed the interaction with the tightly bound terminal NeuNAc 4R (Fig. 5A) with mutations designed to abolish carbohydrate binding either by reducing the number of hydrogen bonds (S274A, T276A, and S274A/T276A), eliminating van der Waals contacts (F75V), or by introducing steric hindrance (L62W, F75W). Mutants were analyzed using growth and re-infection assays. Vero cells were transfected with mutant or WT BKPyV plasmid DNA. Viral gene expression was scored every 3 days over a 22 day growth period. We found that while WT BKPyV resulted in viral production that continued to spread with time, all mutants that targeted the binding site for terminal sialic acid did not propagate, highlighting the importance of this interaction (Fig 5A). To further evaluate the infectivity of each mutant, we collected the supernatant of each mutant at day 22 post transfection and used this to infect freshly seeded Vero cells. The results were similar to the growth assay, in that WT BKPyV containing supernatant was infectious while the supernatants collected from cells infected with non-viable mutants were non-infectious (Fig. 5B). We targeted the binding site of the internal NeuNAc 3R by eliminate the van der Waals contact between H138

and the internal sialic acid by designing the following mutant (H138A). Removal of this van der Waals contact significantly reduced growth and re-infection levels compared to WT (Fig. 5A-B). We also evaluated the effect of the mutation K68S, which takes away a salt bridge and the long lysine side chain, however this will be described in more detail below. We also tested if the aforementioned mutants were able to bind to Vero cells by flow cytometry. Purified mutant or WT pentamers were incubated with Vero cells, and binding detected using a penta-His-tagged antibody. The results show that all mutant pentamers showed reduced binding compared to binding of the WT VP1 pentamer (Fig. 5C). These results taken together demonstrate that the terminal sialic acid interaction is crucial for binding and infection.

Finally, we mutated residues in the putative binding site for the left arm of long b-series gangliosides. Mutant K83A, which likely takes away a hydrogen bond to Gal 4L, exhibited reduced growth as previously demonstrated (Fig. 4 and Fig 5D) (8). Additional mutations predicted from the model (Fig. 4) to interfere with the binding of BKPyV VP1 with Gal 4L include (D59A, D59Y, L67A and L67W). These mutations, with the exception of D59Y which had reduced growth, had minimal effect on BKPyV growth (Fig 5D). Taken together, mutagenesis in the binding site for the second arm of GD1b confirms the structural model, and demonstrates that the interaction with the left arm only subtly modulates BKPyV infection.

Structural basis of binding specificity. The BKPyV binding site for terminal sialic acid is well-conserved among its relatives. In the BKPyV, JCPyV and SV40 receptor complexes, the majority of contacts are made to the terminal sialic acid, which is bound

in the same orientation and analogous positions on VP1 (Fig. 6D). The two hydrogen bonds between VP1 and the carboxylate group of sialic acid are conserved, as well as the hydrogen bond to the N-acetyl group of sialic acid (Fig. 6A-C). In addition, all three proteins feature a rimmed depression that accommodates the glycerol chain of sialic acid, and a cavity for the methyl moiety of the N-acetyl group.

Interestingly, the cavity is tight-fitting and lined with hydrophobic residues in BKPyV and JCPyV, but significantly enlarged and partially hydrophilic in SV40 (Fig. 6A-C). This difference may reflect the different hosts of these viruses, namely humans and monkeys, and the different types of sialic acids characteristic for each host. In contrast to humans, simians carry mostly N-glycolyl neuraminic acid (NeuNGc) (24,42), in which the methyl group is replaced by the larger and more hydrophilic glycolyl (CH₂-OH) group. It is known that SV40 preferentially binds to NeuNGc-GM1, and the glycolyl group is expected to make interactions with polar residues of the cavity (6,28). By contrast, the smaller and more hydrophobic cavity of BKPyV and JCPyV likely cannot accommodate the glycolyl group in a similar manner due to steric clashes.

While terminal sialic acid is engaged similarly in all three viruses, they all recognize different sialylated sequences. SV40 binds the branched α 2,3-linked GM1 oligosaccharide (41), and JCPyV attaches to the linear α 2,6-linked sequence LSTc (27). Specificity for different sialic acid linkages and underlying carbohydrate sequences arises from a small number of unique contacts outside the conserved binding site for terminal sialic acid. JCPyV recognizes an L-shaped conformation of its receptor motif LSTc specific to the α 2,6-linkage of the terminal NeuNAc. The key residue that makes contacts to both legs of the L is N123 (27). BKPyV and SV40 both have a glycine at the

equivalent position, indicating that they cannot form similar contacts. The BKPyV VP1 residues K68 and H138, which are the main contact point for the internal NeuNAc 3R, are not conserved in SV40 or JCPyV, which both have serine and asparagine at these positions. As the serine cannot engage in a salt bridge with the internal sialic acid and the asparagine has a reduced hydrophobic surface, neither SV40 nor JCPyV would be able to specifically interact with α 2,8 disialic acid carrying glycans (27,28). In turn, the long side chain of K68 in BKPyV would lead to clashes with structures that carry a branching α 2,3-linked sialic acid such as the SV40 receptor GM1. Apart from this difference, BKPyV and SV40 VP1 display similar overall surface features and the same main chain conformation in their surface loops (which is somewhat different from the one observed in JCPyV VP1). Thus, the inability of BKPyV to bind to GM1 seems to be determined only by the amino acid at position 68.

A single point mutation retargets BKPyV to recognize GM1. To evaluate the conclusions derived from the structural comparisons, we introduced a K68S mutation into the BKPyV VP1 pentamer expression construct. Purified K68S pentamers were analyzed by STD NMR for binding to GD3 and GM1. Unlike the WT BKPyV-GD3 pair, almost no saturation transfer was observed for the BKPyV K68S and GD3, indicating that the mutation largely abolished binding to the disialic acid motif of GD3 (Fig. 7A). However, saturation transfer from BKPyV K68S VP1 to GM1 was as efficient as for the SV40 VP1-GM1 pair, which was included for comparison (Fig. 7B-E). This indicates that the K68S mutation switches the binding preference of BKPyV VP1 from GD3 to GM1. The STD NMR spectra of SV40 VP1 and BKPyV K68S VP1 with GM1 are nearly

indistinguishable, suggesting that GM1 engages in the same contacts to both proteins. Due to large spectral overlap between 3 and 4 ppm in the GM1 1D ¹H spectrum, not all peaks can be unambiguously assigned in the STD NMR spectra. Among the peaks for which unambiguous assignment was achieved, saturation transfer is observed primarily to protons of the NeuNAc 3R and Gal 4L rings as well as to protons belonging to the GalNAc 3L residue. Resonances from the internal Gal 2 and Glc rings are largely missing in the difference spectra, suggesting little or no saturation transfer to these rings. The insert in Fig. 7 demonstrates that saturation transfer to the anomeric proton is better for Gal 4L than for Gal 2. Both the GalNAc and the NeuNAc methyl groups in GM1 received considerable saturation in the complexes, with the NeuNAc methyl group being more affected. Our observations are in good agreement with the previously reported crystal structure of SV40 VP1 in complex with GM1 (28) and furthermore demonstrate that a single amino acid mutation suffices for BKPyV to adapt to the SV40 receptor, while emphasizing the importance of the internal sialic acid in BKPyV binding and receptor usage.

BKPyV K68S is specific for NeuNAc-GM1. We then probed the specificity of BKPyV K68S VP1 for the human-type and simian-type sialic acids NeuNAc and NeuNGc. The WT BKPyV VP1 and K68S VP1 were analyzed on a focused ganglioside microarray containing b-series gangliosides as well as the species-specific GM1 variants NeuNAc-GM1 and NeuNGc-GM1 (Fig.8A-C). WT BKPyV VP1 bound to the b-series gangliosides but showed no binding to GM1 (Fig 8B). However, BKPyV K68S bound strongly to the two NeuNAc-GM1 variants on the array, which differed only in the

composition of the lipid linker (Fig. 8C). There was no binding to the simian-type NeuNGc-GM1 variants (Fig 8C). In addition, we did not detect binding to the b-series gangliosides GD3, GM3 and GT1b, and only weak binding to GD1b, confirming our STD NMR results (Fig. 8C). The observed specificity of K68S for the human-type NeuNAc-GM1 is consistent with the structure of the BKPyV and SV40 sialic acid binding sites (Fig. 6A-B).

BKPyV K68S uses NeuNAc-GM1 as a receptor on human cells but not on monkey cells. We next tested whether K68S VP1 was able to use NeuNAc-GM1 to attach to cells. K68S and WT BKPyV VP1 pentamers were evaluated for binding by flow cytometry. Purified K68S or WT pentamers were incubated with Vero cells, and binding detected using a penta-His-tagged antibody. The results show that the K68S pentamer has reduced binding compared to WT VP1 pentamer (Fig. 9A). There was no change in the binding of K68S or WT VP1 pentamers to Vero cells that were supplemented with 3 μ M NeuNAc-GM1 prior to incubation with the pentamers (Fig. 9A). The K68S mutation was also assayed in a viral growth assay in which Vero cells, treated or untreated with 3 μ M NeuNAc-GM1 were transfected with K68S or WT BKPyV plasmid DNA. Transfection was scored over a 23 day growth period for the expression of T-Ag. We found that while transfection of WT BKPyV plasmid results in viral propagation and spread, transfection with the K68S plasmid failed to propagate over time (inset) even when cells were treated with NeuNAc-GM1 during the growth assay (Fig. 9B).

We hypothesize that the inability of the K68S mutant to grow even in NeuNAc-GM1 supplemented Vero cells is due to the fact that monkey cells actively convert the

introduced NeuNAc-GM1 to NeuNGc-GM1 (43). We then asked whether the mutant could propagate in human cells that predominantly express NeuNAc-GM1. WT and K68S mutant constructs were transfected into untreated or NeuNAc-GM1 supplemented HEK cells and viral spread measured over time. The mutant spread as efficiently as WT in both untreated and supplemented cells (Fig. 9C). As K68S has the ability to successfully propagate in HEK cells even in the absence of exogenous NeuNAc-GM1, it was important to further establish that NeuNAc-GM1 does in fact play a significant role in binding and propagation. To assess this, a competitive binding assay was performed on untreated and NeuNAc-GM1 supplemented HEK cells in the presence and absence of Cholera toxin subunit B (CTX). As expected supplementation with NeuNAc-GM1 led to increased binding of K68S pentamer to HEK cells (Figs. 9D and E) and CTX abolished binding indicating that the K68S mutant binds directly to GM1 (Fig. 6F). CTX had no effect on the binding of WT BKPyV VP1 pentamer. The results are consistent with the NMR spectral data shown in Fig. 7 and the conclusions drawn from evaluation of the structure of BKPyV and SV40 in Fig. 6. Furthermore, the results provide molecular evidence that introduction of a single point mutation into BKPyV switches the receptor specificity of BKPyV to recognize human GM1 and emphasizes the significance of the internal sialic acid for BKPyV growth and receptor discrimination.

Discussion

The initial interaction between a pathogen and its host cell influences the efficiency of virus infection and spread and may contribute to pathogenicity. In this study, we used infection assays and NMR spectroscopy to define the α 2,8-disialic acid motif found on b-series gangliosides as the minimal binding epitope on carbohydrate receptors for BKPyV. The high-resolution crystal structure of the BKPyV capsid protein VP1 in complex with the oligosaccharide portion of GD3 confirmed this epitope and provides the molecular basis of recognition. Point mutations in the receptor binding site abolished viral spread and infectivity, demonstrating the physiological relevance of the observed interactions. Comparison of the BKPyV VP1-GD3 structure with the closely related SV40 VP1-GM1 complex suggested that the different receptor specificities of the two viruses are largely due to one key amino acid at position 68, which is a lysine in BKPyV and a serine in SV40. Introduction of the K68S point mutation into BKPyV VP1 switched the binding specificity of BKPyV to that of SV40.

In our infectivity assays and NMR experiments, we tested relatives of the established BKPyV ganglioside receptors GD1b and GT1b to assess the binding specificity of BKPyV for b-series gangliosides and demonstrate that gangliosides GD3 and GD2 are also capable of supporting BKPyV infection. This is entirely in line with our structural analysis, which revealed that BKPyV VP1 forms specific contacts with the disialic acid motif present on all b-series gangliosides. A linear motif containing a terminal α 2,3-linked sialic acid has also been implicated as a receptor for BKPyV (7). While it is sterically possible that BKPyV has some affinity for α 2,3-linked NeuNAc, the

favorable interactions with the second sialic acid would be lacking, and the affinity of the interaction would be expected to be very weak. The α 2,8-disialic acid motif bound by BKPyV is not only present on gangliosides, but also on glycoproteins. However, BKPyV's entry route via caveolae points to gangliosides as entry receptors, which can transmit the signal for endocytosis via their lipid tails (11). Furthermore, sialylated proteins are thought to act as decoy receptors that lack that ability to target viral particles such as MyPV along the infectious pathway leading to non-productive infection (32)

We found that b-series gangliosides enhance BKPyV binding and infection, but GD2 and GD3 do not support infection as efficiently as GD1b and GT1b. In the experimental setup we used, this can have a number of reasons. The gangliosides might incorporate into the plasma membrane at different levels, or they might be trafficked and metabolized by cells at different rates. Another possibility would be that BKPyV can engage all these receptors in a similar way, but that they have different efficiencies in promoting cell entry. The second arm of GD1b and likely GT1b make additional contacts with BKPyV VP1 which may act to stabilize the receptor thus improving the interaction and as a result improve infection. It has been shown for SV40 and Polyoma that the interaction of virions with gangliosides induces membrane curvature, which is the signal for viral entry (11). Longer, branched carbohydrates possess higher rigidity due to their restricted conformational space, and this could help to more efficiently induce membrane curvature and cell entry. Since attachment of BKPyV probably requires many simultaneous interactions with carbohydrates, the virus likely engages not only one type of gangliosides, but a mixture of b-series gangliosides depending on the composition of the plasma membrane.

The finding that b-series gangliosides are uniquely important for BKPyV infection may have implications for BKPyV tropism and pathogenesis. Biochemical analysis of kidney glycosphingolipids indicates that the kidney is rich in diverse sphingolipids and is particularly abundant with gangliosides (16,34). Furthermore, GD3, GD2, GD1b and GT1b are resident gangliosides of the human adult kidney and are found differentially expressed in cortical tubular, medullary and glomerular tissues (16). The developmental expression of these gangliosides has not been evaluated in human kidney tissue, but studies with bovine kidney indicate that there are distinct patterns of ganglioside distribution associated with fetal, newborn and adult kidneys, with simpler gangliosides such as GD3 being readily abundant in fetal kidney tissue, and more complex gangliosides such as GD2, GD1b and GT1b being increasingly expressed in the newborn and adult kidney. A similar expression pattern is seen for ganglioside expression in the developing brain of mice and humans (46). The observation that complex gangliosides such as GD1b and GT1b are more efficient in supporting infection leads us to question whether developmental changes associated with ganglioside distribution may play a role in sero-conversion, latency and reactivation.

We identify here a single amino acid switch for receptor recognition and illuminate its effect in atomic detail and in vivo. Alteration of one amino acid was enough to alter the binding specificity of BKPyV from b-series gangliosides to GM1, which carries a branching sialic acid. This was possible because SV40, JCPyV and BKPyV all feature a conserved platform of core residues that allows them to efficiently engage terminal sialic acid in a similar manner. Nevertheless, each of these viruses achieves its distinct receptor specificity with a small number of carefully positioned satellite residues

that form very few contacts with additional carbohydrate moieties. In all three cases, the core residues mediate the vast majority of interactions, and therefore mostly account for the binding affinity. While the satellite residues in some cases only add one or two contacts and thus would contribute little to affinity, they define the context in which a terminal sialic acid can be bound. It is tempting to speculate that at least some members of the polyomavirus family have evolved from an initial sialic-acid binding template through subtle modification of their satellite residues, thereby expanding or possibly restricting their host range and tropism. The switching of specificity can occur naturally in viruses, and often triggers altered pathogenicity and species tropism. In many cases, switching is due to exceedingly small changes in the virus capsid structure. Prominent examples include influenza viruses, measles virus, the canine and feline parvoviruses, and adenoviruses (31,37). In many of these cases, however, the molecular functions of these switches, such as how specific mutations alter the interaction with receptors, are not well understood at the atomic level. We identify here such a single amino acid switch and illuminate in atomic detail its effect on host receptor recognition.

LITERATURE CITED

1. 1994. The CCP4 suite: programs for protein crystallography. *Acta Crystallogr D Biol Crystallogr* **50**: 760-3.
2. **Adams, P.D., P.V. Afonine, G. Bunkoczi, V.B. Chen, I.W. Davis, N. Echols, J.J. Headd, L.W. Hung, G.J. Kapral, R.W. Grosse-Kunstleve, A.J. McCoy, N.W. Moriarty, R. Oeffner, R.J. Read, D.C. Richardson, J.S. Richardson, T.C. Terwilliger, P.H. Zwart.** 2010. PHENIX: a comprehensive Python-based system for macromolecular structure solution. *Acta Crystallogr D Biol Crystallogr* **66**: 213-21.
3. **Bedi, A., C.B. Miller, J.L. Hanson, S. Goodman, R.F. Ambinder, P. Charache, R.R. Arthur, R.J. Jones.** 1995. Association of BK virus with failure of prophylaxis against hemorrhagic cystitis following bone marrow transplantation. *J Clin Oncol* **13**: 1103-9.
4. **Brisson, J.R., H. Baumann, A. Imberty, S. Perez, H.J. Jennings.** 1992. Helical epitope of the group B meningococcal alpha(2-8)-linked sialic acid polysaccharide. *Biochemistry-Us* **31**: 4996-5004.
5. **Brunger, A.T.** 1992. Free R value: a novel statistical quantity for assessing the accuracy of crystal structures. *Nature* **355**: 472-5.
6. **Campanero-Rhodes, M.A., A. Smith, W. Chai, S. Sonnino, L. Mauri, R.A. Childs, Y. Zhang, H. Ewers, A. Helenius, A. Imberty, T. Feizi.** 2007. N-glycolyl GM1 ganglioside as a receptor for simian virus 40. *J Virol* **81**: 12846-58.
7. **Dugan, A.S., S. Eash, W.J. Atwood.** 2005. An N-linked glycoprotein with alpha(2,3)-linked sialic acid is a receptor for BK virus. *J Virol* **79**: 14442-5.
8. **Dugan, A.S., M.L. Gasparovic, N. Tsomaia, D.F. Mierke, B.A. O'Hara, K. Manley, W.J. Atwood.** 2007. Identification of amino acid residues in BK virus VP1 that are critical for viability and growth. *J Virol* **81**: 11798-808.
9. **Eash, S., W.J. Atwood.** 2005. Involvement of cytoskeletal components in BK virus infectious entry. *J Virol* **79**: 11734-41.

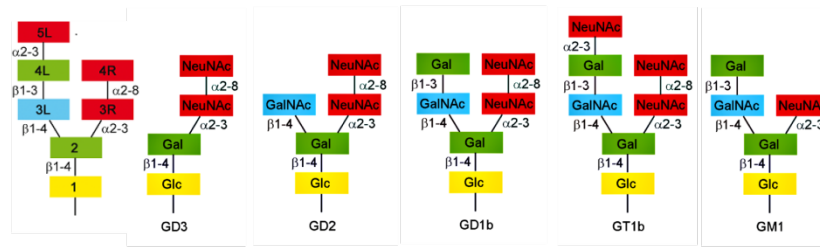
10. **Emsley, P., K. Cowtan.** 2004. Coot: model-building tools for molecular graphics. *Acta Crystallogr D Biol Crystallogr* **60**: 2126-32.
11. **Ewers, H., W. Romer, A.E. Smith, K. Bacia, S. Dmitrieff, W. Chai, R. Mancini, J. Kartenbeck, V. Chambon, L. Berland, A. Oppenheim, G. Schwarzmann, T. Feizi, P. Schwillle, P. Sens, A. Helenius, L. Johannes.** 2010. GM1 structure determines SV40-induced membrane invagination and infection. *Nature cell biology* **12**: 11-8; sup pp 1-12.
12. **Gardner, S.D., A.M. Field, D.V. Coleman, B. Hulme.** 1971. New human papovavirus (B.K.) isolated from urine after renal transplantation. *Lancet* **1**: 1253-7.
13. **Haselhorst, T., H. Blanchard, M. Frank, M.J. Kraschnefski, M.J. Kiefel, A.J. Szyzew, J.C. Dyason, F. Fleming, G. Holloway, B.S. Coulson, M. von Itzstein.** 2007. STD NMR spectroscopy and molecular modeling investigation of the binding of N-acetylneuraminic acid derivatives to rhesus rotavirus VP8* core. *Glycobiology* **17**: 68-81.
14. **Hirsch, H.H.** 2005. BK virus: opportunity makes a pathogen. *Clin Infect Dis* **41**: 354-60.
15. **Hirsch, H.H., J. Steiger.** 2003. Polyomavirus BK. *Lancet Infect Dis* **3**: 611-23.
16. **Holthofer, H., J. Reivinen, A. Miettinen.** 1994. Nephron segment and cell-type specific expression of gangliosides in the developing and adult kidney. *Kidney Int* **45**: 123-30.
17. **Houliston, R.S., B.C. Jacobs, A.P. Tio-Gillen, J.J. Verschuuren, N.H. Khieu, M. Gilbert, H.C. Jarrell.** 2009. STD-NMR used to elucidate the fine binding specificity of pathogenic anti-ganglioside antibodies directly in patient serum. *Biochemistry-Us* **48**: 220-2.
18. **Kabsch, W.** 2010. Integration, scaling, space-group assignment and post-refinement. *Acta Crystallogr D Biol Crystallogr* **66**: 133-44.
19. **Li, T.C., N. Takeda, K. Kato, J. Nilsson, L. Xing, L. Haag, R.H. Cheng, T. Miyamura.** 2003. Characterization of self-assembled virus-like particles of

- human polyomavirus BK generated by recombinant baculoviruses. *Virology* **311**: 115-24.
20. **Liddington, R.C., Y. Yan, J. Moulai, R. Sahli, T.L. Benjamin, S.C. Harrison.** 1991. Structure of simian virus 40 at 3.8-Å resolution. *Nature* **354**: 278-84.
 21. **Low, J.A., B. Magnuson, B. Tsai, M.J. Imperiale.** 2006. Identification of gangliosides GD1b and GT1b as receptors for BK virus. *J Virol* **80**: 1361-6.
 22. **Mayer, M., M. Bernd.** 1999. Characterization of Ligand Binding by Saturation Transfer Difference NMR Spectroscopy. *Angewandte Chemie International Edition* **38**: 1784-88.
 23. **Michon, F., J.R. Brisson, H.J. Jennings.** 1987. Conformational differences between linear alpha (2----8)-linked homosialooligosaccharides and the epitope of the group B meningococcal polysaccharide. *Biochemistry-U.S.* **26**: 8399-405.
 24. **Muchmore, E.A., S. Diaz, A. Varki.** 1998. A structural difference between the cell surfaces of humans and the great apes. *American Journal of Physical Anthropology* **107**: 187-98.
 25. **Murshudov, G.N., A.A. Vagin, E.J. Dodson.** 1997. Refinement of macromolecular structures by the maximum-likelihood method. *Acta Crystallogr D Biol Crystallogr* **53**: 240-55.
 26. **Neu, U., H. Hengel, B.S. Blaum, R.M. Schowalter, D. Macejak, M. Gilbert, W.W. Wakarchuk, A. Imamura, H. Ando, M. Kiso, N. Arnberg, R.L. Garcea, T. Peters, C.B. Buck, T. Stehle.** 2012. Structures of Merkel cell polyomavirus VP1 complexes define a sialic acid binding site required for infection. *PLoS Pathog* **8**: e1002738.
 27. **Neu, U., M.S. Maginnis, A.S. Palma, L.J. Stroh, C.D. Nelson, T. Feizi, W.J. Atwood, T. Stehle.** 2010. Structure-function analysis of the human JC polyomavirus establishes the LSTc pentasaccharide as a functional receptor motif. *Cell host & microbe* **8**: 309-19.
 28. **Neu, U., K. Woellner, G. Gauglitz, T. Stehle.** 2008. Structural basis of GM1 ganglioside recognition by simian virus 40. *Proceedings of the National Academy of Sciences of the United States of America* **105**: 5219-24.

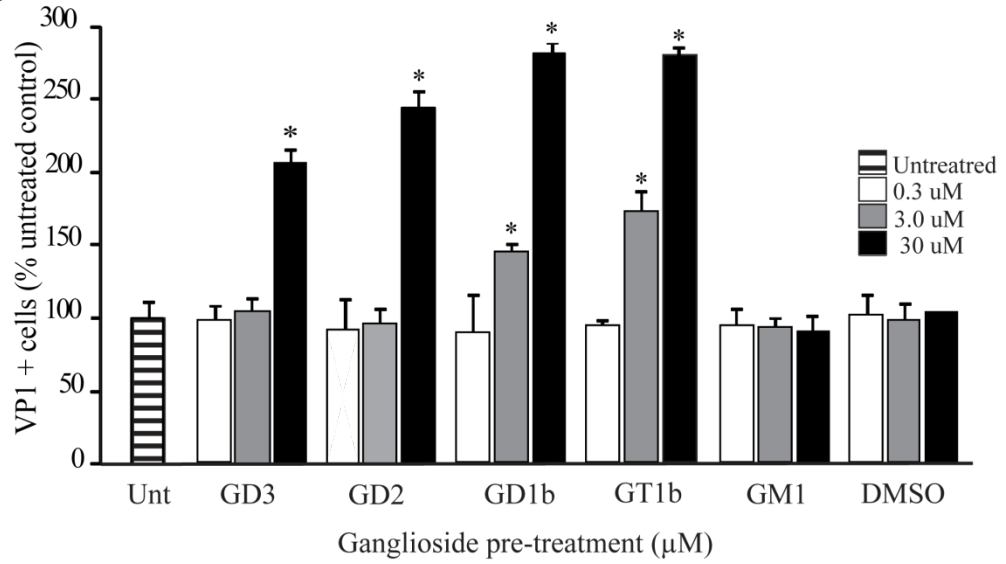
29. **Nickeleit, V., H.H. Hirsch, I.F. Binet, F. Gudat, O. Prince, P. Dalquen, G. Thiel, M.J. Mihatsch.** 1999. Polyomavirus infection of renal allograft recipients: from latent infection to manifest disease. *J Am Soc Nephrol* **10**: 1080-9.
30. **Palma, A.S., T. Feizi, Y. Zhang, M.S. Stoll, A.M. Lawson, E. Diaz-Rodriguez, M.A. Campanero-Rhodes, J. Costa, S. Gordon, G.D. Brown, W. Chai.** 2006. Ligands for the beta-glucan receptor, Dectin-1, assigned using "designer" microarrays of oligosaccharide probes (neoglycolipids) generated from glucan polysaccharides. *J Biol Chem* **281**: 5771-9.
31. **Persson, B.D., S. Muller, D.M. Reiter, B.B. Schmitt, M. Marttila, C.V. Sumowski, S. Schweizer, U. Scheu, C. Ochsenfeld, N. Arnberg, T. Stehle.** 2009. An arginine switch in the species B adenovirus knob determines high-affinity engagement of cellular receptor CD46. *J Virol* **83**: 673-86.
32. **Qian, M., B. Tsai.** 2010. Lipids and proteins act in opposing manners to regulate polyomavirus infection. *Journal of Virology* **84**: 9840-52.
33. **Seganti, L., P. Mastromarino, F. Superti, L. Sinibaldi, N. Orsi.** 1981. Receptors for BK virus on human erythrocytes. *Acta Virol* **25**: 177-81.
34. **Shayman, J.A., N.S. Radin.** 1991. Structure and function of renal glycosphingolipids. *Am J Physiol* **260**: F291-302.
35. **Shinohara, T., M. Matsuda, S.H. Cheng, J. Marshall, M. Fujita, K. Nagashima.** 1993. BK virus infection of the human urinary tract. *J Med Virol* **41**: 301-5.
36. **Sinibaldi, L., P. Goldoni, V. Pietropaolo, C. Longhi, N. Orsi.** 1990. Involvement of gangliosides in the interaction between BK virus and Vero cells. *Arch Virol* **113**: 291-6.
37. **Stehle, T., J.M. Casasnovas.** 2009. Specificity switching in virus-receptor complexes. *Current opinion in structural biology* **19**: 181-8.
38. **Stehle, T., S.C. Harrison.** 1997. High-resolution structure of a polyomavirus VP1-oligosaccharide complex: implications for assembly and receptor binding. *EMBO J* **16**: 5139-48.

39. **Stehle, T., Y. Yan, T.L. Benjamin, S.C. Harrison.** 1994. Structure of murine polyomavirus complexed with an oligosaccharide receptor fragment. *Nature* **369**: 160-3.
40. **Stoll, M.S., T. Feizi.** 2009. Software tools for storing, processing and displaying carbohydrate microarray data. In: Beilstein Symposium on Glyco-Bioinformatics, Potsdam, Germany.
41. **Tsai, B., J.M. Gilbert, T. Stehle, W. Lencer, T.L. Benjamin, T.A. Rapoport.** 2003. Gangliosides are receptors for murine polyoma virus and SV40. *Embo J* **22**: 4346-55.
42. **Varki, A.** 2001. Loss of N-glycolylneuraminic acid in humans: Mechanisms, consequences, and implications for hominid evolution. *Am J Phys Anthropol Suppl* **33**: 54-69.
43. **Varki, A.** 2001. N-glycolylneuraminic acid deficiency in humans. *Biochimie* **83**: 615-22.
44. **Wiseman, A.C.** 2009. Polyomavirus nephropathy: a current perspective and clinical considerations. *Am J Kidney Dis* **54**: 131-42.
45. **Xie, Y., Y. Han, D.P. Wu, A.N. Sun, J.N. Cen, L. Yao, C.G. Ruan.** 2009. [The BK virus load in urine in association with the development of hemorrhagic cystitis after hematopoietic stem cell transplantation]. *Zhonghua Xue Ye Xue Za Zhi* **30**: 524-7.
46. **Yu, R.K., Y. Nakatani, M. Yanagisawa.** 2009. The role of glycosphingolipid metabolism in the developing brain. *J Lipid Res* **50 Suppl**: S440-5.

A



B



C

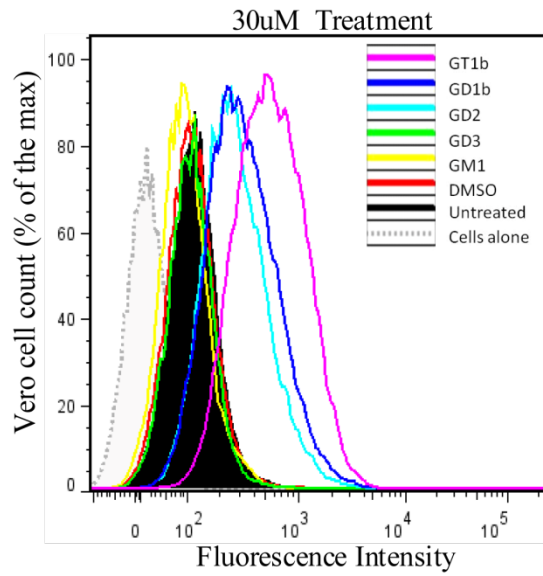


Figure 1: B-series gangliosides are receptors for BKPyV. (A) Representative structures of disialic acid containing gangliosides GD2, GD3, GD1b, GT1b and the monosialylated ganglioside GM1 indicating the labeling and identification of individual components of a ganglioside used in this paper. (B) Vero cells were incubated with disialic acid containing gangliosides GD3, GD2, GD1b, GT1b and monosialylated ganglioside GM1, dissolved in DMSO, or DMSO alone for 17-18 hours. Cells were then challenged with BKPyV and infection scored at 72 hours post-infection by indirect immunofluorescence analysis of VP1 expression. The average number of VP1 positive cells is plotted as a % compared to the untreated control. Error bars represent the standard deviation for triplicate experiments (* $p < .05$ compared to the untreated control). (C) Vero cells were supplemented with 30 μ M disialic acid containing gangliosides GD3, GD2, GD1b, GT1b and monosialylated ganglioside GM1, dissolved in DMSO, or DMSO for 17-18 hours. Cells were incubated with purified Alexa-fluor 488 labeled WT BKPyV pentamer. Cells were fixed and pentamer binding to cells assessed by flow cytometry. Histograms show the fluorescence intensity for the Alexa 488 labeled WT pentamer binding.

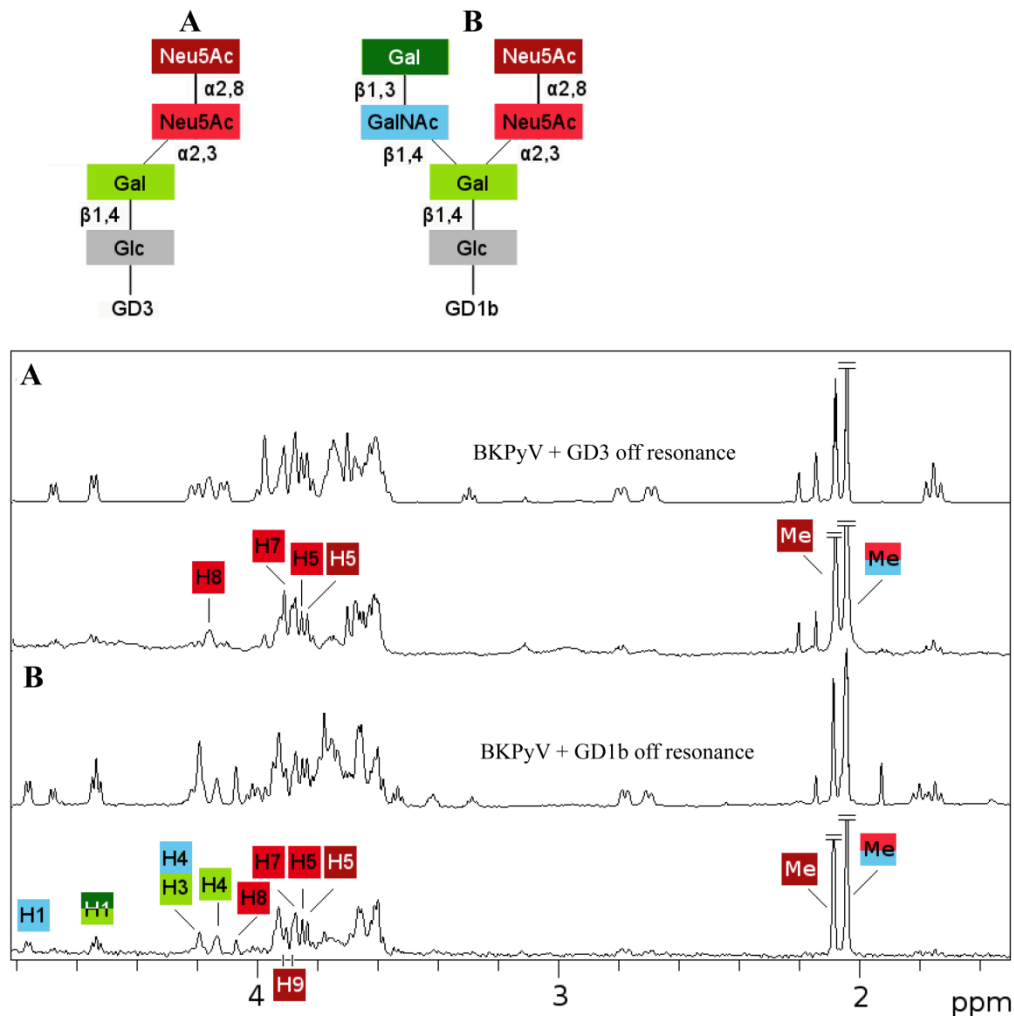


Figure 2: BKPvV primarily engages the disialic acid motif of b—series gangliosides. (A) off-resonance spectrum (top) and STD difference spectrum (bottom) of WT BKPvV VP1 in the presence of 50-fold excess of GD3 oligosaccharide. The off-resonance spectrum was scaled to 3% and is used for assignment of the protons. GD3 resonances in the difference spectrum receive considerable saturation transfer and are labeled/color coordinated to match the sugars of the oligosaccharide that interact with VP1. Regions with strong signal overlap are not labeled because saturation effects in this region cannot be unambiguously assigned. Signals which were truncated are denoted by diagonal bars. (B) off-resonance spectrum (top) and STD difference spectrum (bottom) of wild type BKPvV in the presence of 50-fold excess of GD1b oligosaccharide. The off-resonance spectrum was scaled to 3%. GD1b resonances labeled in the difference spectrum receive considerable saturation transfer from the protein while those labeled in the off-resonance spectrum receive no or negligible saturation transfer. Regions with strong signal overlap are not labeled because saturation effects in this region cannot be unambiguously assigned.

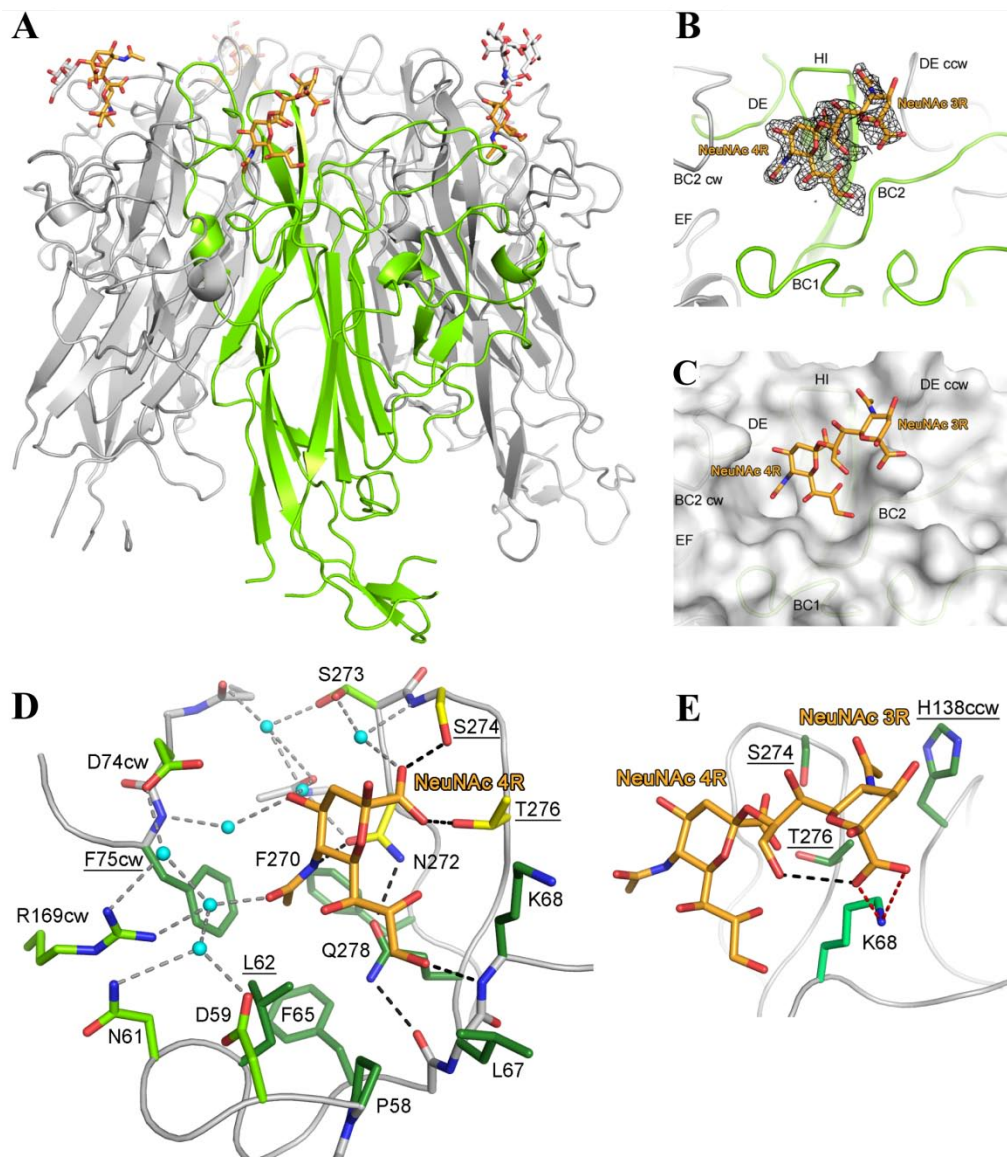


Figure 3: Structure of a BKPyV VP1-GD3 oligosaccharide complex. (A) Structure of a free BKPyV VP1 pentamer in complex with GD3. One VP1 monomer is highlighted in green, the others are coloured gray. The monosaccharides unbiased by crystal contacts are coloured orange, those binding to crystal contacts are coloured white. (B) Composite annealed difference electron density for the terminal disialic acid motif of GD3 oligosaccharide bound to BKPyV VP1 at a σ level of 2.5. The names of VP1 surface loops are indicated. cw/ccw = belonging to the clockwise/counter clockwise neighbouring VP1 monomer within the pentamer. (C) Binding surface for α 2,8-disialic acid on BKPyV VP1. (D) Interactions of terminal sialic acid NeuNAc1. Side chains are coloured by the kind of interaction they make with the sugar: Side chains making hydrogen bonds are coloured yellow, those making van der Waals interactions are coloured dark green, and those making water-mediated hydrogen bonds are coloured light green. Atoms of the protein backbone are shown in gray, and water molecules are in cyan. Direct hydrogen bonds are indicated as black dashed lines, water-mediated ones are gray. (E) Contacts of internal sialic acid NeuNAc2. Only residues in contact with NeuNAc2 are shown. Colours are as in A. The salt bridge between NeuNAc2 and K68 is coloured red.

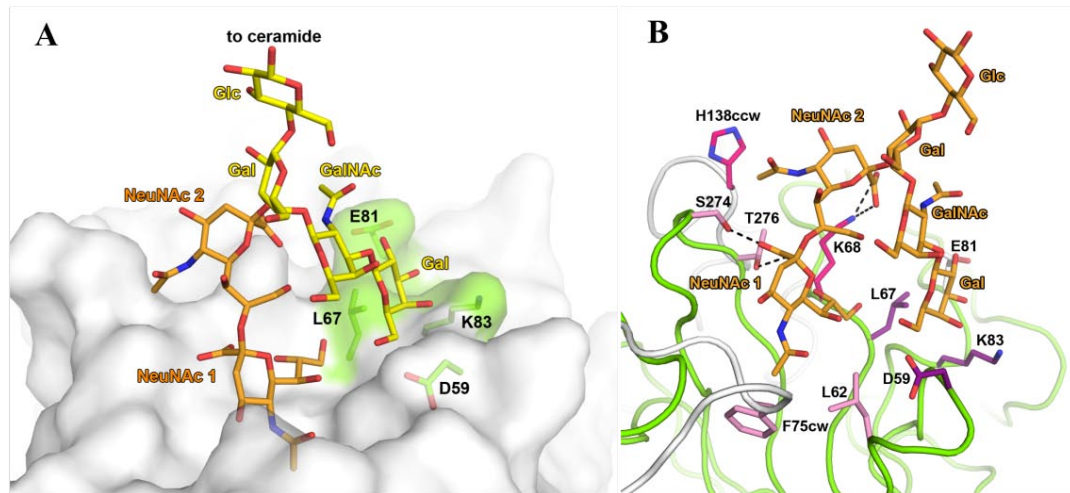


Figure 4: Proposed model of BKPyV VP1-GD1b oligosaccharide complex. (A) Proposed binding surface for the (Gal-(β1,3)-GalNAc) motif of GD1b on BKPyV VP1 using the disialic acid motif (orange stick model) as an anchor. (B) Proposed interactions of GD1b with BKPyV VP1. Side chains making hydrogen bonds to the disialic acid motif are indicated as black dashed lines. Additional interactions for the (Gal-(β1,3)-GalNAc) motif cannot be conclusively assigned.

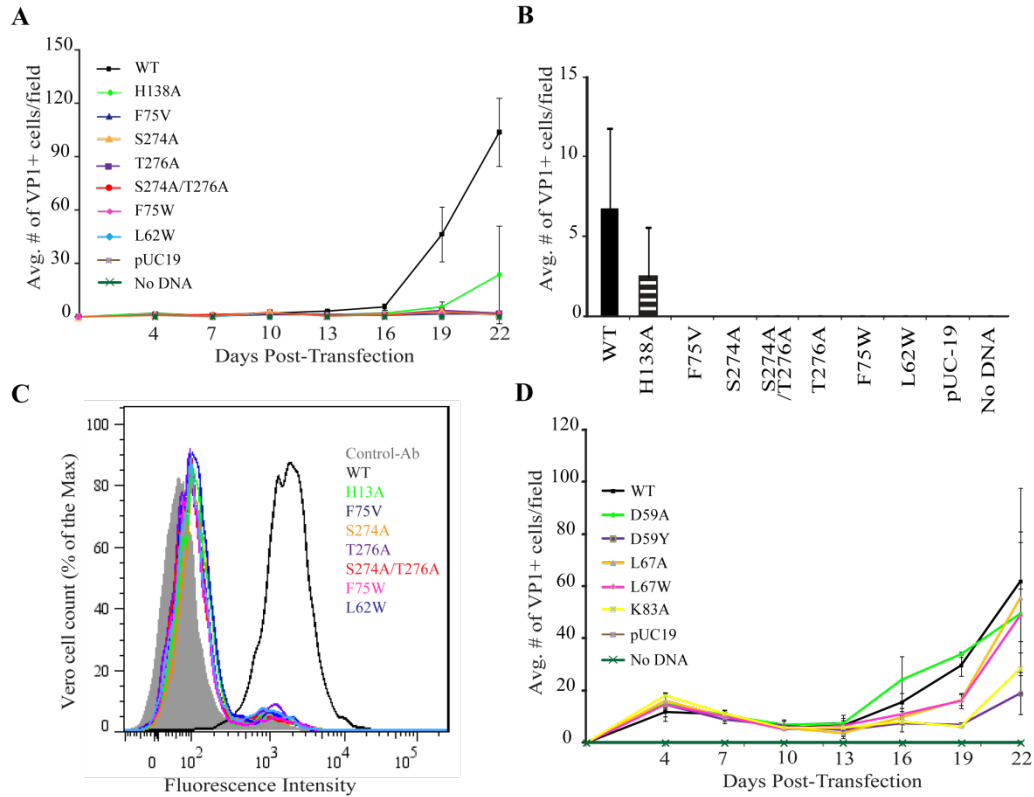


Figure 5: BKPyV engagement of sialic acid is important for spread and infectivity. (A) To assess the importance of the BKPyV engagement of the disialic acid motif, vero cells were transfected with linear WT or mutant BKPyV DNA fixed and stained at 3 day intervals for 22 days. Viral spread was quantified by scoring for cells expressing VP1. The average number of VP1 positive cells is plotted from triplicate experiments with each time point representing the average number of infected cells per visual field for 8 fields. (B) Vero cells were incubated for 2 hours with the infectious supernatant from day 22 to evaluate the re-infection capability of all mutants compared to WT. At 3 days post infection VP1 positive cells were scored as described above. The mean VP1 expression is plotted from three independent experiments. All error bars represent standard deviations. (C) To evaluate the importance of the disialic acid motif for binding, vero cells were incubated with purified His-tagged mutant or WT BKPyV pentamers and an Alexa Fluor 488 conjugated penta-His secondary antibody. Cells were fixed and pentamer binding to cells assessed by flow cytometry. Histograms show the fluorescence intensity of the Alexa 488 antibody alone (gray-filled), WT pentamer (black) or mutants (various color). (D) To assess the importance of the left arm of GT1b, vero cells were transfected with linear WT or mutant BKPyV DNA fixed and stained at 3 day intervals for 22 days. Viral spread was quantified by scoring for cells expressing VP1. The average number of VP1 positive cells is plotted from triplicate experiments with each time point representing the average number of infected cells per visual field for 8 fields.

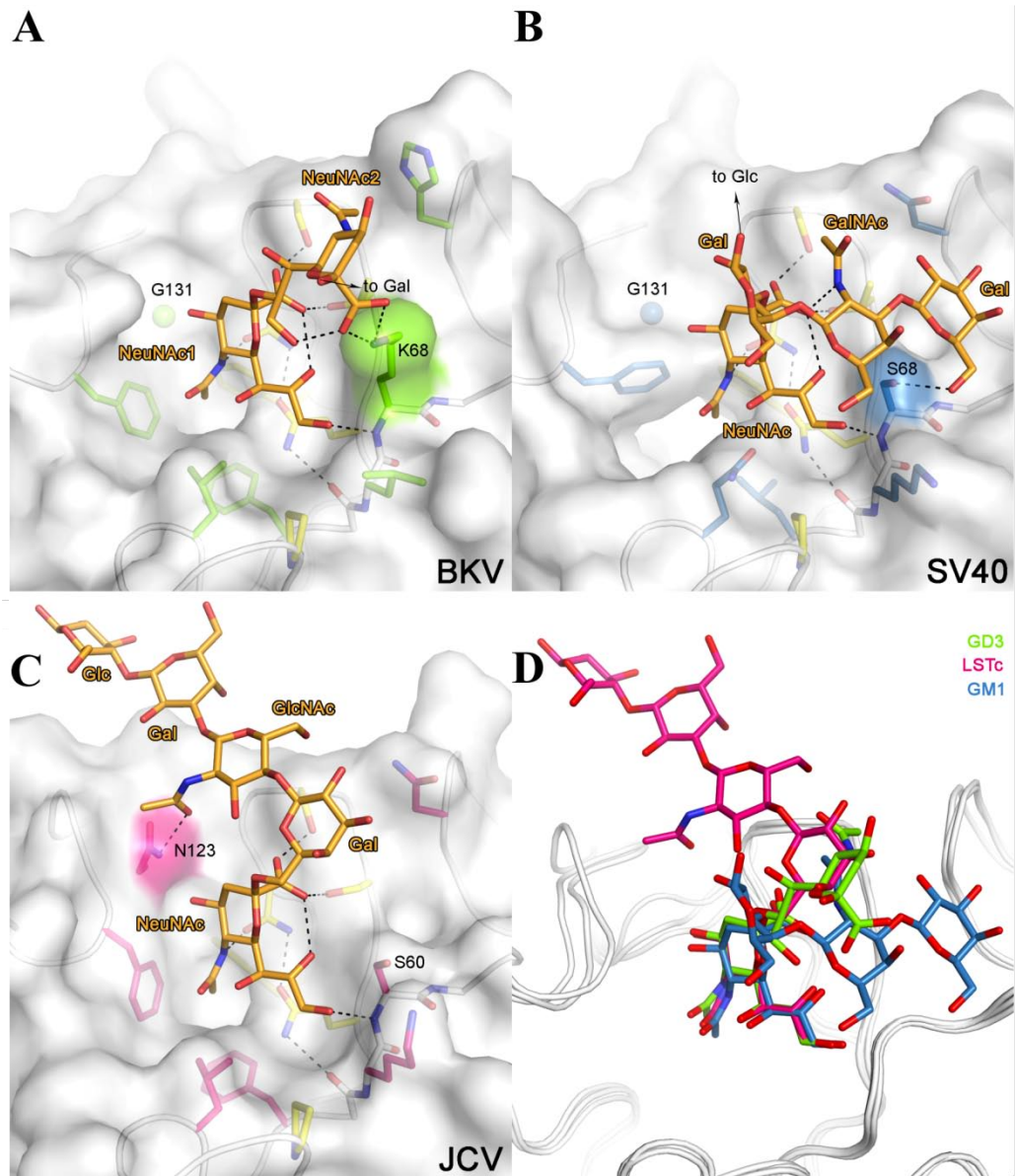


Figure 6: Comparison of carbohydrate binding sites of BKPyV, SV40 and JCPyV. (A+B+C) Recognition of carbohydrate receptors by BKPyV (A), SV40 (B), and JCPyV (C). Only residues making direct hydrogen bonds or van der Waals interactions are shown. Residues that make conserved interactions are coloured in yellow, side chains whose positions are not conserved are shown in green (BKPyV), blue (SV40) and pink (JCPyV). (D) Superimposed receptors of BKPyV, JCPyV and SV40 in their carbohydrate binding site showing that terminal sialic acid binding is conserved.

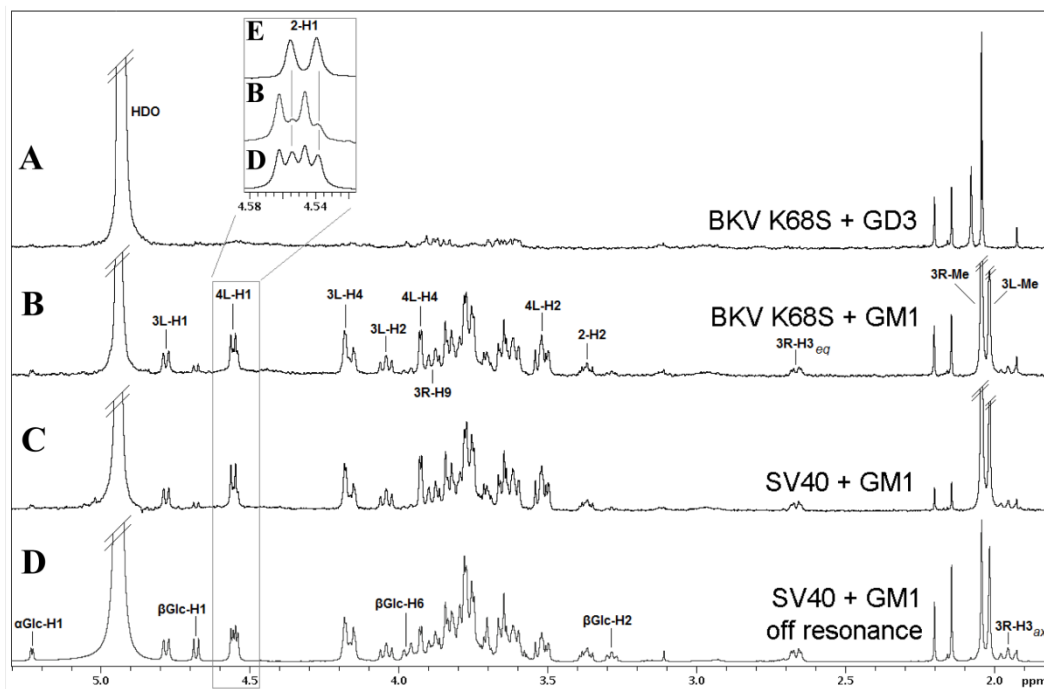
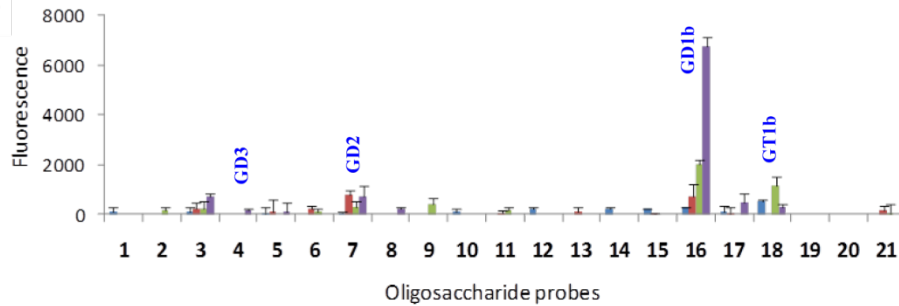


Figure 7: The K68S mutation retargets BKPyV to the SV40 receptor GM1. STD difference spectra of (A) BKPyV K68S with GD3, (B and C, respectively) BKPyV K68S and SV40 with GM1, and (D) SV40-GM1 off-resonance spectrum. A 50-fold excess of oligosaccharide was used for each spectrum. The off-resonance spectrum was scaled to 3%. Resonances labeled in the difference spectra with GM1 (B and C) receive considerable saturation transfer from BKPyV K68S and SV40 while those labeled in the GM1 off-resonance spectrum receive no or negligible saturation transfer. Regions with strong signal overlap are not labeled because they cannot be unambiguously assigned. (A). Enlargement: A 1D ^1H -TOCSY spectrum of the Gal-2 ring (E) allows distinction of both GM1 galactose H1 resonances despite signal overlap in the off-resonance spectrum (D). The anomeric proton of Gal-4L resonates at a slightly higher chemical shift and receives more saturation in the STD difference spectra with BKPyV K68S (B) and SV40 (C). Signals which were truncated are denoted by diagonal bars and impurities are labeled with asterisks. The large signal at 4.7 ppm is due to residual water.

A

Position	Probe	Sequence
1	GM4	NeuAco-3Gal1β-Cer
2	GM3	NeuAco-3Gal1β-4G1cβ-Cer
3	GM3(Gc)	NeuGco-3Gal1β-4G1cβ-Cer
4	GD3	NeuAco-8NeuAco-3Gal1β-4G1cβ-Cer
5	Asialo-GM2	GalNAcβ-4Gal1β-4G1cβ-Cer
6	GM2	NeuAco-3 GalNAcβ-4Gal1β-4G1cβ-Cer
7	GD2	NeuAco-8NeuAco-3 Gal1β-3GalNAcβ-4Gal1β-4G1cβ-Cer
8	Asialo-GM1	Gal1β-3GalNAcβ-4Gal1β-4G1cβ-DH
9	Asialo-GM1-Tetra	Gal1β-3GalNAcβ-4Gal1β-4G1cβ-DH
10	GM1	Gal1β-3GalNAcβ-4Gal1β-4G1cβ-Cer
11	GM1-penta	NeuAco-3 Gal1β-3GalNAcβ-4Gal1β-4G1cβ-DH
12	GM1(Gc)	NeuAco-3 Gal1β-3GalNAcβ-4Gal1β-4G1cβ-Cer
13	GM1(Gc)-penta	NeuGco-3 Gal1β-3GalNAcβ-4Gal1β-4G1cβ-DH
14	GD1a	NeuAco-3Gal1β-3GalNAcβ-4Gal1β-4G1cβ-Cer
15	GD1a-hexa	NeuAco-3 NeuAco-3Gal1β-3GalNAcβ-4Gal1β-4G1cβ
16	GD1b	NeuAco-3 Gal1β-3GalNAcβ-4Gal1β-4G1cβ-Cer
17	GT1a	NeuAco-8NeuAco-3 NeuAco-3Gal1β-3GalNAcβ-4Gal1β-4G1cβ-Cer
18	GT1b	NeuAco-3 NeuAco-3Gal1β-3GalNAcβ-4Gal1β-4G1cβ-Cer
19	GQ1b	NeuAco-8NeuAco-3 NeuAco-3Gal1β-3GalNAcβ-4Gal1β-4G1cβ-Cer
20	LSTc	NeuAco-6Gal1β4-G1cNAcβ3-Gal1β4-G1c-DH
21	LSTa	NeuAco-3Gal1β-3G1cNAcβ-3Gal1β-4G1c-DH

B



C

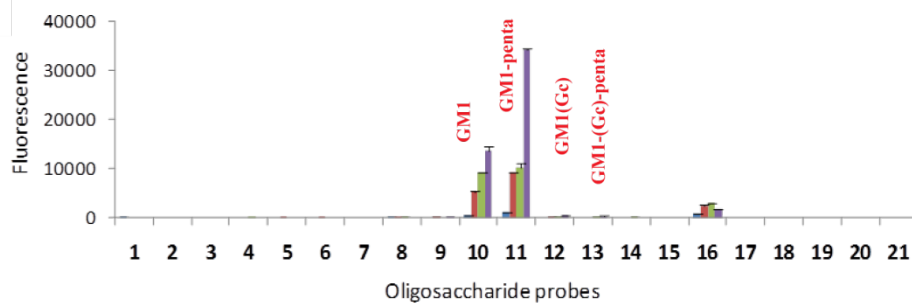


Figure 8: K68S specifically interacts with NeuNAc-GM1. (A) List of oligosaccharide probes on the array. Carbohydrate microarray analyses of recombinant (B) BKPyV VP1 and (C) K68S using 21 lipid-linked oligosaccharide probes. Each oligosaccharide probe was arrayed at four levels (0.3, 0.8, 1.7 and 5 fmol/spot) in duplicate. These are indicated as the coloured panels defined at the bottom of the figure. Numerical scores of the binding signals are means of duplicate spots (with *error bars*).

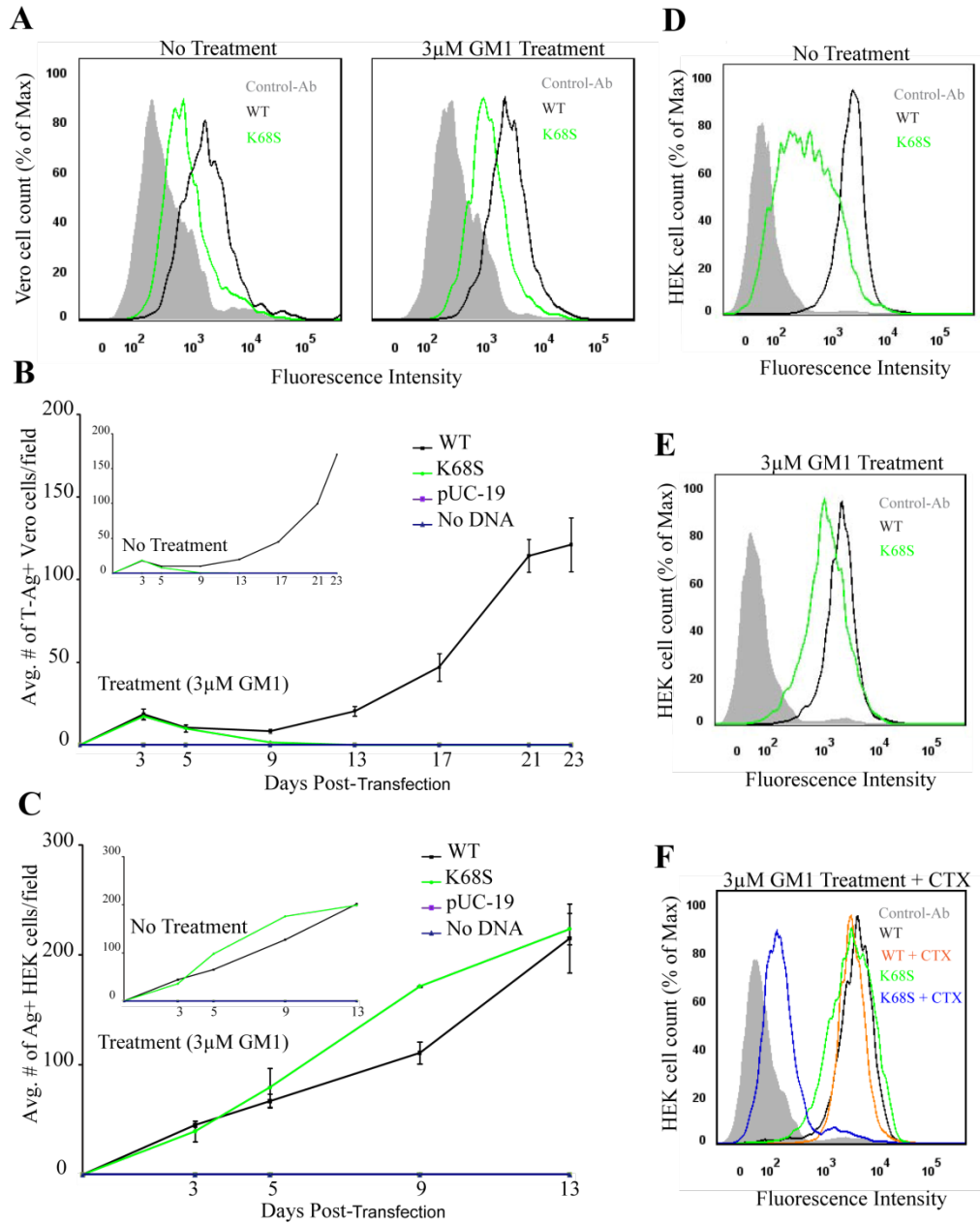


Figure 9: K68S BKPyV uses N-acetyl GM1 as a receptor. (A) Vero cells were incubated with purified His-tagged K68S or WT BKPyV pentamers and an Alexa Fluor 488 conjugated penta-His secondary antibody. Cells were fixed and pentamer binding to cells untreated (left) or treated (right) with NeuNAc-GM1 assessed by flow cytometry. Histograms show the fluorescence intensity of the Alexa 488 antibody alone (gray-filled), K68S pentamer (green) and WT pentamer (black) for 1×10^4 events. (B) Vero cells were transfected as previously described, treated with or without (inset) NeuNAc-GM1, fixed and stained over 23 days. Viral spread was quantified by scoring for cells expressing T-Ag. The average number of T-Ag positive cells is plotted from 3 independent experiments. (C) HEK cells were transfected as previously described, treated with or without (inset) NeuNAc-GM1, fixed and stained over 13 days. Viral spread was quantified as above. (D-F) HEK cells were incubated with purified His-tagged K68S or WT BKPyV pentamers and an Alexa Fluor 488 conjugated penta-His secondary antibody. Cells were fixed and pentamer binding to cells untreated (top), treated with NeuNAc-GM1 (middle) or treated with NeuNAc-GM1 and CTX (bottom) were assessed by flow cytometry. Histograms show the fluorescence intensity of the Alexa 488 antibody alone (gray-filled), K68S pentamer (green) WT pentamer (black) and K68S pentamer with CTX (blue) for 1×10^4 events.

CHAPTER 3

REGULATION OF BKPyV INFECTION BY PKC

Abstract:

The human polyomavirus BK is a clinically relevant virus that causes the diseases Polyomavirus Induced Nephropathy and Hemorrhagic Cystitis in immune suppressed kidney and bone marrow transplant patients. Following interaction with cell surface disialylated gangliosides, entry of BKPyV is mediated by caveolae endocytosis which is regulated by ganglioside localization and PKC activity. We investigate the role of PKC in BKPyV infection using the highly specific PKC inhibitor Bisindolylmaleimide I. We show that transient inhibition of PKC results in virus accumulation at the cells surface and an increase in membrane localization of PKC. Removal of inhibition results in enhanced virus uptake and increased infection, which is prevented by the addition of neutralizing antibody. Additionally, we demonstrate that the BKPyV ganglioside receptor GT1b stimulates increased endocytosis of BKPyV and in combination with PKC inhibition, causes a synergistic increase in infection. The data demonstrates that BKPyV infection is highly regulated by gangliosides and PKC.

Introduction

The human polyomavirus BK (BKPyV) is a member of the family Polyomaviridae. Polyomaviruses are non-enveloped double-stranded DNA (dsDNA) viruses (6,18). Additional human polyomaviruses include the well characterized JC virus (JCPyV), the recently identified Merkel cell polyomavirus (MCPyV), Karolinska Institute polyomavirus (KIPyV), Washington University polyomavirus (WUPyV), Human polyomavirus 6 (hPyV6), Human polyomavirus 7 (hPyV7), and Trichodysplasia-associated polyomavirus (1,6,11-13,18,31,37,38,46).

Initial infection with BKPyV is thought to occur early in childhood through the fecal-oral route (21,44). Following primary infection, BKPyV establishes a persistent asymptomatic infection in the epithelial tissue of the kidney (15,29,40). A combination of the host inflammatory response and the inherent lytic nature of BKPyV results in the development of diseases such as Polyomavirus Induced Nephropathy (PVN) in kidney transplant recipients and Hemorrhagic Cystitis (HC) in bone marrow transplant recipients (2,12,14,50).

Binding and entry are fundamental processes in viral pathogenesis. The process of BKPyV binding, entry and replication begins with engagement of $\alpha(2-3)$ -linked sialic acid on N-linked glycoproteins and as we demonstrate in Chapter 2 engagement of the disialic acid motif found on the disialogangliosides GD3, GD2, GD1b and GT1b (7,24). A proteinaceous receptor for BKPyV has not been identified. Following attachment, BKPyV enters cells by caveolae-mediated endocytosis to a low pH organelle (10,16,27). Once inside BKPyV traffics via an intact microtubule network to the Endoplasmic Reticulum (ER) where the capsid is destabilized (8,16,24,27). BKPyV escapes the ER

and the genome is trafficked to the nucleus where the viral genes are transcribed and replication is undertaken (9).

The signaling events that mediate uptake following attachment of BKPyV to gangliosides are not well understood. Tyrosine kinases are thought to be important for BKPyV infection. The non-specific tyrosine kinase inhibitor Genistein was demonstrated to reduce BKPyV infection (10). Protein Kinase C (PKC) has been shown to be important for glycosphingolipid stimulated caveolar endocytosis. A recent study demonstrated that inhibition of PKC reduced glycosphingolipid stimulated caveolar endocytosis of Bovine Serum Albumin (BSA) (39). Additionally the BKPyV disialylated gangliosides GD3, GD1b and GT1b are shown to specifically induce signaling events, in part, by modulating PKC activity (3,20,22,30,47). PKC has been shown to play a role in BKPyV infection by phosphorylating the BKPyV regulatory protein agnoprotein which plays a role in BKPyV viral propagation (17).

PKC is a family of serine/threonine (Ser/Thr) kinases. In general PKC has a c-terminal catalytic domain, which contains the ATP binding site, and an n-terminal regulatory domain, which contains the phospholipid and diacylglycerol (DAG) binding site (43,48,49). There are at least 12 isoforms of PKC that are closely related but have specific tissue distribution and function (43,48,49). These isoforms are subdivided into three groups based on their structural and functional properties. The groups include the conventional PKC isoforms (cPKC), the novel PKC isoforms (nPKC) and the atypical PKC isoforms (aPKC) (43,48,49). The cPKCs are (calcium) Ca^{2+} dependent, DAG sensitive, phosphatidylserine (PS) dependent and include the isoforms α , β I, β II and γ ; the nPKCs are Ca^{2+} independent, DAG sensitive, PS dependent and include the isoforms δ , ϵ ,

η , θ , and κ ; the α PKCs are Ca^{2+} independent, DAG insensitive PS dependent and include the isoforms ζ , and ι/λ (26,43).

In this report, we examine the role of PKC in BKPyV infection. Using the potent selective inhibitor of PKC, Bisindolylmaleimide I /GF109203X (GFX) we show that PKC is an important regulator of ganglioside stimulated endocytosis of BKPyV.

Materials and Methods

Cells and Virus Vero cells were purchased from the American Type Culture Collection (ATCC, Manassas, VA). They were maintained in a humidified 37°C incubator in Eagles Minimal Essential Medium (MEM) (Mediatech, Inc., Herndon, VA) supplemented with 5% heat inactivated fetal bovine serum (FBS) (Atlanta Biological, Lawrenceville, GA) and penicillin-streptomycin (Mediatech, Inc.). The BKV Dunlop strain used in these experiments was purchased from the (ATCC).

Antibodies, Inhibitors and Plasmids The PKC inhibitor Bisindolylmaleimide I was from (Calbiochem, Billerica, MA). Ganglioside GT1b was from (Matreya, Pleasant Gap, PA). The Alexa Fluor-conjugated 488 secondary antibody was from (Invitrogen, Carlsbad, CA). The monoclonal Anti- Protein Kinase C clone MC5 antibody was from (Sigma Aldrich, St. Louis, MO), and the GAPDH specific monoclonal antibody was from (Ambicon, Grand Island, NY). The IRDye infrared secondary dyes were from (Licor, Lincoln, NE).

Virus purification and labeling BKPyV was purified similar to previously published methods (28). After purification, BKPyV was labeled with Alexa Fluor 405 according to the manufacturer's instructions (Invitrogen). BKPyV was desalted by dialysis in 0.1 M bicarbonate buffer pH 8 using a HiTrap column (GE Healthcare). A volume of 1 mg/ml BKPyV was labeled by adding Alexa Fluor 405 dye at a ratio of 1µl dye to 250 µl virus. This was incubated at room temperature (RT) with rocking for 1 hour (hr). Excess dye was removed by dialysis using a HiTrap column.

Indirect immunofluorescence assay To detect expression of VP1, cells were fixed with 2% paraformaldehyde for 20 minutes at RT and permeabilized for 15 minutes in 1% Triton X-100. Cells were stained with the monoclonal antibody PAB 597 made against SV40, which cross-reacts with BKV. To detect staining of VP1, cells were stained with the secondary antibody Alexa Fluor-488 labeled goat anti-mouse antibody. Cells were observed using a Nikon epifluorescence microscope (Eclipse E800; Nikon, Inc).

Treatment with inhibitors To determine the effects of the PKC inhibitor Bisindolylmaleimide I on BKPyV infection, Vero cells were plated 40% confluent and the next day pretreated with various concentrations (0-40 μ M) of Bisindolylmaleimide I or the highest equivalent amount of Dimethyl Sulfoxide(DMSO) vehicle control in MEM supplemented with 5% FBS. Treatment was removed after 1 hr and cells infected in the presence of the respective concentrations of Bisindolylmaleimide I or DMSO vehicle control in MEM supplemented with 2% FBS. Following a 1 hr infection, the drug was removed and fresh 5% media added. Cells were incubated at 37°C for 72 hrs and analyzed by indirect immunofluorescence as described above.

To determine the effects of GT1b addition on Bisindolylmaleimide I treatment and removal, Vero cells were plated as described above and pre-incubated with 30 μ M ganglioside GT1b, DMSO or media for 17hrs at 37°C. Cells were washed and treated for 1 hr during infection with 20 μ M Bisindolylmaleimide I or DMSO. Cells were infected as described above for 1hr at 37°C. Following infection, the drug was removed and fresh media containing 5% FBS added. Cells were incubated and analyzed as described above.

To determine if Bisindolylmaleimide I blocks BKPyV infection, Vero cells were plated as before and infected with the Dunlop strain of BKPyV for 1 hr. Cells were treated during infection with 20 or 40 μ M Bisindolylmaleimide I or the equivalent DMSO vehicle control in MEM containing 2% FBS at 37°C. Following infection, the media was removed and the drug added back in MEM containing 5% FBS for 2 hrs at 37°C. After 2 hrs the drug treatment was removed and fresh growth media added containing neutralizing Anti-BKV serum (1:5000). Cells were incubated and analyzed as described above.

Fluorescence Microscopy To determine if GT1b enhances BKPyV uptake, Vero cells were plated 2.0×10^5 cells per 35mm cell culture Fluorodish (World Precision instruments, Sarasota, Florida) and treated with 30 μ M GT1b or left untreated for 17 hrs at 37°C. Cells were chilled for 30 minutes on ice and washed with cold 1X Phosphate Buffer Saline (PBS). Cells were pre-incubated with AF405-labeled BKPyV in unsupplemented media for 1 hr on ice. Cells were washed to remove unbound virus and refed with media containing 5% FBS. Cells were shifted to 37°C for 2 hrs. Following incubation, cells were fixed with 4% paraformaldehyde for 15 minutes at RT. BKPyV uptake was analyzed by acquiring Z stacks using a Zeiss LSM 710 confocal laser scanning microscope with a 63 \times 1.4 NA plan apochromat objective with the pinhole set to one Airy unit (Carl Zeiss). Viral entry was assayed using a quenching assay previously described (28). After the first Z-stack was taken trypan blue (0.4% w/v), (Invitrogen) was added to the wells containing 2ml of 1X PBS at a 1:50 dilution to quench extracellular fluorescence. The same Z-stack was taken post trypan blue addition to detect internalized

fluorescence. Images were combined into a single image, showing the maximal fluorescence, and processed using Image J image processing program. Intracellular fluorescence was quantified by analyzing at least 5 images in at least three experiments.

Immunoblot analysis of PKC Vero cells were treated with 20 or 40 μ M Bisindolylmaleimide I for 1 hr at 37°C in MEM supplemented with 2% FBS. Cells were washed with PBS, and harvested by mechanically scraping cells in PBS. Cells were collected as previously described with modifications (25). Cells were pelleted and resuspended in 100 μ l of cold 50 mM Tris (pH 7.6) with protease inhibitor cocktail and phosphatase inhibitor cocktail (Roche, Nutley, NJ) on ice. Samples were sonicated on a low-power setting on ice for 10 sec. and then pelleted at 17,770 \times g at 4°C for 20 minutes. Supernatants (cytosolic fraction) were removed and pellets (membrane fraction) were resuspended in an equal volume of cold Tris Buffer on ice. 30 μ l of cytosolic or membrane fraction was mixed with 10 μ l 4X Laemmli sample buffer (Bio-Rad, Hercules, CA). Samples were boiled at 95°C for 5 minutes, and resolved by SDS-PAGE on 4-15% Tris-Glycine gels (Bio-Rad). Proteins were transferred to polyvinylidene difluoride (PVDF) membranes (Millipore, Temecula, CA) using a semi-dry Trans Blot apparatus (Bio-Rad). Membranes were blocked in 5% milk-PBS for 30 minutes. The blots were processed using a SNAP i.d system (Millipore) as described in the system user guide. After the blot holders containing the blots were placed in the SNAP i.d. system, blocking buffer (1% BSA PBS-T) was added and the vacuum turned on. After the vacuum was turned off primary (PKC 1:1000) and GAPDH (1:10000) antibodies diluted in blocking buffer were added to the blot holders and incubated for 10 minutes at RT. The vacuum

was turned on for 1 minute and then the blots washed three times with 30ml PBS-T. After the vacuum was turned off, the blots were incubated with a Mouse IRDye 800 or Mouse Alexa fluor-680 conjugated secondary antibody diluted in blocking buffer for 10 minutes at RT. The vacuum was turned on and the blots washed as previously described. Membranes were rinsed in PBS and analyzed for protein signal using the LiCor Odyssey (LiCor Biosciences, Lincoln, NE). Images are shown in gray scale.

Results

Transient inhibition of PKC increases BKPyV infection. BKPyV exploits caveolae-mediated endocytosis for entry (10,27). PKC has been shown to be an important regulator of this endocytic pathway (39,41). Inhibition of PKC kinase activity has been shown to block caveolae invagination and ligand uptake (26,33,41). To determine if PKC is required for BKPyV infection we assessed the effect of the widely used and highly specific cell permeable PKC inhibitor Bisindolylmaleimide I (GFX) on BKPyV infection. Vero cells were pre-treated for 1 hr with various non-toxic concentrations (0-40 μ M) of GFX or the highest equivalent amount of DMSO. Following pre-treatment cells were infected for 1hr in the presence of the various respective concentrations of GFX or the highest equivalent amount of DMSO. Complete media was added back without GFX and infectivity assessed 72 hours post infection (HPI) by indirect immunofluorescence for the expression of VP1 (Fig. 1B). GFX is a reversible inhibitor and we exploit this trait by treating with the inhibitor during infection to reduce PKC activity followed by removal of drug treatment to re-establish PKC kinase activity. Upon quantification of VP1 expression we observed that when cells are treated with GFX followed by removal, infection was significantly enhanced with a direct correlation between the concentration of GFX used and the enhancement of infection (Fig. 1A). These results suggest that transient treatment with GFX may stimulate PKC kinase activity resulting in increased caveolae cycling and BKPyV uptake.

GT1b and Bisindolylmaleimide I synergize to increase infection. In chapter 2 we demonstrate that exogenous addition of the gangliosides GT1b increases BKPyV infection. B-series gangliosides such as GT1b have been shown to play a role in signal transduction and to regulate PKC activity in vitro by modulating its association with phospholipids such as phosphatidylserine (19,20). Additionally the exogenous addition of glycosphingolipids is shown to stimulate increased uptake of ligands that are endocytosed by caveolae-mediated endocytosis (4,39). This process is regulated in part by PKC activity which when inhibited blocks caveolae-mediated uptake (39). To evaluate the effects of GT1b on BKPyV uptake, Vero cells were supplemented with 30 μ M GT1b overnight or left untreated. Cells were chilled, washed and bound with Alexa-Fluor 405 labeled BKPyV in media supplemented with 2% FBS at 4°C for 1 hr. Cells were washed and complete media added without GFX. BKPyV was allowed to enter cells for 2 hrs at 37°C. Cells were fixed and the amount of virus internalized quantified by confocal microscopy using a Trypan blue assay previously described in the literature (Fig. 2A) (28,34). Quantification of viral internalization showed that GT1b significantly enhanced BKPyV uptake compared to the untreated control (Fig. 2B). This data demonstrates that GT1b as a functional receptor increases BKPyV infection by enhancing uptake. Additionally, it supports the finding that glycosphingolipids stimulate caveolae endocytosis.

Because GT1b enhanced BKPyV uptake and has been demonstrated to modulate PKC activity we wanted to assess the combined effects of the exogenous addition of GT1b and GFX treatment and removal (Fig 2C) (20,22). Vero cells were exogenously treated with 30 μ M GT1b and the equivalent volume of DMSO overnight. Cells were

washed and infected with BKPyV in the presence of media alone, 20 μ M GFX or the DMSO equivalent. Treatment with GFX or GT1b alone significantly increased BKPyV infection compared to the untreated control as previously demonstrated above and in Chapter 2 (Fig. 2C). When cells are treated with both GT1b and GFX followed by drug removal, we observed a synergistic increase resulting in a greater than 2 fold increase in infection compared to infection in the presence of the individual treatments (Fig. 2C). These data demonstrate that combining glycosphingolipid stimulation of endocytosis with GFX stimulation of endocytosis has an additive effect thus further supporting the idea that PKC regulates caveolae mediated BKPyV uptake and infection.

Bisindolylmaleimide I localizes PKC to the plasma membrane. GFX seems to be highly selective for cPKCs and nPKCs (42,45). cPKCs and nPKCs undergo a conformational change upon activation resulting in translocation to the plasma membrane (42,43). In un-stimulated cultured cells, a population of PKC is constitutively active and localized to caveolae domains (26,41). It has been shown that upon inhibition, with a potent inhibitor of caveolae internalization, this population of PKC no longer associates with caveolae lipid domains but becomes localized to the plasma membrane fraction (41). GFX is a state dependent inhibitor that stabilizes activated PKC and prolongs its association with the plasma membrane (42). We assessed the localization of PKC following GFX treatment by western blot with a pan-PKC antibody (Fig. 3). Vero cells were treated for 1 hr with 20 or 40 μ M GFX or the respective equivalent volume of DMSO in media supplemented with 2% FBS at 37°C. Cells were collected and fractionated into the cytosolic and particulate fraction and analyzed for PKC translocation

by western blotting (Fig. 3A). Quantification of signal intensity showed that GFX increased membrane association of PKC in a dose dependent manner (Fig. 3B). These data confirm that treatment with GFX prolongs PKC membrane association. We speculate that this membrane association of PKC may result in increased kinase activity once drug treatment is removed resulting in increased caveolae invagination and the observed enhanced infection.

Transient inhibition of PKC causes BKPyV accumulation at the plasma membrane. Since inhibition of PKC with GFX localizes PKC to the membrane and, as demonstrated in the literature, blocks membrane invagination, we wanted to assess if the increase in BKPyV infection was due to synchronization of BKPyV at the plasma membrane (33). To assess this, vero cells were treated during infection and for an additional 2 hrs with GFX or the respective equivalent DMSO control at 37°C. Drug treatment was removed and replaced with complete media supplemented with-BKPyV neutralizing serum to prevent the endocytosis of any virus remaining on the cell surface after the drug has been removed. Positive control cells were infected with BKPyV in the presence of media alone and maintained in media without anti-BKPyV neutralizing serum. Infectivity was assessed 72 HPI by indirect immunofluorescence for the expression of VP1 (Fig. 4B). Quantification of VP1 expression revealed a dose dependent decrease in BKPyV infection (Fig. 4A). This indicated that inhibition blocked BKPyV uptake as BKPyV was susceptible to antibody neutralization. The results support the idea that GFX blocks caveolae invagination and may indicate that BKPyV localized to the

exterior of the cell can be endocytosis upon removal of inhibition similar to the effects of a synchronized infection.

Discussion

Following engagement of cellular receptors, BKPyV is endocytosed by caveolae-mediated endocytosis. This process is tightly regulated by a network of signaling events which ensures the efficiency of viral internalization. Glycosphingolipids localize to caveolae domains and are facilitators of signal transduction. BKPyV engages the b-series gangliosides, which have been shown to modulate PKC Kinase activity. In this study we show that ganglioside mediated internalization of BKPyV is regulated by PKC.

Bisindolylmaleimide I is a state dependent ATP-competitive inhibitor, as such it competes with ATP and the PKC pseudo-substrate in the catalytic domain and blocks PKC kinase activity (42). Bisindolylmaleimide I seems to specifically inhibit cPKCs and nPKCs, which are shown to require membrane association for activation. We demonstrated that treatment of Vero cells with Bisindolylmaleimide I increased PKC membrane association (Fig. 3). Our data is consistent with previous research that has shown that Bisindolylmaleimide I prolongs PKC membrane association by stabilizing PKC in its active confirmation (42). This outcome was further confirmed in a study that showed that Bisindolylmaleimide I blocks vesicle trafficking and prevents PKC down regulation for degradation (33).

Exploiting the reversibility of inhibition with Bisindolylmaleimide I, we showed that transient inhibition of PKC increases BKPyV infection (Fig. 1 and Fig 2). This observation led us to speculate that the observed improved efficiency may likely be due to synchronization of both BKPyV on the exterior of the plasma membrane and caveolae

vesicle on the interior of the plasma membrane resulting in increased uptake and kinase activity once inhibition is removed. We demonstrated in support of this argument that in addition to increasing PKC membrane association (Fig.3), transient inhibition of PKC caused BkPyV accumulation at the plasma membrane making it susceptible to antibody neutralization (Fig.4). In addition to our findings, our speculation is supported by various studies characterizing caveolar cycling and PKC regulation of caveolae. One study showed that knocking down six key kinases, three of which are ser/thr kinases, reduces caveolar stability, increases multivalent caveolar assembly and reduces caveolar cycling leading to accumulation of caveolae at the membrane (32). Furthermore, studies with PKC α , which is constitutively present in caveolar domains shows that PKC α phosphorylation of a 90kDA substrate found in caveolae domains stimulates caveolae invagination. (26,33).

Glycosphingolipids stimulate caveolar endocytosis and this process had been demonstrated to be regulated by PKC (39). Several studies indicate a role for gangliosides in modulating PKC kinase activity. Some studies characterize gangliosides as negative regulators of PKC activity while others characterize them as positive regulators of PKC kinase activity. The discrepancy between the two observations may be attributed to differences in the signaling micro-environments where various gangliosides reside and to differences in cell type expression of signaling molecules in these micro-environments (47). The b-series gangliosides have been identified as potent inhibitors of PKC kinase activity in-vitro; this inhibition is reversed in the presence of phosphatidylserine which activates PKC (20). The enhanced uptake seen with GT1b may likely be due to conformational changes in caveolae that result in PKC associating with

phosphatidylserine at the plasma membrane. We demonstrate that the exogenous addition of GT1b increases BKPyV infection and uptake and synergistically increases BKPyV infection when combined with PKC inhibitor treatment and removal (Fig.2). This further supports the argument that the increase in infection efficiency seen with drug treatment and removal may be due in part to increased PKC activity and caveolae cycling.

This is the first study defining the role of PKC in BKPyV entry. It remains to be determined whether inhibition of PKC alters the distribution of the caveolae scaffolding domain protein caveolin-1 (Cav-1) during BKPyV infection and if GT1b can rescue uptake of BKPyV in the presence of PKC inhibition and antibody neutralization. Answering these questions would further strengthen the argument that PKC regulates caveolae-mediated BKPyV infection and further characterize the relationship between glycosphingolipid stimulated endocytosis and PKC. Additional areas of interest include the role of PKC in replication and transcriptional regulation. PKC has been previously shown to play a role late in BKPyV infection by phosphorylating the regulatory protein agnoprotein (17). This suggests a possible role for PKC in BKPyV virion assembly and release. Additionally, PKC has been shown to play a role in the activation of primary response genes during SV40 infection and as such PKC could also play a role in transcriptional regulation for BKPyV (5). The role of PKC in endocytosis and trafficking has also been studied in other viruses such as Influenza viruses and Respiratory Syncytial virus (RSV) (35,36). Interestingly inhibition of PKC blocks Influenza and RSV infection by blocking uptake and membrane fusion respectively indicating that PKC regulation of uptake may extend to multiple endocytic pathways (35,36).

Most isoforms of PKC are found distributed in the normal kidney tissue (23). A role for PKC in the pathology of organ transplant and kidney disease has been documented. Understanding the mechanism of BKPyV internalization is important as this could likely lead to the development of entry specific antiviral therapies. This could in turn improve prospects for patients who develop PVN or HC following reactivation of BKPyV.

In summary, we provide the first evaluation of a role for PKC in BKPyV endocytosis. Our data suggests that PKC is an important regulator of ganglioside mediated caveolae uptake of BKPyV.

LITERATURE CITED

1. **Allander, T., K. Andreasson, S. Gupta, A. Bjerkner, G. Bogdanovic, M.A. Persson, T. Dalianis, T. Ramqvist, B. Andersson.** 2007. Identification of a third human polyomavirus. *J Virol* **81**: 4130-6.
2. **Bedi, A., C.B. Miller, J.L. Hanson, S. Goodman, R.F. Ambinder, P. Charache, R.R. Arthur, R.J. Jones.** 1995. Association of BK virus with failure of prophylaxis against hemorrhagic cystitis following bone marrow transplantation. *J Clin Oncol* **13**: 1103-9.
3. **Chen, N., S. Furuya, H. Doi, Y. Hashimoto, Y. Kudo, H. Higashi.** 2003. Ganglioside/calmodulin kinase II signal inducing cdc42-mediated neuronal actin reorganization. *Neuroscience* **120**: 163-76.
4. **Choudhury, A., D.L. Marks, K.M. Proctor, G.W. Gould, R.E. Pagano.** 2006. Regulation of caveolar endocytosis by syntaxin 6-dependent delivery of membrane components to the cell surface. *Nature cell biology* **8**: 317-28.
5. **Dangoria, N.S., W.C. Breau, H.A. Anderson, D.M. Cishek, L.C. Norkin.** 1996. Extracellular simian virus 40 induces an ERK/MAP kinase-independent signalling pathway that activates primary response genes and promotes virus entry. *J Gen Virol* **77 (Pt 9)**: 2173-82.
6. **Delbue, S., M. Comar, P. Ferrante.** 2012. Review on the relationship between human polyomaviruses-associated tumors and host immune system. *Clin Dev Immunol* **2012**: 542092.
7. **Dugan, A.S., S. Eash, W.J. Atwood.** 2005. An N-linked glycoprotein with alpha(2,3)-linked sialic acid is a receptor for BK virus. *J Virol* **79**: 14442-5.
8. **Eash, S., W.J. Atwood.** 2005. Involvement of cytoskeletal components in BK virus infectious entry. *J Virol* **79**: 11734-41.
9. **Eash, S., K. Manley, M. Gasparovic, W. Querbes, W.J. Atwood.** 2006. The human polyomaviruses. *Cellular and molecular life sciences : CMLS* **63**: 865-76.

10. **Eash, S., W. Querbes, W.J. Atwood.** 2004. Infection of vero cells by BK virus is dependent on caveolae. *J Virol* **78**: 11583-90.
11. **Feng, H., M. Shuda, Y. Chang, P.S. Moore.** 2008. Clonal integration of a polyomavirus in human Merkel cell carcinoma. *Science* **319**: 1096-100.
12. **Gardner, S.D., A.M. Field, D.V. Coleman, B. Hulme.** 1971. New human papovavirus (B.K.) isolated from urine after renal transplantation. *Lancet* **1**: 1253-7.
13. **Gaynor, A.M., M.D. Nissen, D.M. Whiley, I.M. Mackay, S.B. Lambert, G. Wu, D.C. Brennan, G.A. Storch, T.P. Sloots, D. Wang.** 2007. Identification of a novel polyomavirus from patients with acute respiratory tract infections. *PLoS Pathog* **3**: e64.
14. **Hirsch, H.H.** 2002. Polyomavirus BK nephropathy: a (re-)emerging complication in renal transplantation. *Am J Transplant* **2**: 25-30.
15. **Hirsch, H.H., J. Steiger.** 2003. Polyomavirus BK. *Lancet Infect Dis* **3**: 611-23.
16. **Jiang, M., J.R. Abend, B. Tsai, M.J. Imperiale.** 2009. Early events during BK virus entry and disassembly. *J Virol* **83**: 1350-8.
17. **Johannessen, M., M.R. Myhre, M. Dragset, C. Tummler, U. Moens.** 2008. Phosphorylation of human polyomavirus BK agnoprotein at Ser-11 is mediated by PKC and has an important regulative function. *Virology* **379**: 97-109.
18. **Johne, R., C.B. Buck, T. Allander, W.J. Atwood, R.L. Garcea, M.J. Imperiale, E.O. Major, T. Ramqvist, L.C. Norkin.** 2011. Taxonomical developments in the family Polyomaviridae. *Arch Virol* **156**: 1627-34.
19. **Kasahara, K., Y. Sanai.** 2000. Functional roles of glycosphingolipids in signal transduction via lipid rafts. *Glycoconj J* **17**: 153-62.
20. **Katoh, N.** 1995. Inhibition by gangliosides GM3, GD3 and GT1b of substrate phosphorylation by protein kinase C in bovine mammary gland and its reversal by phosphatidylserine. *Life sciences* **56**: 157-62.

21. **Knowles, W.A.** 2006. Discovery and epidemiology of the human polyomaviruses BK virus (BKV) and JC virus (JCV). *Advances in experimental medicine and biology* **577**: 19-45.
22. **Kreutter, D., J.Y. Kim, J.R. Goldenring, H. Rasmussen, C. Ukomadu, R.J. DeLorenzo, R.K. Yu.** 1987. Regulation of protein kinase C activity by gangliosides. *J Biol Chem* **262**: 1633-7.
23. **Li, J., G. Gobe.** 2006. Protein kinase C activation and its role in kidney disease. *Nephrology* **11**: 428-34.
24. **Low, J.A., B. Magnuson, B. Tsai, M.J. Imperiale.** 2006. Identification of gangliosides GD1b and GT1b as receptors for BK virus. *J Virol* **80**: 1361-6.
25. **Maginnis, M.S., S.A. Haley, G.V. Gee, W.J. Atwood.** 2010. Role of N-linked glycosylation of the 5-HT_{2A} receptor in JC virus infection. *J Virol* **84**: 9677-84.
26. **Mineo, C., Y.S. Ying, C. Chapline, S. Jaken, R.G. Anderson.** 1998. Targeting of protein kinase Calpha to caveolae. *The Journal of cell biology* **141**: 601-10.
27. **Moriyama, T., J.P. Marquez, T. Wakatsuki, A. Sorokin.** 2007. Caveolar endocytosis is critical for BK virus infection of human renal proximal tubular epithelial cells. *J Virol* **81**: 8552-62.
28. **Nelson, C.D., A. Derdowski, M.S. Maginnis, B.A. O'Hara, W.J. Atwood.** 2012. The VP1 subunit of JC polyomavirus recapitulates early events in viral trafficking and is a novel tool to study polyomavirus entry. *Virology* **428**: 30-40.
29. **Nickeleit, V., H.H. Hirsch, I.F. Binet, F. Gudat, O. Prince, P. Dalquen, G. Thiel, M.J. Mihatsch.** 1999. Polyomavirus infection of renal allograft recipients: from latent infection to manifest disease. *J Am Soc Nephrol* **10**: 1080-9.
30. **Ortaldo, J.R., A.T. Mason, D.L. Longo, M. Beckwith, S.P. Creekmore, D.W. McVicar.** 1996. T cell activation via the disialoganglioside GD3: analysis of signal transduction. *Journal of leukocyte biology* **60**: 533-9.

31. **Padgett, B.L., D.L. Walker, G.M. ZuRhein, R.J. Eckroade, B.H. Dessel.** 1971. Cultivation of papova-like virus from human brain with progressive multifocal leucoencephalopathy. *Lancet* **1**: 1257-60.
32. **Pelkmans, L., M. Zerial.** 2005. Kinase-regulated quantal assemblies and kiss-and-run recycling of caveolae. *Nature* **436**: 128-33.
33. **Prevostel, C., V. Alice, D. Joubert, P.J. Parker.** 2000. Protein kinase C(alpha) actively downregulates through caveolae-dependent traffic to an endosomal compartment. *J Cell Sci* **113 (Pt 14)**: 2575-84.
34. **Rejman, J., V. Oberle, I.S. Zuhorn, D. Hoekstra.** 2004. Size-dependent internalization of particles via the pathways of clathrin- and caveolae-mediated endocytosis. *Biochem J* **377**: 159-69.
35. **Root, C.N., E.G. Wills, L.L. McNair, G.R. Whittaker.** 2000. Entry of influenza viruses into cells is inhibited by a highly specific protein kinase C inhibitor. *J Gen Virol* **81**: 2697-705.
36. **San-Juan-Vergara, H., M.E. Peeples, R.F. Lockey, S.S. Mohapatra.** 2004. Protein kinase C-alpha activity is required for respiratory syncytial virus fusion to human bronchial epithelial cells. *J Virol* **78**: 13717-26.
37. **Schowalter, R.M., D.V. Pastrana, K.A. Pumphrey, A.L. Moyer, C.B. Buck.** 2010. Merkel cell polyomavirus and two previously unknown polyomaviruses are chronically shed from human skin. *Cell host & microbe* **7**: 509-15.
38. **Scuda, N., J. Hofmann, S. Calvignac-Spencer, K. Ruprecht, P. Liman, J. Kuhn, H. Hengel, B. Ehlers.** 2011. A novel human polyomavirus closely related to the african green monkey-derived lymphotropic polyomavirus. *J Virol* **85**: 4586-90.
39. **Sharma, D.K., J.C. Brown, A. Choudhury, T.E. Peterson, E. Holicky, D.L. Marks, R. Simari, R.G. Parton, R.E. Pagano.** 2004. Selective stimulation of caveolar endocytosis by glycosphingolipids and cholesterol. *Molecular biology of the cell* **15**: 3114-22.

40. **Shinohara, T., M. Matsuda, S.H. Cheng, J. Marshall, M. Fujita, K. Nagashima.** 1993. BK virus infection of the human urinary tract. *J Med Virol* **41**: 301-5.
41. **Smart, E.J., Y.S. Ying, R.G. Anderson.** 1995. Hormonal regulation of caveolae internalization. *The Journal of cell biology* **131**: 929-38.
42. **Smith, I.M., N. Hoshi.** 2011. ATP competitive protein kinase C inhibitors demonstrate distinct state-dependent inhibition. *PloS one* **6**: e26338.
43. **Steinberg, S.F.** 2008. Structural basis of protein kinase C isoform function. *Physiological reviews* **88**: 1341-78.
44. **Stolt, A., K. Sasnauskas, P. Koskela, M. Lehtinen, J. Dillner.** 2003. Seroepidemiology of the human polyomaviruses. *J Gen Virol* **84**: 1499-504.
45. **Toullec, D., P. Pianetti, H. Coste, P. Bellevergue, T. Grand-Perret, M. Ajakane, V. Baudet, P. Boissin, E. Boursier, F. Loriolle, et al.** 1991. The bisindolylmaleimide GF 109203X is a potent and selective inhibitor of protein kinase C. *J Biol Chem* **266**: 15771-81.
46. **van der Meijden, E., R.W. Janssens, C. Lauber, J.N. Bouwes Bavinck, A.E. Gorbalenya, M.C. Feltkamp.** 2010. Discovery of a new human polyomavirus associated with trichodysplasia spinulosa in an immunocompromized patient. *PLoS Pathog* **6**: e1001024.
47. **Wang, X.Q., P. Sun, A.S. Paller.** 2002. Ganglioside modulation regulates epithelial cell adhesion and spreading via ganglioside-specific effects on signaling. *J Biol Chem* **277**: 40410-9.
48. **Way, K.J., E. Chou, G.L. King.** 2000. Identification of PKC-isoform-specific biological actions using pharmacological approaches. *Trends in pharmacological sciences* **21**: 181-7.
49. **Webb, B.L., S.J. Hirst, M.A. Giembycz.** 2000. Protein kinase C isoenzymes: a review of their structure, regulation and role in regulating airways smooth muscle tone and mitogenesis. *British journal of pharmacology* **130**: 1433-52.

50. **Xie, Y., Y. Han, D.P. Wu, A.N. Sun, J.N. Cen, L. Yao, C.G. Ruan.** 2009. [The BK virus load in urine in association with the development of hemorrhagic cystitis after hematopoietic stem cell transplantation]. *Zhonghua Xue Ye Xue Za Zhi* **30**: 524-7.

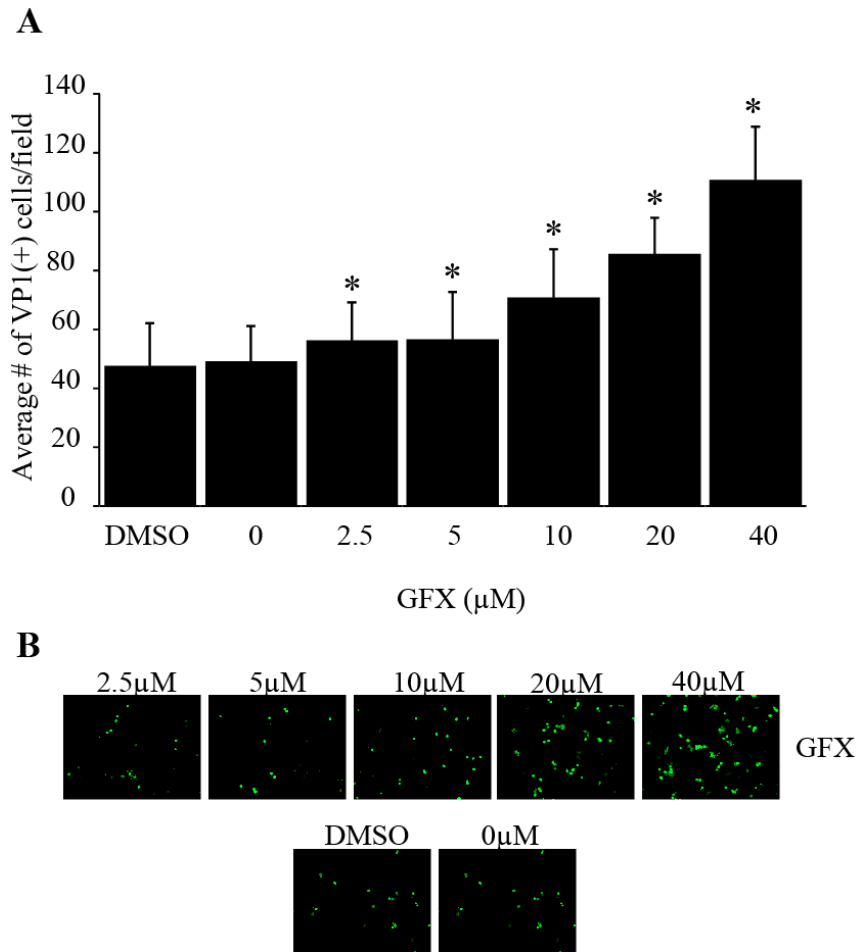


Figure 1: Transient inhibition of PKC increases BKPyV infection. (A) Vero cells were pre-treated and infected in the presence of GFX (0-40µM) for 1 hr at 37°C. After infection, cells were refed with growth media. Cells were fixed and infection scored by indirect immunofluorescence for VP1 expression 72 hrs post-infection. The data represents the number of VP1 positive cells in each field of view for 8 non-overlapping random fields of view for three replicate experiments. Error bars indicate standard deviation (*p<.05 compared to the DMSO control). (B) Representative indirect immune-fluorescence images of VP1 positive cells.

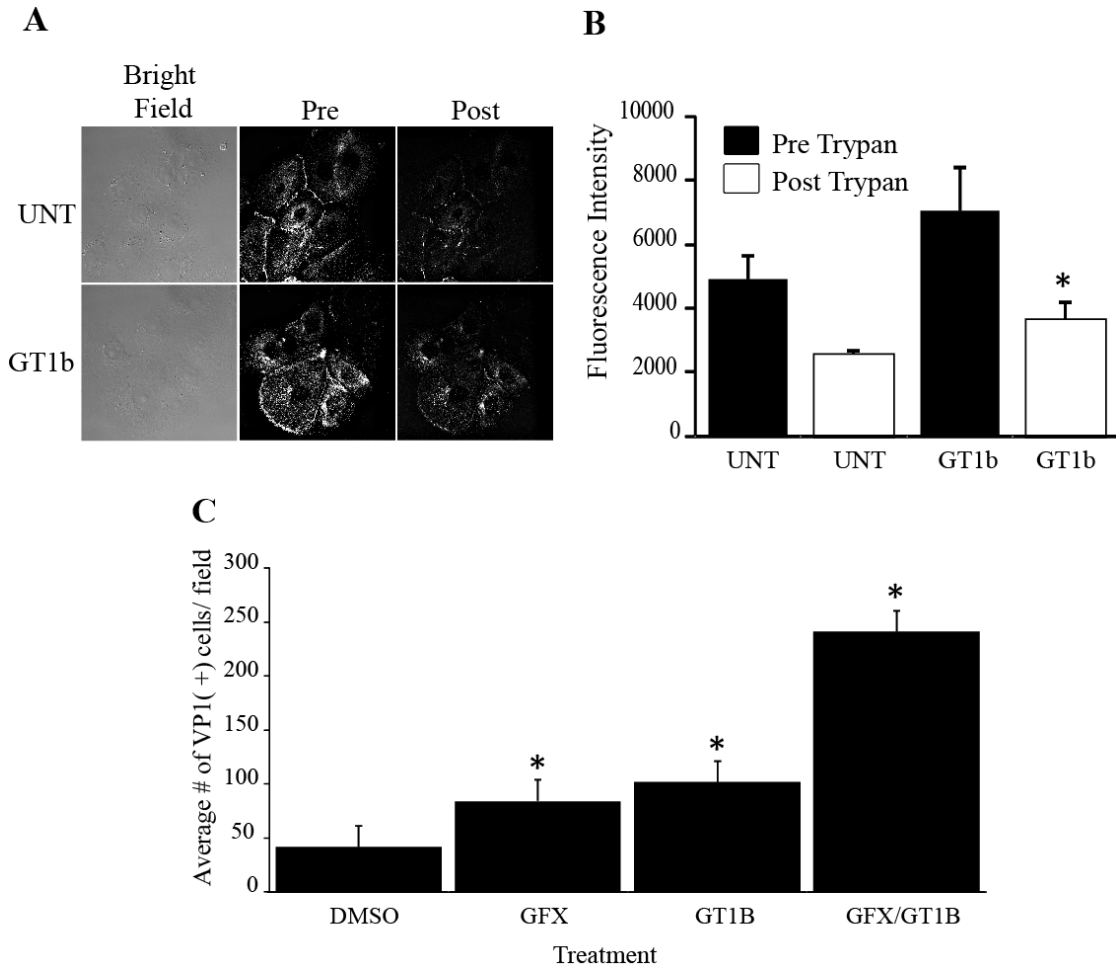


Figure 2: GT1B and GFX synergize to further enhance BKPyV infection (A) Vero cells were supplemented with 30 μ M of GT1b or left untreated for 17 hrs at 37°C. Following supplementation cells were chilled and bound with labeled BKPyV for 1 hr at 4°C. Cells were washed and incubated for 2 hrs at 37°C. Cells were fixed and imaged by confocal microscopy (pre) to detect fluorescence. After imaging, extracellular fluorescence was quenched with Trypan blue and the same sample re-imaged to detect internalized BKPyV (post). (B) Endocytosis was quantified using Image J imaging software by outlining at least 5 individual cells per sample from three replicate experiments and determining fluorescence intensity. (C) Vero cells were supplemented as above and treated during infection with 20 μ M GFX or DMSO for 1 hr at 37°C. After infection, cells were incubated with growth media. Cells were fixed and infection scored by indirect immunofluorescence for VP1 expression 72 hrs post-infection. The data represents the number of VP1 positive cells in each field of view for 8 non-overlapping random fields of view for three replicate experiments. Error bars indicate standard deviation (*p<.05 compared to the mock treated (UNT) in panel A and B or DMSO control in panel C).

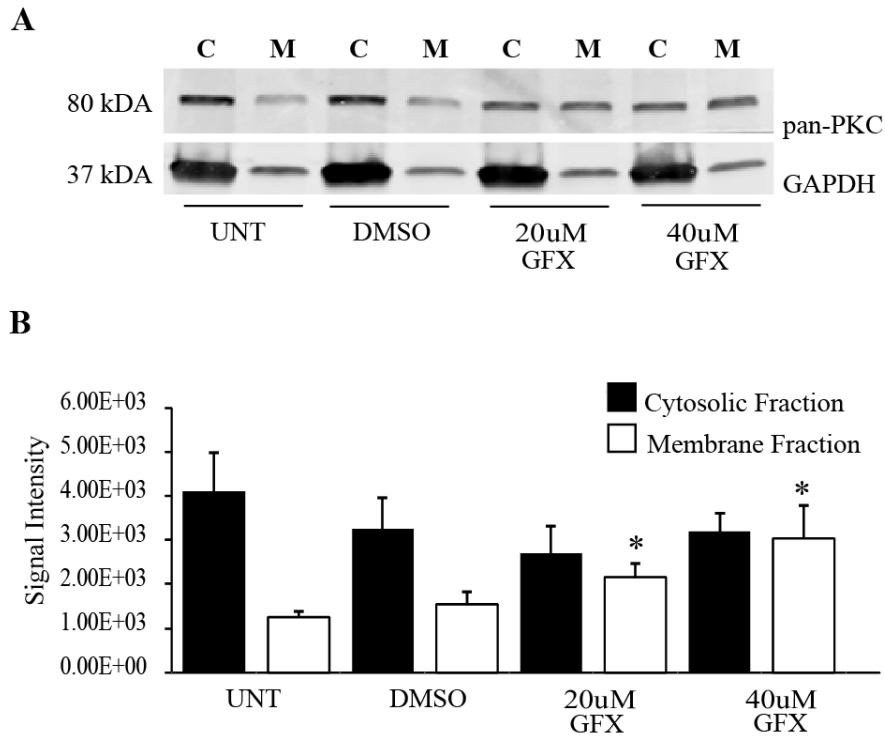


Figure 3: Inhibition of PKC causes membrane localization. Vero cells were treated with GFX (20 or 40 μ M), the vehicle or mock treated (UNT). Cells were harvested after 1 hr and the cell lysates fractionated into cytosolic (C) and membrane (M) fractions. Fractions were resolved by SDS-PAGE, transferred to a PVDF membrane and blotted using a pan-PKC mouse monoclonal antibody or a GAPDH mouse monoclonal antibody as a cytosolic marker to determine fractionation efficiency and an anti-mouse IR-800CW or Alexa 680 antibody respectively (A). Membranes were analyzed using a LiCor Odyssey and are shown in gray scale. The bar graphs are the absolute optical density (OD) volume PKC (B). The data shown are mean from three separate experiments. Error bars represent standard deviation for three independent experiments and asterisks the p-value (* $p < .05$ compared the respective DMSO control).

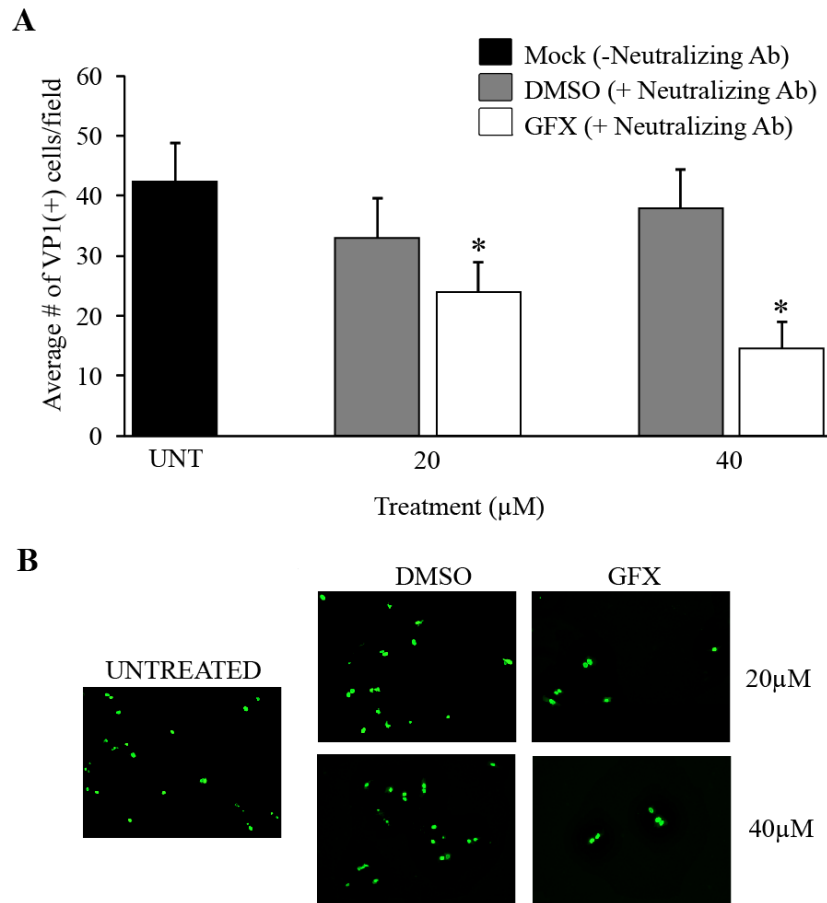


Figure 4: Inhibition of PKC causes BKPyV accumulation in an antibody sensitive location. (A) Vero cells were infected in the presence of 20 or 40µM of GFX for 1 hr at 37°C. After infection cells were treated with media containing 20 or 40µM of GFX for an additional 2 hrs. Cells were refed with growth media supplemented with anti-BKPyV neutralizing serum. Cells were fixed and infection scored by indirect immunofluorescence for VP1 expression 72 hrs post – infection. The data represents the number of VP1 positive cells in each field of view for 8 non-overlapping random fields of view for three replicate experiments. Error bars indicate standard deviation (*p<.05 compared to the DMSO control). (B) Representative indirect immunofluorescence images of VP1 positive cells.

CHAPTER 4

DISCUSSION & FUTURE DIRECTIONS

BKPyV engagement of b-series gangliosides

The first aim of this dissertation was to determine the binding epitope for BKPyV on gangliosides GD1b and GT1b. The prerequisite for successful viral infection includes: engagement of cellular receptor(s), penetration of the plasma membrane and finally deposit of the viral genome at the site of replication. Previous research revealed that BKPyV engages cells via $\alpha(2-3)$ -linked sialic acid on N-linked glycoprotein (s) and uses gangliosides GD1b and GT1b, which are branched structures, as receptors (7,21). Additionally, it was shown that BKPyV binding and infection of cells is specifically dependent on the $\alpha(2-3)$ sialic acid linkage (8). This is interesting as the independent finding that gangliosides GD1b and GT1b are receptors, further supports this observation because both gangliosides have at least one $\alpha(2-3)$ linkage in their structures (21). We show that in addition to the previously identified receptors, gangliosides GD2 and GD3 can also serve as receptors for BKPyV. We observed that GD2, GD3, GD1b and GT1b which are members of the b-series group of gangliosides share a common disialic acid motif on the right arm of their structures.

The interaction between sialic acid and the outer loops of BKPyV has been characterized using the prototypical polyomaviruses MPyV and SV40 (29,41-43). These studies serve as models for the characterization of BKPyV with its sialic acid containing receptors. Using the insight gained from the characterization of SV40, Dugan *et. al.* determined that a collection of amino acid residues on the outer loops of BKPyV predicted by molecular model to engage sialic acid are critical for viability and growth, as mutations of a subset of these amino acids significantly reduced or abolished binding

and growth (9). Additionally, this study highlighted the importance of the BC loop of BKPyV for engagement of sialic acid as a majority of the defective mutants were localized to this loop (9). Using crystallographic studies, we not only characterized the engagement of BKPyV VP1 with sialic acid but determined that the common disialic acid motif of b-series gangliosides directly engages the outer loops (BC, HI and DE) of BKPyV VP1. Characterizing the interaction of the individual sialic acids showed that the terminal sialic acid is the primary interacting sialic acid and makes extensive contacts with BKV VP1 similar to predicted model of sialic acid interaction proposed by Dugan *et. al.* (9). Sialic acid has four functional groups (carboxylate, hydroxyl, N-Acetyl and the glycerol group) that engage BKPyV VP1. To evaluate the importance of terminal sialic acid engagement of BKPyV VP1 we used the structural information generated from the crystal structure of BKPyV VP1 with the disialic acid motif to make more informed decisions regarding what amino acids to mutate. As expected when we mutated specific amino acids residues on BKPyV VP1 that primarily interact with the functional groups of the terminal sialic acid, we observed that BKPyV no longer grows or has significantly reduced growth.

Engagement of terminal sialic acid is conserved for the closely related human polyomavirus JCPyV and the non human polyomavirus SV40. SV40 engages cells via GM1, which has a terminal $\alpha(2-3)$ linked sialic and JCPyV engages cells via the lactoseries tetrasaccharide c (LSTc) motif which contains an $\alpha(2-6)$ linked sialic (28,48). SV40 and JCPyV VP1 share significant sequence homology and their crystal structures reveal that they have similar receptor binding pockets which presumably accounts for the fact that they bind sialic acid in a similar position and orientation (28,29). Beyond the

human polyomaviruses, engagement of sialic acid seems to be an important requirement for a number of human pathogens such as Human Rotavirus, which is the leading cause of gastroenteritis in children, and Influenza which is highly contagious and potentially deadly (27,38,46). A recent review compared engagement of terminal sialic acid by the viral attachment proteins of 3 polyomaviruses and 7 additional viruses that share no homology, differ in their viral envelope, and genome type. This study revealed that despite these differences, sialic acid interacted with the various attachment proteins in a similar orientation (27). Furthermore, the conserved orientation was found to be strongly influenced by conserved intermolecular interactions between amino acids on the attachment proteins and two function groups on sialic acid. These interactions involve hydrogen bonds or a salt bridge between an amino acid and the carboxylate group and the interaction between an amino acid and the nitrogen of the N-Acetyl group (27). Both interactions are conserved in BKPyV engagement of terminal sialic acid. The widespread use and conserved engagement of sialic acid may suggest that while evolutionary pressure may have influenced changes in receptor types in humans, pathogens have evolved to take advantage of this common functional component for attachment.

In addition to characterizing BKPyV engagement of terminal sialic acid, we also evaluated the influence of the second sialic acid for BKPyV binding. Previous research has shown that small differences in the sequence homology of the VP1 binding region define receptor specificity (22,27,28). Neu et. al compared the receptor binding site of JCPyV VP1 and SV40 VP1 and found that unique amino acid differences between JCPyV and SV40 dictate how each virus' respective receptor interacts with the binding site (28). Additionally, a study to characterize how changes to the receptor binding site of

SV40 influence receptor usage and tropism found that a small number of mutations in the SV40 binding region can switch SV40 receptor usage from GM1 to some unknown receptor, and also change the viral tropism. By comparing the respective ganglioside engagement of BKPyV VP1 and SV40 VP1 we determined that a single amino acid residue is a major determinant of receptor specificity for BKPyV. Lysine 68 (K68) in the BKPyV VP1 binding pocket interacts via a salt bridge with the internal sialic acid of the disialic acid motif and influences BKPyV engagement of disialic acid containing gangliosides. Previous characterization of K68 by Dugan et.al, showed that mutation of K68 to an Alanine (A) resulted in reduced binding and growth highlighting its importance in BKPyV viability (9). A comparison of this amino acid residue in SV40 and JCPyV shows that while the corresponding amino acid residue differs from BKPyV it is conserved for both SV40 and JCPyV as a Serine 68 (S68) (28,29). To evaluate the role of this amino acid in determining receptor specificity, we mutated residue K68 to S68 in BKPyV VP1. This mutation resulted in a receptor switch from GD3 to GM1 as demonstrated by STD-NMR, Glycan array screen and flow cytometry. The most striking observation however was that even though K68S retain some binding to the normally permissive African Green Monkey Kidney Cells (Vero cells), when tested for its ability to grow in cell culture, it could no longer grow Vero cells. The mutant however grew in Human Embryonic Kidney (HEK) cells. These results indicate that not only does the amino acid K68 influence receptor specificity, but it also influences species specificity for BKPyV. Our observations support the idea that recognition of different sialic acid types influences changes in tissue and host tropism and range (22,27).

Characterization of SV40 with potential carbohydrate receptors revealed that recognition of sialic acid variants can influence species tropism. SV40 interacts with two analogs of GM1, which confer different sialic acid types. SV40 binds with high specificity to the N-Glycolyl GM1 analog, which is expressed by simians, compared to its binding to the N-Acetyl analog of GM1, which is the predominant sialic acid type in humans (3,26,49,50). Structural analysis of SV40 binding to GM1 showed that while both analogues of GM1 can interact with the VP1 surface without creating steric hindrance, the binding of the N-Glycolyl analog produced more efficient binding, which may be explained by the relatively large hydrophobic cavity that accommodates the large N-Glycolyl functional group of the N-Glycolyl GM1 analog (3,22,27). BKPyV being a human virus likely interacts more favorably with the N-Acetyl analogy of b-series or GM1 receptor types. Additionally, the hydrophobic pocket of BKPyV is much smaller than that of SV40 and may likely be better suited to accommodate the smaller N-Acetyl functional group of N-Acetyl GM1 or b-series analogs. This may explain in part, why the K68S mutation has such restricted species tropism and when evaluated by glycan array screen was observed to bind specifically to the N-Acetyl analog of GM1. The human polyomavirus JCPyV also has a small hydrophobic cavity, which further supports the idea that the structure of VP1 influences recognition of sialic acid variants and species tropism (27,28). This structure-function relationship of neuraminic acid and VP1 has also been evaluated with MPyV and the results support the aforementioned points, as substitution of the N-Acetyl functional group of neuraminic acid with various analogs showed variable effects on growth depending on the type of modification (12,18).

In addition to influencing receptor specificity and species tropism, mutations in the BKPyV binding site have been hypothesized to influence risk factors for the development of PVN. Studies to characterize mutations in VP1 sequences of various BKPyV strains from the urine of kidney transplant recipients who were diagnosed or not diagnosed with PVN revealed that amino acid changes were present in both groups (19,47). These studies found no link between amino acid changes and PVN or increased viral load in renal transplant patients (19,47). However in one particular study, it was observed that a common mutation at K68 was exclusively found in samples from PVN patients (47). The prevalent substitution observed is a Lysine to an Arginine (K68R) (47). Though they differ in their side chains, both Lysine and Arginine have positively charged polar side chains. It is not clear why a mutation at this site is commonly found in PVN urine samples. It is possible that the Arginine mutation simply maintains the interaction of BKPyV VP1 with the internal sialic acid of the disialic acid motif on b-series gangliosides and thus confers no advantage for receptor interactions. On the other hand the mutation could enhance the interaction to the disialic acid motif or allow for interaction with a different receptor(s) thus improving the virus' receptor repertoire and refining the requirements for tissue tropism. Modification of the K68 in BKPyV VP1 could therefore serve as a risk factor for reactivation and predispose a renal transplant patient to PVN.

Though we identified additional disialic acid containing gangliosides as receptors, the previously identified gangliosides GD1b and GT1b are more efficient receptors for BKPyV. Both gangliosides share a common (Gal-(β 1,3)-GalNac) branch, also known as the left arm, similar to the left arm of SV40 GM1. Previous research with GM1 showed

that this left arm interacts with residues in the HI and BC loop of VP1(29). Comparison of the interaction between BKPyV VP1 with GD1b, which has the most similar structure in the left arm and SV40 with GM1, showed that while the amino acid profile in the binding pocket is conserved, there are considerable differences in the amino acid profile in the peripheral of VP1. Interestingly, this is the region where the left arm interacts with VP1. Additionally, a comparison of the BKPyV strains revealed that only a few amino acid differences exist between the strains, which localize to the periphery of the binding pocket. These differences between BKPyV and SV40, and the strains of BKPyV may alter receptor specificity and affinity. To evaluate the importance of the left arm for influencing receptor specificity and BKPyV viability we mutated a small number of amino acids that were predicted to interact with the galactose of the left arm. A few amino acids in this region that were predicted to involve engagement of the left arm were previously characterized by Dugan *et. al.* and found to either have no effect or reduced infection when mutated. When we mutated two amino acid residues that interact with the galactose of the left arm there was no change or a moderate reduction in the growth of BKPyV. These results indicate that interaction with the left arm may primarily influence receptor affinity.

It is quite striking that BKPyV has the ability to use multiple receptor subtypes. Though the binding affinity of BKPyV to each subtype may vary, collectively the presence of the various subtypes may improve the avidity of interaction. Additionally the multiple subtypes, may influence the age of sero-conversion, the site of infection and subsequent pathogenesis. The b-series gangliosides have been shown to be differentially expressed at various times during development in rat and bovine, with the simpler

gangliosides being expressed in fetal development and in newborns and the more complex gangliosides (GD1b and GT1b), being expressed at a more mature age (14,54). This developmental expression pattern may explain why sero-conversion primarily occurs in childhood and not during the neonatal years. In addition to developmental expression, the b-series ganglioside subtypes have been shown have varied cell type expression and localization within the kidney (14). This may also influence how well BKPyV can propagate in various cells types and within the various segments of the genitourinary tract. Finally, various ganglioside receptors have been shown to localize to specific lipid raft domain with a tightly regulated group of signaling molecules (4,52,53). By engaging multiple receptor subtypes, BKPyV can potentially sequentially activate multiple signally pathways, thus improving the chances of a productive infection.

Future studies will evaluate whether mutations made to disrupt the interaction of the left arm of GD1b with BKPyV VP1 that have reduced growth also disrupt binding to cells. Also since the glycan array indicated that the K68S mutation still has weak interactions with GD1b, it would be interesting to see the effect of supplementing human and monkey cells with GD1b on K68S growth and binding. Another area of interest for future studies includes evaluating amino acid changes in urine isolates from PVN patients. Because K68 defines receptor specificity, and this amino acid residue is mutated to an arginine in urine samples from PVN patients, we would like to characterize the effects of this mutation for binding to b-series gangliosides, and growth in both human and monkey cells. Finally, because a small number of amino acid interactions play such a critical role in determining receptor specificity and engagement, we are interested in

comparing the four subtypes of BKPyV to evaluate how the amino acid differences influence binding to b-series gangliosides.

PKC regulation of BKPyV entry

The second aim of this dissertation was to investigate ganglioside mediated signaling events in BKPyV entry. Viruses exploit the coordinated signaling machinery used by cells to communicate information from the exterior of the cell to the interior of the cell. Virus engagement of cellular receptors triggers signals that lead to internalization and subsequent replication of their viral genomes. Caveolae raft domains are enriched with signaling molecules and are thought to be platforms for signal transduction. A number of studies have evaluated the molecular signaling mechanisms of caveolae endocytosis and have demonstrated that caveolae mediated endocytosis is highly regulated by tyrosine kinases and serine threonine kinases (5,30-32,35,36,39). Tyrosine kinases and Ser/Thr kinases have been shown to directly interact with caveolins, which negatively regulate their activity in the absence of cargo or a stimulus (2,36).

Tyrosine kinases are enriched in caveolae and influence recruitment or exclusion of signaling molecules to caveolae domains (2,16,45). They have been shown to regulate the release and internalization of caveolae vesicles by phosphorylating caveolin-1, caveolin-2 and dynamin-2 (32,45). Previous research shows that as pathogens that rely on caveolae-mediated endocytosis for entry, both BKPyV and SV40 require tyrosine kinase activity for infection. For example, both BKPyV and SV40 infection are inhibited in the presence of the tyrosine kinase inhibitor Genistein (1,5,10). Like tyrosine kinases, Ser/Thr kinase signaling seems to be compartmentalized to caveolae as multiple isoforms of PKC, for example, have been observed to be localized to caveolae domains (24,40). Compared to tyrosine kinases, Ser/Thr kinases have been less characterized for their role

in caveolae mediated endocytosis. Pelkman et al showed that silencing of the ser/thr kinases ARF1, KIAA0999 and MAP3K2 cause instability of caveolin-1 and reduced caveolae cycling and SV40 uptake (33). Additionally, Sharma et al. and Prevostel et al demonstrated that the inhibition of PKC blocks glycosphingolipid stimulated caveolar endocytosis by blocking caveolae invagination (39).

PKC has been the most extensively characterized with regards to Ser/Thr kinase regulation of caveolae mediated endocytosis. Because of this, PKC was selected for evaluation as a ser/thr kinase that regulates BKPyV uptake. PKC has been demonstrated to play a role late in BKPyV infection by phosphorylating the regulatory protein Agnoprotein (15). Additionally, previous research established a role for PKC in polyomavirus SV40 induced signaling and activation of primary response genes that influence SV40 uptake (6). To evaluate the relationship between PKC and BKPyV infection we transiently inhibited PKC kinase activity using a highly selective ATP competitive kinase inhibitor, Bisindolylmaleimide I. We believe that transient inhibition stimulates PKC activity, which in turn regulates caveolae endocytosis. Our reasoning is supported by work from Mineo *et. al.* which showed that a 90kDa substrate is specifically phosphorylated in caveolae domains by PKC α during invagination. Additionally, Smart et. al showed that upon PKC α inhibition, PKC α was displaced from caveolae domains but once the drug was removed, PKC α returned to caveolae domains (24,40). The result of this experiment revealed that transient inhibition of PKC increased BKPyV infection and localized PKC to the membrane during inhibition. These combined observations support our hypothesis and indicates that PKC regulates BKPyV infection through its spatial location and its modulation of vesicle trafficking.

We then wanted to more specifically evaluate the effects of PKC inhibition on BKPyV uptake. To evaluate this, we transiently inhibited PKC activity and used a BKPyV neutralizing antibody to prevent uptake of virus not endocytosed during PKC inhibition. We speculated that if inhibition of PKC blocks caveolae uptake, then it should block BKPyV uptake also. Additionally, previous research showed that use of Bisindolmaleimide I blocks caveolae invagination and trafficking (34). We demonstrated that inhibition of PKC activity during the time course of BKPyV entry blocked BKPyV uptakes and infection. This was observed because BKPyV was susceptible to anti-BKPyV antibody neutralization. This indicates that transient inhibition of PKC may cause BKPyV accumulation at the plasma membrane. Taken together, it is possible that PKC inhibition and removal creates the perfect storm of virus synchronization on the outside of the cell and PKC localization at the plasma membrane leading to the observed increase in infection.

The function of glycosphingolipids in signaling and endocytosis has been well characterized. A recent study with ganglioside GM1 showed that the structure of glycosphingolipids influences membrane invagination (11). This supports the idea that glycosphingolipids mediate signal transduction through their tails (16). Additionally, antibody crosslinking, and ligand crosslinking of glycosphingolipids causes redistribution of signaling molecules in caveolae domains resulting in efficient crosstalk among signaling pathways (16). The addition of exogenous gangliosides can mimic the effects of antibody or ligand crosslinking and induce changes in the localization and conformation of signaling molecules (39). Interestingly, a review of the literature indicates that disialogangliosides interact with and modulate PKC activity (17,20,23,53).

Disialogangliosides have been shown to stimulate calcium release from intracellular stores which is particularly significant because the activation of the cPKCs and nPKCs require calcium (4,16). In the presence of increased intracellular calcium cPKCs and nPKCs are activated when calcium binding increases their affinity for membranes (37,44). Disialogangliosides have also been shown to interact with PKC and inhibit its activity. However this effect is reversed in the presence of phosphatidylserine (17).

We demonstrated in Chapter 2 that the disialogangliosides can increase BKPyV infection. We evaluate how the disialoganglioside GT1b increases infection and assessed the role GT1b in PKC regulated infection. To do this, we supplemented cells with ganglioside GT1b and evaluated BKPyV uptake. We showed that the addition of GT1b enhanced BKPyV uptake. From this we conclude that disialogangliosides such as GT1b increase infection by increasing uptake. This result supports the finding that glycosphingolipids stimulate enhanced caveolae uptake (39). We also evaluated the effects of combining the exogenous addition of GT1b with transient inhibition of PKC. We showed that this resulted in a synergistic increase in BKPyV infection. This result further supports the idea that PKC regulated glycosphingolipid stimulated caveolae endocytosis.

Signaling molecules regulate caveolae mediated endocytosis and as a result BKPyV endocytosis. Tyrosine kinases and serine/threonine kinases play a significant and consorted role in regulating caveolae mediated endocytosis. These kinases are potential targets for drug development to prevent entry of polyomaviruses that utilize caveolae-mediated endocytosis for entry. Understanding the signaling events associated with

binding and entry is an important aspect of characterizing the polyomavirus life cycle. Our assessment of how PKC regulates BKPyV uptake is essential as PKC has been shown to play a role in kidney disease. Studies show that PKC activity for some PKC isoforms increase during ischemic injury after organ transplantation (25). This is significant because kidney transplant patients are susceptible to ischemic injury, which is a risk factor for reactivation of latent BKPyV (13). PKC is therefore a likely target for development of antiviral therapies to block BKPyV infection and prevent complications from BKPyV reactivation. Interestingly, a recent study evaluated the effects of a pan-PKC inhibitor sotrastaurin (AEB071) on increased viral replication of Hepatitis C (HCV) and Hepatitis B (HBV) (51). Sotrastaurin is interesting because it is in phase II trials as an immunosuppressant for use during solid organ transplant (51). The study found that unlike other drugs that enhance viral replication as a side effect of immunosuppression, treatment with Sotrastaurin does not increase viral replication of HCV or Hepatitis B HBV due to its inhibition of PKC which is required for replication of both viruses (51). A drug like Sotrastaurin shows promise as a multifunctional therapy for kidney transplant recipients as it could likely serve as both an immunosuppressant and an inhibitor of PKC activity and BKPyV reactivation.

In the future we would like to determine if engagement of b-series gangliosides by BKPyV directly stimulates PKC activity. We would also like to confirm that inhibition of PKC causes BKPyV accumulation at the plasma membrane as the explanation for the observed susceptibility to antibody neutralization. Because BKPyV infection is increased when PKC is transiently inhibited, we would like to evaluate the localization of caveolae during transient inhibition of PKC to confirm that the observed increase in infection is

due to increased caveolae cycling. Finally, because bisindolmaleide I shows specificity for cPKCs, and some cPKC have been associated with kidney nephropathy, we would like to determine which isoforms of the cPKCs are important for PKC regulated BKPyV infection.

Summary

The objective of this work was to characterize how BKPyV engages the ganglioside receptors GD1b and GT1b and to determine how this engagement induces signaling events necessary for BKPyV entry. We hypothesized that the binding epitope for BKPyV is the disialic acid motif present on b-series gangliosides. Characterization of the binding epitope resulted in the identification of two additional gangliosides, GD2 and GD3, as potential receptors for BKPyV. Gangliosides GD2 and GD3 share a common disialic acid motif with gangliosides GD1b and GT1b. Our studies demonstrate that each sialic acid of the disialic acid motif plays an important function in BKPyV receptor engagement and receptor specificity. BKPyV engagement of its cellular receptors is mediated primarily by BKPyV VP1 interaction with the terminal sialic acid. We demonstrate that mutations of amino acids on BKPyV VP1 that prevent or alter the interaction of BKPyV VP1 with the functional groups of terminal sialic acid abolished or reduced viral growth. Additionally we show that a single amino acid on BKPyV VP1 defines receptor specificity. We demonstrate that mutating this amino acid, to more closely resemble that of SV40, switches BKPyV receptor engagement to that of the monosialylated ganglioside GM1. Further characterization of BKPyV engagement of GD1b revealed that while the left arm interacts with BKPyV VP1, this interaction is not critical to BKPyV growth. We show that mutating amino acids to abolish the interaction between BKPyV VP1 and the left arm of GD1b resulted in moderate to no reduction in BKPyV growth. Lastly we characterize ganglioside mediated internalization of BKPyV. We hypothesized that the serine/threonine kinase PKC regulates BKPyV entry. We demonstrate that transient inhibition of PKC stimulates increased BKPyV infection and is

associated with increased PKC localization to the membrane. This increase in infection is further enhanced by GT1b treatment, which stimulates increased BKPyV uptake. We also demonstrate that transient inhibition of PKC caused BKPyV susceptibility to antibody neutralization suggesting that BKPyV accumulates at the plasma membrane.

LITERATURE CITED

1. **Anderson, H.A., Y. Chen, L.C. Norkin.** 1996. Bound simian virus 40 translocates to caveolin-enriched membrane domains, and its entry is inhibited by drugs that selectively disrupt caveolae. *Molecular biology of the cell* **7**: 1825-34.
2. **Anderson, R.G.** 1998. The caveolae membrane system. *Annual review of biochemistry* **67**: 199-225.
3. **Campanero-Rhodes, M.A., A. Smith, W. Chai, S. Sonnino, L. Mauri, R.A. Childs, Y. Zhang, H. Ewers, A. Helenius, A. Imberty, T. Feizi.** 2007. N-glycolyl GM1 ganglioside as a receptor for simian virus 40. *J Virol* **81**: 12846-58.
4. **Chen, N., S. Furuya, H. Doi, Y. Hashimoto, Y. Kudo, H. Higashi.** 2003. Ganglioside/calmodulin kinase II signal inducing cdc42-mediated neuronal actin reorganization. *Neuroscience* **120**: 163-76.
5. **Chen, Y., L.C. Norkin.** 1999. Extracellular simian virus 40 transmits a signal that promotes virus enclosure within caveolae. *Exp Cell Res* **246**: 83-90.
6. **Dangoria, N.S., W.C. Breau, H.A. Anderson, D.M. Cishek, L.C. Norkin.** 1996. Extracellular simian virus 40 induces an ERK/MAP kinase-independent signalling pathway that activates primary response genes and promotes virus entry. *J Gen Virol* **77 (Pt 9)**: 2173-82.
7. **Dugan, A.S., S. Eash, W.J. Atwood.** 2005. An N-linked glycoprotein with alpha(2,3)-linked sialic acid is a receptor for BK virus. *J Virol* **79**: 14442-5.
8. **Dugan, A.S., M.L. Gasparovic, W.J. Atwood.** 2008. Direct correlation between sialic acid binding and infection of cells by two human polyomaviruses (JC virus and BK virus). *J Virol* **82**: 2560-4.
9. **Dugan, A.S., M.L. Gasparovic, N. Tsomaia, D.F. Mierke, B.A. O'Hara, K. Manley, W.J. Atwood.** 2007. Identification of amino acid residues in BK virus VP1 that are critical for viability and growth. *J Virol* **81**: 11798-808.

10. **Eash, S., W. Querbes, W.J. Atwood.** 2004. Infection of vero cells by BK virus is dependent on caveolae. *J Virol* **78**: 11583-90.
11. **Ewers, H., W. Romer, A.E. Smith, K. Bacia, S. Dmitrieff, W. Chai, R. Mancini, J. Kartenbeck, V. Chambon, L. Berland, A. Oppenheim, G. Schwarzmann, T. Feizi, P. Schwille, P. Sens, A. Helenius, L. Johannes.** 2010. GM1 structure determines SV40-induced membrane invagination and infection. *Nature cell biology* **12**: 11-8; sup pp 1-12.
12. **Herrmann, M., C.W. von der Lieth, P. Stehling, W. Reutter, M. Pawlita.** 1997. Consequences of a subtle sialic acid modification on the murine polyomavirus receptor. *J Virol* **71**: 5922-31.
13. **Hirsch, H.H., C.B. Drachenberg, J. Steiger, E. Ramos.** 2006. Polyomavirus-associated nephropathy in renal transplantation: critical issues of screening and management. *Advances in experimental medicine and biology* **577**: 160-73.
14. **Holthofer, H., J. Reivinen, A. Miettinen.** 1994. Nephron segment and cell-type specific expression of gangliosides in the developing and adult kidney. *Kidney international* **45**: 123-30.
15. **Johannessen, M., M.R. Myhre, M. Dragset, C. Tummler, U. Moens.** 2008. Phosphorylation of human polyomavirus BK agnoprotein at Ser-11 is mediated by PKC and has an important regulative function. *Virology* **379**: 97-109.
16. **Kasahara, K., Y. Sanai.** 2000. Functional roles of glycosphingolipids in signal transduction via lipid rafts. *Glycoconj J* **17**: 153-62.
17. **Katoh, N.** 1995. Inhibition by gangliosides GM3, GD3 and GT1b of substrate phosphorylation by protein kinase C in bovine mammary gland and its reversal by phosphatidylserine. *Life sciences* **56**: 157-62.
18. **Keppler, O.T., P. Stehling, M. Herrmann, H. Kayser, D. Grunow, W. Reutter, M. Pawlita.** 1995. Biosynthetic modulation of sialic acid-dependent virus-receptor interactions of two primate polyoma viruses. *J Biol Chem* **270**: 1308-14.

19. **Krautkramer, E., T.M. Klein, C. Sommerer, P. Schnitzler, M. Zeier.** 2009. Mutations in the BC-loop of the BKV VP1 region do not influence viral load in renal transplant patients. *J Med Virol* **81**: 75-81.
20. **Kreutter, D., J.Y. Kim, J.R. Goldenring, H. Rasmussen, C. Ukomadu, R.J. DeLorenzo, R.K. Yu.** 1987. Regulation of protein kinase C activity by gangliosides. *J Biol Chem* **262**: 1633-7.
21. **Low, J.A., B. Magnuson, B. Tsai, M.J. Imperiale.** 2006. Identification of gangliosides GD1b and GT1b as receptors for BK virus. *J Virol* **80**: 1361-6.
22. **Magaldi, T.G., M.H. Buch, H. Murata, K.D. Erickson, U. Neu, R.L. Garcea, K. Peden, T. Stehle, D. DiMaio.** 2012. Mutations in the GM1 binding site of simian virus 40 VP1 alter receptor usage and cell tropism. *J Virol* **86**: 7028-42.
23. **Min, K.J., H.K. Pyo, M.S. Yang, K.A. Ji, I. Jou, E.H. Joe.** 2004. Gangliosides activate microglia via protein kinase C and NADPH oxidase. *Glia* **48**: 197-206.
24. **Mineo, C., Y.S. Ying, C. Chapline, S. Jaken, R.G. Anderson.** 1998. Targeting of protein kinase Calpha to caveolae. *The Journal of cell biology* **141**: 601-10.
25. **Mochly-Rosen, D., K. Das, K.V. Grimes.** 2012. Protein kinase C, an elusive therapeutic target? *Nature reviews. Drug discovery* **11**: 937-57.
26. **Muchmore, E.A., S. Diaz, A. Varki.** 1998. A structural difference between the cell surfaces of humans and the great apes. *American Journal of Physical Anthropology* **107**: 187-98.
27. **Neu, U., J. Bauer, T. Stehle.** 2011. Viruses and sialic acids: rules of engagement. *Current opinion in structural biology* **21**: 610-8.
28. **Neu, U., M.S. Maginnis, A.S. Palma, L.J. Stroh, C.D. Nelson, T. Feizi, W.J. Atwood, T. Stehle.** 2010. Structure-function analysis of the human JC polyomavirus establishes the LSTc pentasaccharide as a functional receptor motif. *Cell host & microbe* **8**: 309-19.

29. **Neu, U., K. Woellner, G. Gauglitz, T. Stehle.** 2008. Structural basis of GM1 ganglioside recognition by simian virus 40. *Proceedings of the National Academy of Sciences of the United States of America* **105**: 5219-24.
30. **Pelkmans, L., E. Fava, H. Grabner, M. Hannus, B. Habermann, E. Krausz, M. Zerial.** 2005. Genome-wide analysis of human kinases in clathrin- and caveolae/raft-mediated endocytosis. *Nature* **436**: 78-86.
31. **Pelkmans, L., J. Kartenbeck, A. Helenius.** 2001. Caveolar endocytosis of simian virus 40 reveals a new two-step vesicular-transport pathway to the ER. *Nature cell biology* **3**: 473-83.
32. **Pelkmans, L., D. Puntener, A. Helenius.** 2002. Local actin polymerization and dynamin recruitment in SV40-induced internalization of caveolae. *Science* **296**: 535-9.
33. **Pelkmans, L., M. Zerial.** 2005. Kinase-regulated quantal assemblies and kiss-and-run recycling of caveolae. *Nature* **436**: 128-33.
34. **Prevostel, C., V. Alice, D. Joubert, P.J. Parker.** 2000. Protein kinase C(alpha) actively downregulates through caveolae-dependent traffic to an endosomal compartment. *J Cell Sci* **113 (Pt 14)**: 2575-84.
35. **Razani, B., C.S. Rubin, M.P. Lisanti.** 1999. Regulation of cAMP-mediated signal transduction via interaction of caveolins with the catalytic subunit of protein kinase A. *J Biol Chem* **274**: 26353-60.
36. **Razani, B., S.E. Woodman, M.P. Lisanti.** 2002. Caveolae: from cell biology to animal physiology. *Pharmacological reviews* **54**: 431-67.
37. **Ron, D., M.G. Kazanietz.** 1999. New insights into the regulation of protein kinase C and novel phorbol ester receptors. *Faseb J* **13**: 1658-76.
38. **Schneider-Schaulies, J.** 2000. Cellular receptors for viruses: links to tropism and pathogenesis. *J Gen Virol* **81**: 1413-29.
39. **Sharma, D.K., J.C. Brown, A. Choudhury, T.E. Peterson, E. Holicky, D.L. Marks, R. Simari, R.G. Parton, R.E. Pagano.** 2004. Selective stimulation of

caveolar endocytosis by glycosphingolipids and cholesterol. *Molecular biology of the cell* **15**: 3114-22.

40. **Smart, E.J., Y.S. Ying, R.G. Anderson.** 1995. Hormonal regulation of caveolae internalization. *The Journal of cell biology* **131**: 929-38.
41. **Stehle, T., S.C. Harrison.** 1996. Crystal structures of murine polyomavirus in complex with straight-chain and branched-chain sialyloligosaccharide receptor fragments. *Structure* **4**: 183-94.
42. **Stehle, T., S.C. Harrison.** 1997. High-resolution structure of a polyomavirus VP1-oligosaccharide complex: implications for assembly and receptor binding. *EMBO J* **16**: 5139-48.
43. **Stehle, T., Y. Yan, T.L. Benjamin, S.C. Harrison.** 1994. Structure of murine polyomavirus complexed with an oligosaccharide receptor fragment. *Nature* **369**: 160-3.
44. **Steinberg, S.F.** 2008. Structural basis of protein kinase C isoform function. *Physiological reviews* **88**: 1341-78.
45. **Sverdlov, M., A.N. Shajahan, R.D. Minshall.** 2007. Tyrosine phosphorylation-dependence of caveolae-mediated endocytosis. *Journal of cellular and molecular medicine* **11**: 1239-50.
46. **Taube, S., M.X. Jiang, C.E. Wobus.** 2010. Glycosphingolipids as Receptors for Non-Enveloped Viruses. *Viruses-Basel* **2**: 1011-49.
47. **Tremolada, S., S. Delbue, L. Castagnoli, S. Allegrini, U. Miglio, R. Boldorini, F. Elia, J. Gordon, P. Ferrante.** 2010. Mutations in the external loops of BK virus VP1 and urine viral load in renal transplant recipients. *J Cell Physiol* **222**: 195-9.
48. **Tsai, B., J.M. Gilbert, T. Stehle, W. Lencer, T.L. Benjamin, T.A. Rapoport.** 2003. Gangliosides are receptors for murine polyoma virus and SV40. *Embo J* **22**: 4346-55.

49. **Varki, A.** 2001. Loss of N-glycolylneuraminic acid in humans: Mechanisms, consequences, and implications for hominid evolution. *Am J Phys Anthropol Suppl* **33**: 54-69.
50. **Varki, A.** 2001. N-glycolylneuraminic acid deficiency in humans. *Biochimie* **83**: 615-22.
51. **von Hahn, T., A. Schulze, I. Chicano Wust, B. Heidrich, T. Becker, E. Steinmann, F.A. Helfritz, K. Rohrmann, S. Urban, M.P. Manns, T. Pietschmann, S. Ciesek.** 2011. The novel immunosuppressive protein kinase C inhibitor sotrastaurin has no pro-viral effects on the replication cycle of hepatitis B or C virus. *PloS one* **6**: e24142.
52. **Vyas, K.A., H.V. Patel, A.A. Vyas, R.L. Schnaar.** 2001. Segregation of gangliosides GM1 and GD3 on cell membranes, isolated membrane rafts, and defined supported lipid monolayers. *Biological chemistry* **382**: 241-50.
53. **Wang, X.Q., P. Sun, A.S. Paller.** 2002. Ganglioside modulation regulates epithelial cell adhesion and spreading via ganglioside-specific effects on signaling. *J Biol Chem* **277**: 40410-9.
54. **Yu, R.K., Y. Nakatani, M. Yanagisawa.** 2009. The role of glycosphingolipid metabolism in the developing brain. *J Lipid Res* **50 Suppl**: S440-5.